UNDERSTANDING AND OVERCOMING LIMITATIONS OF VESICULAR
STOMATITIS VIRUS AS AN ONCOLYTIC AGENT AGAINST PANCREATIC
DUCTAL ADENOCARCINOMA

by

Eric Lawrence Hastie

A dissertation submitted to the faculty of
The University of North Carolina at Charlotte
in partial fulfillment of the requirements
for the degree of Doctor of Philosophy in
Biology

Charlotte

2014

Approved by:

_____
Dr. Valery Grdzelishvili

_____
Dr. Didier Dréau

_____
Dr. Ian Marriott

_____
Dr. Christine Richardson

_____
Dr. Jennifer Weller

ABSTRACT

ERIC LAWRENCE HASTIE. Understanding and overcoming limitations of vesicular stomatitis virus as an oncolytic agent against pancreatic ductal adenocarcinoma (Under the direction of DR. VALERY Z. GRDZELISHVILI)

Vesicular stomatitis virus (VSV) is a prototypic nonsegmented negative-strand RNA virus. Lack of preexisting immunity against VSV, inherent oncotropism, and genetic malleability make VSV a widely used platform for vaccine, oncolytic, and gene therapy vectors. VSV proteins and host cellular proteins both determine VSV success as an oncolytic therapy. This dissertation focuses on two host proteins in pancreatic ductal adenocarcinoma (PDAC) that may affect VSV oncolytic efficacy: human Mucin 1 (MUC1) and tumor suppressor TP53 (p53). As MUC1 is known to inhibit other viruses, we tested VSV against murine PDAC cell lines expressing human MUC1 or MUC1-null, and found that VSV demonstrates significant oncolytic ability independent of MUC1 expression status *in vitro* and *in vivo*. Importantly, we tested VSV against murine PDAC xenografts for the first time in immunocompetent mice. *In vivo* VSV treatment resulted in significant reduction of tumor growth for tested mouse PDAC xenografts (+MUC1 or MUC1 null), although the antitumor effect was transient. The antitumor effect was further improved when the virus was combined with the chemotherapeutic drug gemcitabine. Another approach to improve oncolytic therapy is to engineer VSV to express anticancer genes. We generated rVSV encoding a chimeric human p53 that evades inhibition by cellular dominant-negative mutant p53 and confirmed that virus-encoded p53 is functional in cancer cells. As p53 is known to enhance antiviral responses in nonmalignant cells, it was important to determine if the transgene would attenuate

VSV in PDACs. Surprisingly, our analysis of global gene expression in infected PDAC cells suggests that the p53 transgene inhibits, rather than attenuates, antiviral responses in cancer cells thereby making the virus a viable option for therapeutic use. In agreement with this, the oncolytic efficacy of VSV expressing p53 against 11 human PDAC cell lines *in vitro* was not attenuated compared to the parental strain in all cell lines.

DEDICATION

To my parents, my family,

and

my partner in wine, Michael.

ACKNOWLEDGEMENTS

This work was made possible by the guidance and support of Dr. Valery Grdzelishvili; thank you for the opportunity to work in your lab and your mentorship. Importantly, Megan Moerdyk-Schauwecker, M.S. was an endless source of technical knowledge, encouragement, friendship, and delicious baked goods. I would like to thank my committee: Dr. Ian Marriott, Dr. Didier Dréau, Dr. Christine Richardson, and Dr. Jennifer Weller for their important feedback and support. Thank you to the members of the Grdzelishvili lab, Dr. Andrea Murphy and Dr. Nirav Shah, Natascha Moestl, Carlos Molestino, Dr. Marcela Cataldi, Sebastien Felt, and Cuyler Pittan for their assistance and friendship throughout my graduate career. Thank you to Dr. Pinku Mukherjee and her laboratory, especially Dr. Dahlia Besmer, for providing materials and expertise in pancreatic cancer in our MUC1 studies. Also, I want to thank Dr. Nury Steuerwald and her lab for processing and analysis of cellular RNA and genomic DNA samples for the p53 studies. I would like to thank The University of North Carolina at Charlotte Graduate School for the Graduate Assistant Support award for funding my graduate education. Lastly, I would like to acknowledge my friends: Jennifer Beck, Dr. Ben and Lianna Conforti, and Patrick Richardson, you questioned my sanity but made sure I crossed the finish line. Thank you.

TABLE OF CONTENTS

LIST OF FIGURES

LIST OF TABLES

LIST OF ABBREVIATIONS

5-FC	5-fluorocytosine
5-FU	5-fluorouracil
Abs	antibodies
BCL-2	b-cell lymphoma 2
CCP	clathrin-coated pit
CD	cytosine deaminase
CKII	casein kinase II
CNS	central nervous system
CPA	cyclophosphamide
CypA	cyclophilin A
DI	defective interfering
dsRNA	double stranded RNA
EF-1	elongation factor-1 (EF-1)
eIF4E	eukaryotic translation initiation factor 4F
ER	endoplasmic reticulum
FADD	fas-associated protein with death domain
G	glycoprotein
GFP	green fluorescent protein
HPV	human papilloma viruses
HSV	herpes simplex virus
IFN	interferon

IFNAR1/2	interferon receptor
IL	interleukin
IRF	interferon regulatory factor
ISG	interferon stimulated gene
JAK	janus kinase
L	large polymerase
LCMV	lymphocytic choriomeningitis virus
LDLR	low density lipoprotein receptor
M	matrix protein
Mcl-1	meloid cell leukaemia 1 protein
MDA5	melanoma differentiation-associated protein 5
MEK/ERK	mitogen-Activated Protein kinase kinase kinase 5 signaling
MHC-I	major histocompatibility complex class I
MOI	multiplicity of infection
mRNA	messenger RNA
MTT	3-(4,5-dimethyl-2-thiazolyl)-2,5-diphenyl-2H-tetrazolium bromide
MxA	myxovirus (influenza virus) resistance 1
MyD88	myeloid differentiation primary response gene 88
N	nucleocapsid protein
NDV	newcastle disease virus
NIS	sodium iodide symporter
NK	natural killer cells

OAS	2'–5' oligoadenylate synthetase
OPD	o-phenylenediamine
ORF	open reading frame
OV	oncolytic virus
OVA	ovalbumin
P	phosphoprotein
PDAC	pancreatic ductal adenocarcinoma
PKR	double-stranded RNA-activated protein kinase
PRR	pattern recognition receptors
PS	phosphatidylserine
RdRp	RNA dependent RNA polymerase
RIG-I	retinoic-acid-inducible gene
RNP	ribonucleoprotein
Rp	repeated passage
RSV	respiratory syncytial virus
rVSV	recombinant VSV
S.C.	subcutaneous
ScFv	single-chain variable fragment
STAT	signal transducer and activator of transcription
TAA	tumor-associated antigen
TK	thymidine kinase
TLR	toll-like receptor
UPRT	uracil phosphoribosyltransferase

VSV   vesicular stomatitis virus

VSV IN   VSV Indiana serotype

VSV NJ   VSV New Jersey serotype

WT   wild type

CHAPTER 1: INTRODUCTION

1.1 Introduction

Viruses are commonly thought of as intracellular parasites that hijack host cell machinery to facilitate replication with resulting infections that cause such diseases as the common cold, AIDS, or lead to cancer. However, some viruses can also be used as therapeutic agents for various vaccines, gene therapy, and more recently, cancer therapy applications. Oncolytic virus (OV) therapy is an emerging approach that utilizes viruses to preferentially infect and kill cancer cells, while not harming non-malignant, normal cells. Scientists have observed tumor regression after virus infection since 1893 (1), yet most research in the field has occurred in the last 15 years, when almost every major group of animal virus has been tested for OV potential. Impressive preclinical successes have been reported (2).

This work focuses on using VSV as an OV. Numerous preclinical studies demonstrated the effectiveness of VSV against various malignancies (51) and a VSV recombinant encoding the interferon (IFN)-β gene is currently in a phase I clinical trial against hepatocellular carcinoma (trial NCT01628640). In the last 10 years, a great number of recombinant VSVs (rVSVs) have been generated via reverse genetics, with the goal of generating more potent OVs that work synergistically with host immunity and/or other therapies to reduce or eliminate tumor burden (51). The aim of this dissertation is to improve efficacy of VSV as an OV against pancreatic ductal

adenocarcinoma (PDAC). Given that host proteins can play a role in influencing the VSV life cycle, it is critical to understand the biology of VSV (section 1.2) before focusing on host proteins that may influence the therapeutic efficacy of VSV. In an effort to focus this dissertation on VSV as an OV, this section is mainly focused on VSV biology relevant to its OV potential. Section 1.3 is focused on VSV as an oncolytic agent against various cancers by providing generalities about the virus tropism for cancer and oncolytic action of VSV. Finally, section 1.4 discusses VSV specifically in the context of PDAC by focusing on two host proteins examined in this dissertation: MUC1 and p53. This section highlights the importance of MUC1 as a potential inhibitor of VSV therapy against PDAC as well as how virus-based delivery of exogenous p53 may be a useful tool to enhance VSV therapy.

1.2 VSV Biology

VSV is a prototypic, non-segmented negative sense RNA virus (order *Mononegavirales*, family *Rhabdoviridae*) and one of the best-studied animal viruses. Two major wild type (WT) VSV serotypes, Indiana (VSV-IN) and New Jersey (VSV-NJ), are endemic to much of Central and South America and parts of the USA (3). Natural hosts include horses, cattle, pigs and a range of other mammals and their insect vectors. Among livestock, WT VSV outbreaks occur seasonally and most infections are non-lethal, manifesting as fever and blister-like lesions of the oral cavity, feet, and teats (4, 5). Five genes are encoded by the 11-kb VSV genome: nucleocapsid protein (N), phosphoprotein (P), matrix protein (M), glycoprotein (G), and large polymerase (L) that assemble as an enveloped, bullet-shaped virion measuring 185 nm × 75 nm (6). Below are the detailed steps of the VSV life cycle: entry, replication, and exit (Figures 1 - 2).

Biology of VSV: Entry

The VSV G protein is the main viral determinant of entry (7), and is involved in two of the initial steps of the infectious process: virus attachment to the host cell surface and viral-induced pH-dependent endosomal membrane fusion. VSV G enables infection of most, if not all, human cell types, and of organisms as distant as zebrafish and Drosophila (8-10). Currently, low density lipoprotein receptor (LDLR) and its family members have been proposed to be the cell surface receptors for VSV (11). The study suggests that LDLR serves as the major receptor for VSV entry in human and mouse cells, whereas LDLR family members serve as alternative receptors. The widespread expression of LDLR family members would account for the pantropism (wide tropism) of VSV.
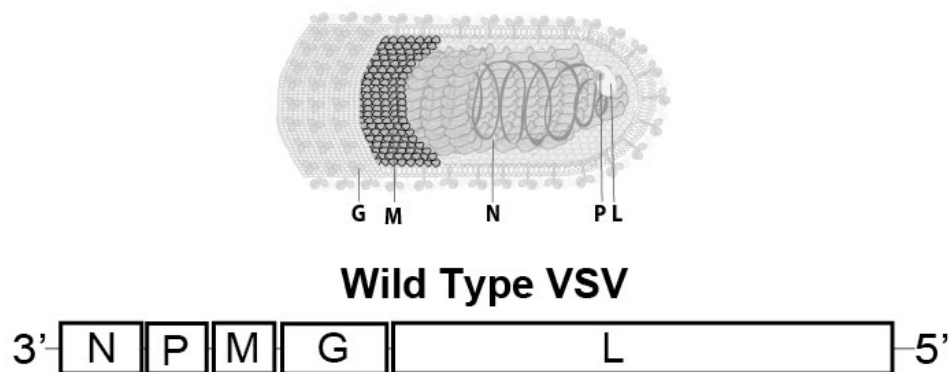
Wild Type VSV

Figure 1: Structure and genome of wild type VSV. VSV is a prototypic, non-segmented negative sense RNA genome that encodes 5 genes: N, P, M, G, L that assemble as an enveloped, bullet-shaped virion. This illustration was created by Eric Hastie.

After binding to the cell surface, VSV particles enter the cell through endocytosis, in a clathrin-based, dynamin-2-dependent manner (12). The virus can enter either through a preformed clathrin-coated pit (CCP) or by de novo induction of pit formation (13). Interestingly, because VSV is significantly larger than the dimensions of a typical clathrin-coated vesicle, the vesicles used by the virus for entry are only partially clathrin-coated, and require actin polymerization for efficient uptake (14).

Following internalization membrane fusion occurs rapidly in early endosomes (13). It has long been assumed that the viral envelope fuses directly to the limiting endosomal membrane, but it has also been suggested that VSV G targets the membrane of intraendosomal vesicles first (15). The authors propose a two-step process, with the initial fusion event occurring with internal vesicles followed by release of the viral NC into the cytosol by back-fusion of the internal vesicle with the limiting membrane of late endosomes. This alternative mechanism is supported by *in vitro* experiments demonstrating that the presence of lipid bis(monoacylglycero)phosphate on the endosomal internal vesicles selectively promotes VSV G-mediated membrane fusion (16). The authors concluded the two-step model remains controversial but that differential composition of endosomal domains across cell types may allow the virus to either fuse directly from the early endosome or enter via back-fusion in late endosomes.

Biology of VSV: Replication

The ability of VSV to enter a cell does not guarantee successful virus replication. Permissive cells must provide an optimal environment (including host factors) for viral genome transcription, replication, and viral messenger RNA (mRNA) translation. Importantly, VSV also needs to evade the host cell innate antiviral

responses.

Following release from the endosome, the VSV ribonucleoprotein (RNP) complex, composed of the VSV nucleocapsid and associated VSV L and P proteins, is released into the cytoplasm. VSV L protein, a multifunctional RNA dependent RNA polymerase (RdRp), forms a complex with VSV P, a multifunctional polymerase co-factor, to begin primary transcription of viral mRNAs (17, 18). Viral transcripts are synthesized, capped, methylated, and polyadenylated by the L protein (19-28). VSV mRNAs are virtually indistinguishable from host mRNAs and are translated by host cell ribosomes (30-33). Unlike viral mRNA synthesis, VSV genome replication requires N protein, which is used to encapsidate newly produced antigenomic or genomic RNA but also is a component of the polymerase complex specifically involved in genome replication rather than mRNA synthesis (34-36). While transcription of viral mRNAs appears to occur throughout the cytoplasm, there is evidence to suggest that genome replication occurs in cytoplasmic inclusions. It remains unclear if these are virus developed inclusions or stress granules induced by cellular response to infection (37, 38). At this step in the life cycle, primary transcription still occurs, but it appears that mRNA transcripts are transported away from the inclusion sites in a microtubule dependent manner (38).

As with other RNA viruses, the VSV polymerase lacks proofreading activities and makes an error every 10^3 to 10^4 nucleotides (39-41). This generates genetically differing viruses, so called quasi-species, which makes VSV extremely adaptable to changing environments. The broad tropism of VSV suggests viral proteins may be responsible for the bulk of enzymatic activity required for viral gene transcription and
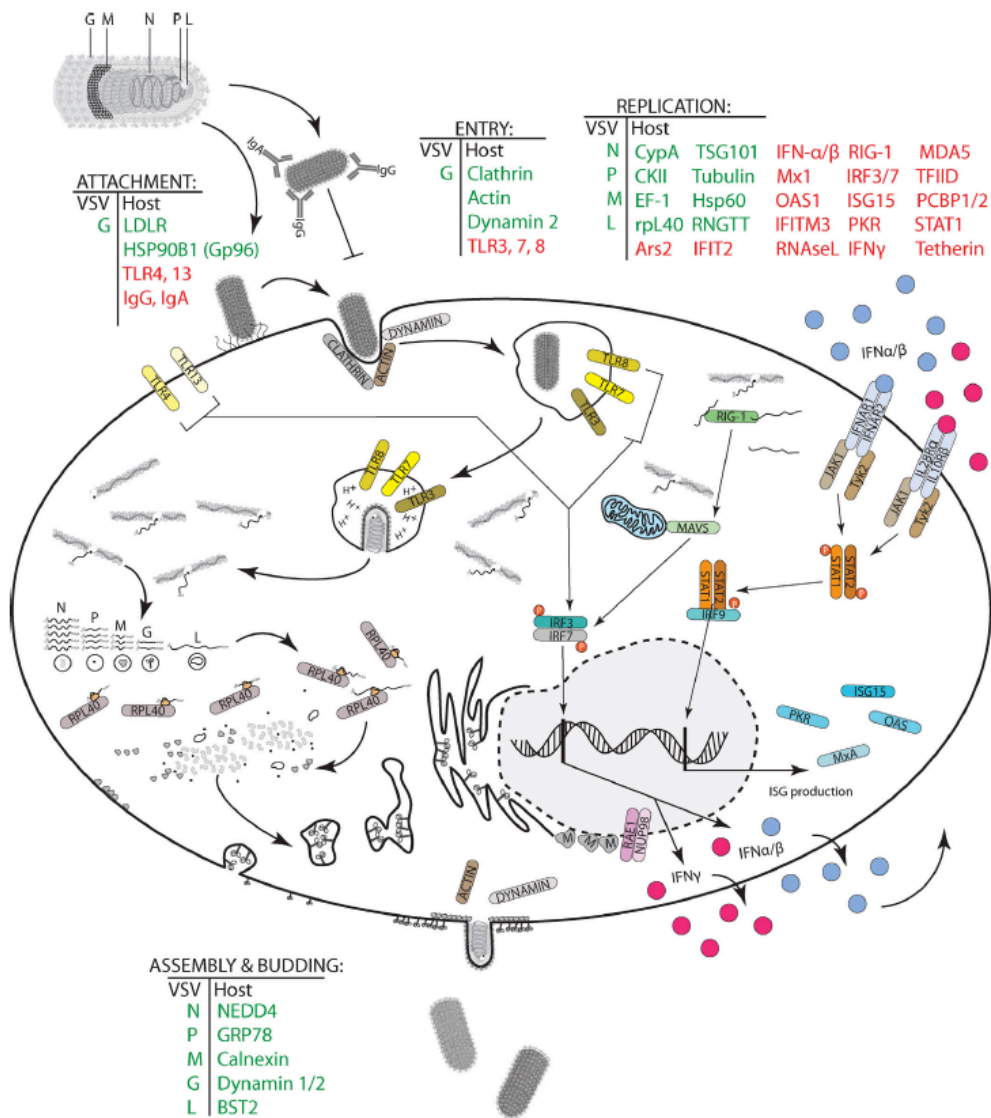
Figure 2: Life cycle of VSV. Host and viral proteins are involved (positively or negatively) in VSV infection and replication. Different viral and host proteins are involved in VSV attachment, entry, replication, assembly, or release. Proteins known to be involved in the VSV life cycle are shown at each step: green indicates viral or host proteins known to assist VSV while red indicates putative host proteins as well as host proteins responsible for an antiviral response (29). This illustration was created by Eric Hastie.

genome replication, or that conserved host proteins assist virus replication. Importantly, the success of VSV replication and spread can be influenced by the formation of defective interfering (DI) particles. DIs arise as a result of one or more RNA recombination events at a variety of viral genomic sites (42, 43). These truncated genomes can still be encapsidated and form virus-like particles. Although these particles cannot sustain an infection by themselves, they are able to replicate in cells coinfected with a helper VSV, resulting in substantial reductions in virus titer (42).

<div align="center">Biology of VSV: Exit/Release</div>

Even if a cell provides a hospitable environment for virus infection and replication, there is no guarantee that progeny virions will be produced or that produced virions will be highly infectious. VSV virions acquire an envelope by budding through sites in the host plasma membrane enriched in VSV G protein (44). Viral RNPs are transported to the site of budding in a microtubule dependent manner (3, 38, 45). Association of the RNP with VSV M results in RNP condensation and facilitates budding (44). VSV budding depends on the interactions of M protein with host factors (3). The N terminus of VSV M interacts with dynamins 1 and 2 (46, 47) and is thought to affect endocytic vesicle trafficking as blocking the M-dynamin interaction inhibited budding and resulted in accumulation of nucleocapsids at the plasma membrane (47). Additionally, ubiquitination of M also appears to be required, possibly for recruitment of host factors, as a decrease in availability of cytoplasmic ubiquitin reduces VSV titers (48). As a consequence of budding through the cellular plasma membrane, in addition to all five VSV proteins, host factors from the cytoplasm and plasma membrane can be incorporated into progeny virions. Our proteomic analysis using mass spectrometry

showed a large number of host proteins associated with virions of VSV, and this profile

was dependent on the cell type (BHK-21, A549, or 4T-1) used to generate virions (49,

50). Virions purified from these cell lines also differed by more than an order of

magnitude in the number of infectious particles per μg of total protein, suggesting

properties of the host cell may influence the infectivity of the resulting virions.

1.3 VSV as an Oncolytic Agent Against Cancer

OV therapy is an emerging anti-cancer approach that utilizes viruses to

preferentially infect and kill cancer cells and impressive preclinical successes have been

reported (2). As a result, the adenovirus H101 was approved for clinical use in China in

2006 (52), and three other OVs based on VV, herpes simplex virus (HSV) and reovirus

are currently in late-phase clinical trials and could soon be approved in the USA (2).

This work focuses on using VSV as an OV (Figure 3). Compared with

other OVs, VSV is advantageous due to a combination of several factors, including its

well-studied biology, relative independence of a specific receptor or cell cycle phase,

ability to infect a wide range of laboratory cell lines and to produce very high virus

yields, cytoplasmic replication without risk of host-cell transformation, a small, easily

manipulated genome, and lack of pre-existing immunity in humans. Regarding

oncolytic therapy, VSV preferentially infects and kills cancer cells while leaving

nonmalignant "normal" cells unharmed. Numerous preclinical studies demonstrated the

effectiveness of VSV against various malignancies (51) and a VSV recombinant

encoding the interferon (IFN)-β gene is currently in a phase I clinical trial against

hepatocellular carcinoma (trial NCT01628640). In the last 10 years, a great number of

recombinant VSVs (rVSVs) have been generated via reverse genetics, with the goal of
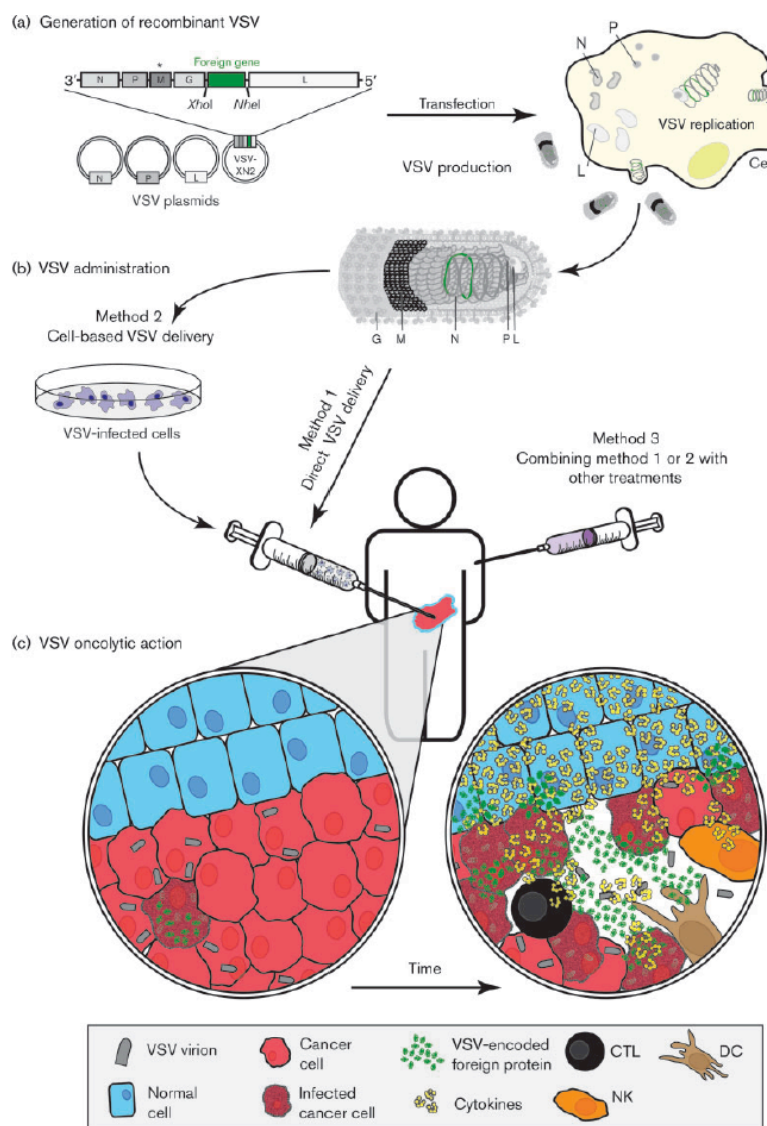
Figure 3: Scheme of VSV-based OV therapy. (a) Reverse genetics allows generation of a recombinant VSV encoding a foreign gene of interest between the VSV G and L genes. The asterisk above M indicates M protein mutation(s) resulting in VSV attenuation in normal cells. Plasmids encoding VSV replication machinery and the modified genome are co-transfected into a cell line, and complete virions are produced and amplified using good manufacturing practices. (b) For evaluation of oncolytic efficacy, VSV can be administered directly, via cell-based delivery, or in combination with other treatments (chemotherapy, radiotherapy or other OVs). (c) In infected cells, VSV recombinants may express a foreign gene that facilitates killing of the adjacent uninfected cancer cells (e.g. suicide-gene approach or immunostimulation). Innate antiviral responses and other mechanisms prevent cell death in normal cells. Ideally, stimulation of innate and adaptive immune cells by VSV and/or the foreign gene product should lead to tumor-specific immune responses, including memory responses that prevent cancer recurrence (51). This illustration was created by Eric Hastie.

generating more potent OVs that work synergistically with host immunity and/or other therapies to reduce or eliminate tumor burden (51).

In general, pre-existing immunity to VSV in human populations is very low, and VSV infection in humans is generally asymptomatic and limited to agricultural and laboratory workers (3). Only one case of WT VSV-IN-mediated encephalitis in humans has been reported (53). To address concerns for therapeutic use, VSV neurotoxicity has been studied extensively in different rodent and non-human primate systems. In principle, VSV can cause neurotoxicity in mice or rats when administered intracranially (54), intranasally (55), intravascularly (56) and intraperitoneally (57). Neurotoxicity following intranasal VSV infection (WT or non-attenuated rVSVs) is very efficient and has been studied extensively. When administered intranasally, WT or non-attenuated rVSVs replicate rapidly in the nasal epithelium, spread to olfactory neurons, then move retrograde axonally to the brain, where they replicate and cause neuropathogenesis (58-60). Following infection of the central nervous system (CNS), the onset of encephalitis was shown to be T-cell-independent as it is seen in athymic mice, and WT VSV neuropathology appears to be more related to the cytopathological nature of VSV infection rather than to T-cell-mediated mechanisms (61), (62). Both innate (nitric oxide produced by neurons and glial cells) and adaptive (expression of MHC molecules and T-cell infiltration) immunity are required for clearance of VSV from the CNS (58). In collaboration with Dr. Ian Marriott's laboratory, our research demonstrated that WT VSV can infect microglia and astrocytes *in vitro* and *in vivo*, and suggests that infection of glial cells results in the production of inflammatory cytokines that may facilitate encephalitis (63-65). VSV-mediated encephalitis has been observed in non-human

primates (NHPs). Fortunately, the undesirable natural neurotoxicity of WT VSV has been addressed by the generation of various VSV-based recombinants retaining their oncolytic activities but lacking neurotoxicity, reviewed in (51). VSV-ΔM51 lacks neurotoxicity and is the basis for many recombinant VSVs used for OV therapy, Table 1. The attenuated VSV-ΔM51 virus has a deletion of the methionine at amino acid position 51 of the VSV M protein (66), and this mutation hones VSV oncoselectivity by preventing WT M protein's ability to shut down cellular gene expression (67-69), thus limiting virus replication to cells, like cancer, that lack an intact antiviral response. Additionally, this mutation to the VSV M protein may also affect how VSV induces cell death as an OV. Interestingly, while WT VSV induces apoptosis primarily via the intrinsic pathway, VSV M51 mutants induce apoptosis primarily via the extrinsic pathway (70, 71). Importantly, it appears that this ΔM51 mutation does not inhibit the oncolytic efficacy of the virus.

However, perhaps the most significant determinant of VSV oncoselectivity and success as a therapy is the type I IFN-associated antiviral response of a cell. Although normal cells can be infected by VSV, they sense virus infection and produce, secrete and respond to type I IFNs to impede virus replication by inducing an antiviral state in the cell. In many cancer cells, VSV oncoselectivity is based largely on defective or reduced type I IFN responses (69, 72-74). In many cancer cells, specific genes associated with type I IFN responses are downregulated or functionally inactive (75-78). In addition, IFN signaling can be inhibited by MEK/ERK signaling, a cascade often upregulated in cancer cells (79). Abrogation of IFN signaling in cancer cells can also be caused by epigenetic silencing of IFN-responsive transcription factors IRF7 or IRF5

(80). In addition to defective IFN signaling, continuously proliferating cancer cells often have abnormal translation machinery that favors VSV replication (81). Several cellular proteins, including PKR, eIF2β, eIF4E, AKT and NFAR1/2, have been shown to play a role in mRNA translation as a determinant of VSV oncoselectivity (82, 83). Defects in the IFN pathway are not surprising, considering that IFN responses generally create conditions unfavorable for tumor formation, as they are anti-proliferative, anti-angiogenic and pro-apoptotic (84).

However, some cancer cells do not have these defects and resist VSV infection like normal cells (74, 85). This includes some mesotheliomas (86), melanomas (87, 88), lymphomas (89), bladder and (90) renal cancers (91) and possibly others (69). Understanding the mechanisms of VSV oncoselectivity is important for creating new, safe OVs designed for selective replication in cancer cells.

1.4 VSV and Pancreatic Ductal Adenocarcinoma

Pancreatic cancer has the worst prognosis of all cancers and is estimated to be the fourth leading cause of cancer-related deaths in the United States (92). About 95% of pancreatic cancers are pancreatic ductal adenocarcinomas (PDACs), which are known to be highly invasive, with aggressive local growth and rapid metastases (93). To date, surgery remains the only potential cure for PDAC. Other therapies, such as radiation therapy and chemotherapy, have shown little efficacy (94, 95). Thus, the development of new treatment strategies against PDAC is of utmost importance.

VSV has shown promising results against an array of cancers in preclinical studies (51) and is currently in a phase I clinical trial against hepatocellular carcinoma (trial NCT01628640). The undesirable neurotoxicity of WT VSV has been addressed by

Table 1: VSV-XN2 and attenuated VSV-M51

Recombinant VSV	Virus description	Reference(s)	Designed to improve:				
			Oncoselectivity	Safety	Oncotoxicity	VSV survival	Tumour immunity
WT and miscellaneous							
WT VSV ('Rose lab')	The parental rWT VSV for most VSV-based OVs. The L gene and the N-terminal 49 residues of the N gene are derived from the Mudd-Summers strain, the rest is from the San Juan strain (both Indiana serotype)	Lawson et al. (1995)					
VSV-WT-XN2 (or XN1)	Derivative of rWT VSV ('Rose lab'). Generated using pVSV-XN2 (or pVSV-XN1), a full-length VSV plasmid containing unique XhoI and NheI sites flanked by VSV transcription start and stop signals between G and L genes. pVSV-XN2 (or pVSV-XN1) is commonly used to generate recombinant VSVs encoding an extra gene	Schnell et al. (1996)					
WT VSV ('Wertz lab')	Alternative rWT VSV. The N, P, M and L genes originate from the San Juan strain; G gene from the Orsay strain (both Indiana serotype). Rarely used in OV studies	Whelan et al. (1995)					
M mutants							
VSV-M51R	The M51R mutation was introduced into M	Kopecky et al. (2001)	X		X		
VSV-ΔM51, VSV-ΔM51-GFP, - RFP, -FLuc, -Luc, - LacZ	The ΔM51 mutation was introduced into M. In addition, some recombinants encode a reporter gene between the G and L	Stojdl et al. (2003), Power & Bell (2007), Wu et al (2008)	X		X		
VSV-*Mmut	VSV with a single mutation or combination of mutations at the following M positions: M33A, M51R, V221F and S226R	Hoffmann et al. (2010)	X		X		

the generation of various VSV-based recombinants retaining their oncolytic activities but lacking neurotoxicity, Table 1 (51). Before VSV can be successful against a PDAC, it is important to understand characteristics of the cancer that may inhibit virus efficacy.

Activating mutations in the KRAS proto-oncogene generally drive PDAC and progression through the stages of pancreatic intraepithelial (PanIN) lesions to invasive cancer is characterized by deregulation of several genes, including mucins (96, 97) (Figure 4). In a tumor setting, the membrane-tethered glycoprotein mucin 1 (MUC1) becomes overexpressed and aberrantly glycosylated in more than 80% of human PDACs and in 100% of metastatic lesions (96). MUC1 plays an important role in the development and progression of PDAC and other cancers and is a major marker for poor prognosis (98-102) (Figures 4 - 5).
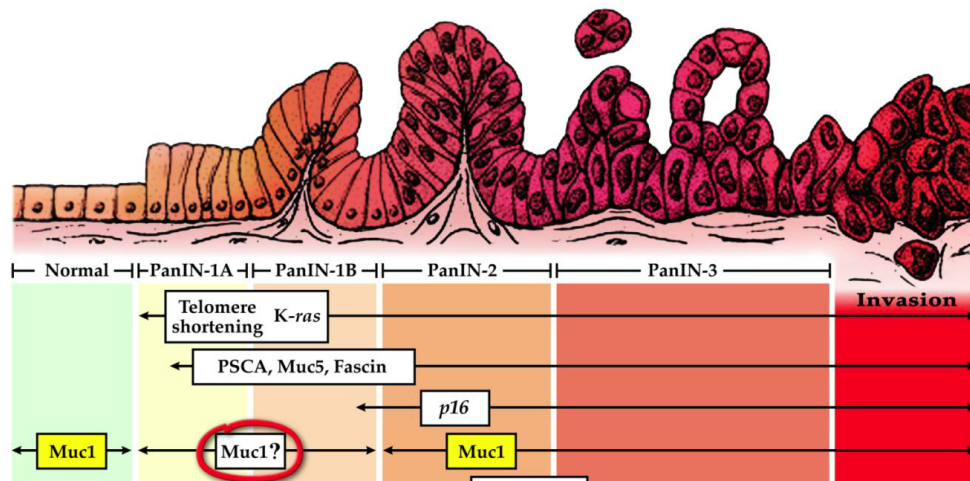
Figure 4. Pancreatic cancer progression. Pancreatic intraepithelial (PanIN) lesions are most often driven by KRAS mutations that promote continuous proliferation. Secondary mutations, like MUC1, are thought to enhance progression and may also act to inhibit virus-based oncolytic therapy either directly at the cell surface or through signaling mechanisms that are not entirely understood. Adapted from (103).

Our studies analyzed several rVSVs in an array of human PDAC cell lines *in vitro* (104, 105) and *in vivo* in xenografts in athymic mice (105) (Chapter 2). For these studies, however, there was a correlation between cells that were resistant to VSV oncolysis and MUC1 expression. While the role of MUC1 in VSV infection or OV therapy has never been studied before, the O-linked carbohydrates of MUC1 purified from human breast milk can inhibit poxvirus (106), HIV (106, 107), and rotavirus (108), and MUC1 expression can block adeno-associated virus attachment (109). These studies were the basis for our hypothesis that MUC1 may play an inhibitory role in VSV infection and its success as an oncolytic virus.
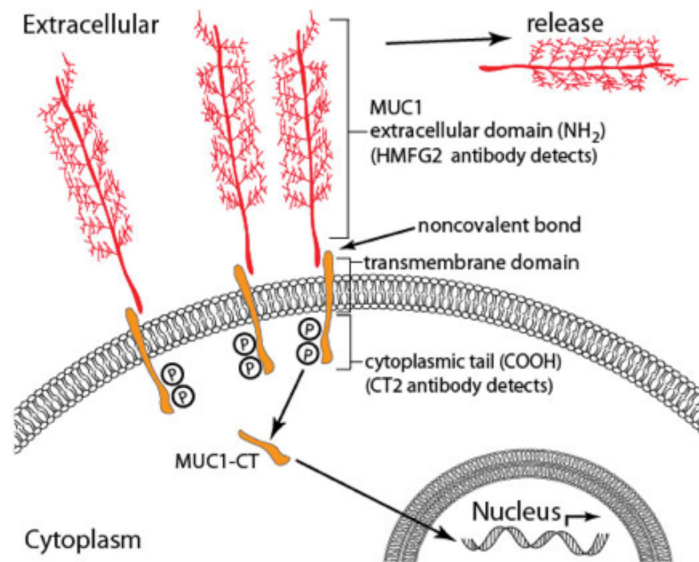
Figure 5: Diagram of MUC1 at the cell surface and cytoplasm. MUC1 is a membrane-tethered protein that becomes overexpressed and aberrantly glycosylated in pancreatic cancer. The protein exists as three domains: extracellular, transmembrane, and a cytoplasmic tail. The cytoplasmic tail can relocate to the nucleus where it is thought to be involved in cell signaling that promotes cell cycle progression, survival, and even migration. This illustration was created by Eric Hastie.

In this work, VSV was evaluated for the first time in MUC1 positive or null immunocompetent mouse models of PDAC. As mentioned above, the use of MUC1 in these models is important, as previous studies have shown MUC1 to be a major marker for poor prognosis and drug resistance of PDAC (100, 102). It was unclear if the presence of MUC1 might also be a marker for the resistance to VSV as an OV and the studies in chapter 2 address this topic.

In contrast to potential host factors inhibiting virus therapy, some may actually enhance OV therapeutic outcomes. In fact, many labs have attempted to strengthen VSV as an OV by arming the virus with transgenes with antitumor effects. VSV is able to stably maintain expression of an additionally inserted gene, especially when it is inserted between the G and L genes (110, 111) (Figure 1). Such stability is highly beneficial for VSV as a vector and vaccine delivery agent. Currently, a large number of VSV recombinants expressing heterogeneous genes have been generated and characterized, and many studies have demonstrated stable expression of these genes (Tables 1 and 8).

In this work we aimed to enhance the oncolytic effect of VSV by generating recombinant VSVs encoding TP53 gene for human tumor suppressor, p53. Mutation of p53 in cancer cells is often a secondary mutation that promotes PDAC progression and we found that none of our 11 PDAC cell lines retained wild type p53 expression. As a therapy, restoration of WT p53 activity has been reviewed extensively and is canonically known to induce cell-cycle arrest, apoptosis, and senescence (Figure 6). Additionally, more recently identified functions include regulation of metabolism and promotion of enhanced antiviral and antitumor immunity (112-114). What role any of

these pathways may have in enhancing the oncolytic effect of VSV remains to be explored.

Overall, the work in this dissertation will address host factor involvement in the oncolytic efficacy of VSV against PDAC. By focusing specifically on a potential inhibitory role of MUC1 (chapter 2) and viral-expression of tumor suppressor p53 (chapter 3), we aim to characterize the involvement of these two proteins in VSV therapy and provide methods to enhance VSV-based therapy.

CHAPTER 2: ROLE OF MUC1 IN SUSCEPTIBILITY OF PDAC CELLS TO
VSV *IN VITRO* AND *IN VIVO* IN IMMUNOCOMPETENT MICE

2.1 Abstract

VSV is a promising oncolytic agent against various malignancies. Here, we
wanted to determine the role of MUC1 in susceptibility of PDAC cells to VSV.
Moreover, for the first time, we tested VSV *in vitro* and *in vivo* in a clinically relevant,
immunocompetent mouse model of PDAC. Our system allows the study of virotherapy
against PDAC in the context of overexpression (80% of PDAC patients) or no
expression of human MUC1, a major marker for poor prognosis in patients. *In vitro*, we
tested three rVSVs: WT VSV, VSV-green fluorescent protein (VSV-GFP), and a safe
oncolytic VSV-ΔM51-GFP, against mouse PDAC cell lines that expressed human
MUC1 or were MUC1 null. All viruses demonstrated significant oncolysis, independent
of MUC1 expression, although VSV-ΔM51-GFP was somewhat less effective in two
PDAC cell lines. *In vivo* administration of VSV-ΔM51-GFP resulted in significant
reduction of tumor growth for murine PDAC xenografts (+MUC1 or MUC1 null), and
efficacy was improved when the virus was combined with the chemotherapeutic drug
gemcitabine. The antitumor effect was transient in all tested groups. The developed
system can be used to study therapies involving various oncolytic viruses and
chemotherapeutics, with the goal of inducing tumor-specific immunity while preventing
premature virus clearance.

2.2 Introduction

Pancreatic cancer has the worst prognosis of all cancers and is estimated to be the fourth leading cause of cancer-related deaths in the United States (92). About 95% of pancreatic cancers are pancreatic ductal adenocarcinomas (PDACs), which are known to be highly invasive, with aggressive local growth and rapid metastases (93). To date, surgery remains the only potential cure for PDAC. Other therapies, such as radiation therapy and chemotherapy, have shown little efficacy (94, 95). Thus, the development of new treatment strategies against PDAC is of utmost importance.

PDAC is generally driven by activating mutations in the *KRAS* proto-oncogene and is characterized by deregulation of several genes, including mucins (96, 97). In a tumor setting, the membrane-tethered glycoprotein MUC1 becomes overexpressed and aberrantly glycosylated in more than 80% of human PDACs and in 100% of metastatic lesions (96). MUC1 plays an important role in the development and progression of PDAC and other cancers and is a major marker for poor prognosis (98-102). Importantly, while the role of MUC1 in VSV infection or OV therapy has never been studied before, the *O*-linked carbohydrates of MUC1 purified from human breast milk can inhibit poxvirus (106), HIV (107, 117), and rotavirus (108), and MUC1 expression can block adeno-associated virus attachment (109).

OV therapy is an emerging therapeutic approach largely based on defects in the innate immunity of cancer cells or other abnormalities that increase cancer cell susceptibility to viral infection and virus-mediated death compared to healthy cells. VSV, a prototypic nonsegmented negative-strand RNA virus, has shown promising results against an array of cancers in preclinical studies (51) and is currently in a phase I

clinical trial against hepatocellular carcinoma (trial NCT01628640). The undesirable natural neurotoxicity of WT VSV has been addressed by the generation of various VSV-based recombinants retaining their oncolytic activities but lacking neurotoxicity (51).

One such oncolytic recombinant, VSV-ΔM51-GFP, has a deletion of the methionine at amino acid position 51 of the VSV M protein, as well as a green fluorescent protein (GFP) open reading frame (ORF) inserted in position 5 of the viral genome (66). The ΔM51 mutation improves VSV oncoselectivity by preventing WT M protein's ability to shut down cellular gene expression (67-69). Therefore, VSV-ΔM51-GFP is unable to successfully replicate in healthy cells with intact type I IFN responses. However, as many cancer cells are believed to have defective type I IFN signaling (118), they remain susceptible to VSV-ΔM51-GFP infection.

Our recent studies analyzed several VSV recombinants in an array of human PDAC cell lines *in vitro* (104, 105) and in xenografts in athymic mice (105). These studies demonstrated excellent abilities of VSV recombinants to infect and kill a majority of tested human PDACs and revealed that intact type I IFN signaling in some PDACs was responsible for their resistance to OV therapy (104). However, tumors in immunocompetent animals generate additional challenges for viruses, including the potential elimination of viruses before complete tumor killing can occur. Here, VSV was evaluated for the first time in an immunocompetent mouse PDAC model. This system is based on xenografts of murine PDAC cells originating from mice with spontaneous KRAS^{G12D}-driven PDACs (referred to as KC) either expressing human MUC1 (KCM cells) or MUC1 null (KCKO cells) (Figure 7) and thus allows for study

of OV therapy in the context of MUC1 overexpression or lack of expression. This system can also be used to study combinational therapies involving chemotherapeutics or other combinational therapies. Therefore, we also examined VSV-ΔM51-GFP in combination with gemcitabine, the standard drug for treatment of pancreatic cancer.
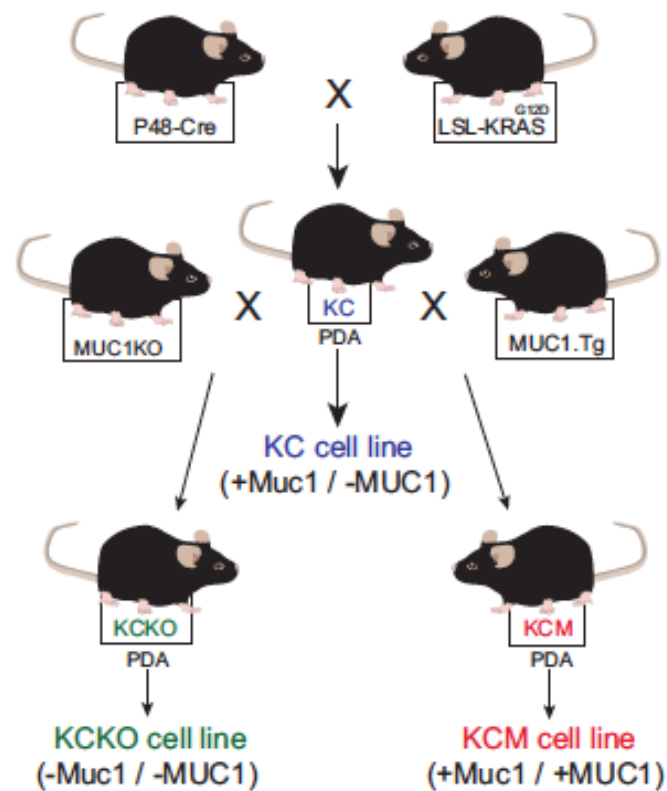
Figure 6: Mouse PDAC cell lines used in MUC1 study. KC mice producing KRAS^{G12D}-driven spontaneous PDACs (KC cells) were crossed with mice expressing human MUC1 (MUC1.Tg) or MUC1 null (MUC1KO) to generate the MUC1-positive KCM or MUC1-null KCKO cell lines, respectively (119). This illustration was created by Eric Hastie.

2.3 Materials and Methods

Cell Lines and Culture

The KC, KCM, and KCKO cell lines were generated from spontaneous CC tumors in the corresponding mice (Figure 6). KC mice were generated on the C57BL/6 background by mating the P48-Cre mice with the LSL-KRAS^{G12D} mice (120). We generated the KC cell line (in which only mouse Muc1 is expressed) for this study using spontaneous PDAC tumors from KC mice. The KCM and KCKO cells have been generated and characterized previously (98). The KCKO cells completely lack mouse Muc1 and human MUC1, while KCM cells express both mouse Muc1 and human MUC1. The murine cell line Panc02-Neo (transfected with neomycin empty vector) and Panc02-MUC1 (expressing full-length human MUC1) murine PDAC cell line were a generous gift from Tony Hollingsworth (University of Nebraska) (121). In addition, 4T1 (murine mammary carcinoma; ATCC CRL-2539) and BHK-21 (Syrian golden hamster kidney fibroblasts; ATCC CCL-10) were used to grow VSV and/or as controls for viral replication. KCKO, KCM, KC, Panc02-MUC1, Panc02-Neo, and 4T1 cells were maintained in Dulbecco's modified Eagle's medium (DMEM; with 4.5 g/liter glucose, l-glutamine, and sodium pyruvate; Cellgro), and BHK-21 cells were maintained in modified Eagle's medium (MEM; Cellgro). MEM was also supplemented with 0.3% glucose (wt/vol). All cell growth media were supplemented with 9% fetal bovine serum (FBS; Gibco), 3.4 mM l-glutamine, 90 units (U) per ml penicillin, and 90 µg/ml streptomycin (Cellgro). Cells were kept in a 5% CO_2 atmosphere at 37°C. The antibiotic G418 (30 mg/ml) was added to every other passage of Panc02-MUC1 and

Panc02-Neo to select for cells maintaining the vector. For all experiments, cell lines were passaged no more than 10 times.

Immunofluorescence

Cells were seeded in borosilicate glass chamber slides (Labtek catalog no. 155411) to be approximately 30% confluent in 24 h. Cells were washed with phosphate-buffered saline (PBS; Mediatech, Inc.) and then fixed with 3% paraformaldehyde (PFA) (Sigma-Aldrich) in distilled water (dH_2O) for 15 min. Cells were permeabilized with a solution containing 20 mM HEPES (pH 7.5), 300 mM sucrose, 50 mM NaCl, 3 mM $MgCl_2$, and 0.5% Triton X-100 on ice for 15 min, washed with PBS, and then blocked with 5% bovine serum albumin (BSA; Sigma-Aldrich) in PBS for 30 min, after which they were incubated with 1:100 HMFG2 antibody in 5% BSA at 4°C overnight. Cells were then incubated with secondary 1:100 anti-mouse-fluorescein isothiocyanate antibody (catalog no. sc-2010; Santa Cruz Biotechnology, Inc.) in 5% BSA for 2 h at room temperature and then stained with 1 μM Hoechst and 1 mg/ml wheat germ agglutinin. Cells were washed with PBS and used for confocal imaging.

Western Blotting

Cellular lysates and Western blots were prepared as previously described (104). For MUC1, polyvinylidene difluoride membranes were incubated with 1:2,000 Armenian hamster monoclonal anti-human MUC1 cytoplasmic tail (122), or 1:2,000 mouse HMFG2 monoclonal anti-human MUC1 (123) antibodies in Tris-buffered saline-Tween 20 (TBS-T) with 5% milk and 1% of 2% sodium azide. The HMFG2 antibody targets sparsely glycosylated variable-number tandem repeats within the human MUC1 extracellular domain. The CT2 antibody recognizes the last 17 amino acids

(SSLSYNTPAVAATSANL) of the cytoplasmic tail of human MUC1 (124). Neither antibody allows for efficient detection of murine Muc1; the presence of murine Muc1 could not be confirmed. In addition, the following primary antibodies were used in TBS-T with 5% BSA and 1% of 2% sodium azide: 1:5,000 rabbit polyclonal anti-VSV antibodies (raised against VSV virion proteins), 1:1,000 rabbit anti-MX1/2/3 (catalog no. sc-5059; Santa Cruz Biotechnology, Inc.), 1:3,000 mouse anti-GFP (catalog no. 600-301-215; Rockland). Also used were the following antibodies from Cell Signaling (1:1,000): anti-STAT1 (catalog no. 9172), Stat1-P (catalog no. 9171), and IRF3-P (catalog no. 4947). The following horseradish peroxidase (HRP)-conjugated secondary antibodies in TBS-T with 5% milk antibodies were used: 1:4,000 goat antibody against Armenian hamster (Santa Cruz Biotechnology, Inc.; catalog no. sc-2443), and 1:4,000 goat anti-mouse and 1:2,000 goat anti-rabbit (catalog no. 115-035-003 and 111-035-003, respectively; Jackson-ImmunoResearch). The Amersham ECL Western Blotting Detection kit (catalog no. RPN2106; GE Healthcare) was used for detection. Membranes were reprobed with mouse anti-actin antibody (clone C4) to verify sample loading (125).

Viruses

Recombinant wild-type VSV (VSV-rWT, Indiana serotype) (126) and VSV-ΔM51-GFP (66) were kindly provided by Jack Rose (Yale University), and VSV-GFP (45) was kindly provided by Asit Pattnaik (University of Nebraska). VSV stocks were prepared using BHK-21 cells infected at a multiplicity of infection (MOI) of 0.005 CIU (cell infectious units) and incubated at 37°C in MEM-based medium containing 5% FBS. Virus-containing medium was collected at 24 h postinfection (p.i.) and centrifuged

at 3,000 × g for 10 min at room temperature to remove large cellular debris. Virus was

purified by the method of Kalvodova et al. (127), with slight modifications. In brief,

clarified supernatants were underlaid with 5 ml 20% (wt/vol) sucrose in HEN buffer (10

mM HEPES [pH 7.4], 1 mM EDTA, 100 mM NaCl) and centrifuged at 28,000 rpm for

3.5 h at 4°C in a Beckman SW32 Ti rotor. The resulting viral pellet was resuspended in

HEPES buffered saline (HBS) (pH 7.5) (21 mM HEPES, 140 mM NaCl, 45 mM KCl,

0.75 mM Na_2HPO_4, 0.1% [wt/vol] dextrose) at 4°C overnight and then centrifuged in a

7.5 to 27.5% continuous gradient of Optiprep (Axis Shield) in HBS at 26.5×10^3 rpm

for 30 min at 4°C using a Beckman SW40 Ti rotor. The virus-containing band was

collected from the gradient, diluted with ET buffer (1 mM Tris-HCl, pH 7.5, 1 mM

EDTA), pelleted by centrifugation at 27,000 rpm for 1.5 h at 4°C using a Beckman

SW40 Ti rotor, then resuspended in PBS.

Cell Viability Assay

Cells (in triplicate) were seeded in 96-well plates so that they reached

approximately 80% confluence at 24 h and then were infected with VSV at an MOI of

0.001, 0.1, or 10 CIU/cell (based on titration on KCKO cells) or mock infected in

growth medium without FBS. Virus-containing medium was aspirated 1 h p.i. and

replaced with growth medium containing 5% FBS. Virus replication was measured by

GFP fluorescence readings approximately every 12 h p.i. for 5 days (CytoFluor Series

4000, with excitation filter of 450/20 nm, emission filter of 530/25 nm, and gain of 63;

Perseptive Biosystems). Cell viability was analyzed 120 h p.i. by a 3-(4,5-dimethyl-2-

thiazolyl)-2,5-diphenyl-2H-tetrazolium bromide (MTT) cell viability assay (Biotium).

Type I IFN Sensitivity

Cells were seeded in 24-well plates so that they reached approximately 80% confluence at 24 h. Cells were mock treated or treated with 5,000, 15,000, or 30,000 U/ml human IFN-α (catalog no. 407294; Calbiochem) in growth medium containing 5% FBS. Twenty-four hours post treatment, the cells were infected with serial dilutions of VSV-ΔM51-GFP, and infectious foci were counted at 12 h p.i. by fluorescence microscopy. Treatments and infections were performed in duplicate.

Plaque Reduction Neutralization Test

BHK-21 cells were seeded in 96-well plates to reach confluence in 24 h. Mouse serum was first diluted 1:20 to 1:40,960 for analysis. VSV-ΔM51-GFP stock diluted 1:32,000 (a dilution determined to produce approximately 50 infectious foci per well) was incubated with the serum dilutions for 1 h at 37°C. Serum/virus dilutions were then used to infect cells for 1 h at 37°C, rocking every 10 min. Serum/virus dilutions were removed and the cells overlaid with growth media with 5% FBS and 1% Bacto agar. Foci were counted by fluorescence microscopy at 16 h p.i. Antibody dilution titers were calculated as the inverse of the serum dilution resulting in one-half of the number of foci obtained with VSV-ΔM51-GFP alone. All serum samples were tested in triplicate.

Detecting Antibodies Generated Against KCM Cells

KCM cells were seeded in 96-well plates to reach confluence in 24 h. Cells were fixed and permeabilized as described above. Cells were blocked with 5% BSA in PBS for 20 min at room temperature and then incubated with mouse serum dilutions as prepared for the plaque reduction neutralization assay, but without incubating with virus, overnight at 4°C. Cells were washed with PBS and then incubated with peroxidase-conjugated goat anti-mouse IgG antibodies (1:300; Jackson

ImmunoResearch) for 1 h. For detection, cells were washed with PBS and then incubated with o-phenylenediamine (OPD; Thermo Scientific) for 15 min. OPD was inactivated by addition of 2.5 M sulfuric acid. Optical density was read at 490 nm. All serum samples were tested in triplicate.

MUC1.Tg Mice

Mice were handled and maintained under veterinary supervision in accordance with the University of North Carolina at Charlotte Institutional Animal Care and Use Committee (IACUC) approved protocol. All experiments were conducted using MUC1.Tg mice (Fig. 3). Previously generated and characterized MUC1.Tg mice (inbred CS7BI/6 background) express human MUC1 under its own promoter and in a tissue-specific manner, and these mice exhibit T and B cell tolerance when immunized with human MUC1 antigen, making it a relevant model to study (128). For genotypic confirmation, DNA from MUC1.Tg mice was isolated from tail clippings when mice were 11 to 17 days old and analyzed by PCR. Primers used for identification of MUC1-positive MUC1.Tg mice were 5′-CTTGCCAGCCATAGCACCAAG-3′ and 5′-CTCCACGTCGTGGACATTGATG-3′. Genotype was confirmed by the presence of a 340-bp amplification product seen on 1% agarose gels (129).

In vivo Treatment of Tumors with VSV-ΔM51-GFP

All cell lines used in animal experiments were negative for an extended panel of pathogens as tested by Charles River Laboratories. For the short-term *in vivo* efficacy study, 16- to 18-week-old male MUC1.Tg mice ($n = 29$) were injected in the right flank with 1×10^6 KCM in 100 μl of PBS. Mice were palpated for tumor formation starting on day 5 post-tumor injection (p.t.i.) and then randomly divided into 5 groups: PBS,

VSV-ΔM51-GFP, UV-killed VSV-ΔM51-GFP, VSV-ΔM51-GFP + gemcitabine, and gemcitabine alone ($n = 6$ per group, $n = 5$ for UV-killed VSV-ΔM51-GFP). At 5 days p.t.i., mice were treated once with a single intraperitoneal (i.p.) injection of either 50 μl PBS or gemcitabine (50 mg/kg of body weight) dissolved in 50 μl PBS. On days 7, 9, and 11 p.t.i., the PBS and gemcitabine groups received intratumoral (i.t.) administration of either 50 μl PBS or 1×10^8 CIU in 50 μl PBS (based on BHK-21 titer) of infectious VSV-ΔM51-GFP or UV-killed VSV-ΔM51-GFP. The same amounts of particles for infectious VSV-ΔM51-GFP or UV-killed VSV-ΔM51-GFP were used (based on virus titration prior to UV-mediated inactivation of the killed virus). Tumor size was monitored by caliper measurements every day until day 12 and every other day afterward. Body weight was measured once weekly. Tumor volume was calculated according to the following formula: volume in mm^3 = [length in cm × (width in cm)^2]/2. Mice were sacrificed 18 days p.t.i., at which time the animals showed no clinical signs indicating severe morbidity. To conduct a survival study using VSV-ΔM51-GFP against KCKO and KCM tumors, 8- to 11-week-old MUC1.Tg male mice were subcutaneously injected in the flank with either 1×10^6 KCM or KCKO cell lines in 100 μl of PBS ($n = 8$ each). Mice were palpated for tumor formation starting at 5 days p.t.i. and then were randomly divided into 2 groups per cell line ($n = 4$ per group). One group per cell line served as a control and received i.t. administration of 50 μl PBS on days 8, 10, and 12 p.t.i. The other group received i.t. administration of VSV-ΔM51-GFP on days 8, 10, and 12 p.t.i. with an initial dose of 7.2×10^7 CIU in 50 μl PBS (based on BHK-21 titer) followed by two doses of 4.3×10^7 CIU in 50 μl PBS. Tumor size was monitored by caliper measurements every other day, and body weight was measured once weekly.

Tumor volume was calculated according to the following formula: volume in mm^3 =

[length in cm × (width in cm)^2]/2. Mice were sacrificed when the length or width of the

tumor reached 1.5 cm, the tumors became ulcerated, or the mice presented with clinical

signs indicating severe morbidity. Data were analyzed using GraphPad software and are

expressed as means ± standard errors of the means (SEM). Comparison of groups was

done by two-way analysis of variance (ANOVA) only when the groups had the same

number of animals (*, $P < 0.05$; **, $P < 0.01$; ***, $P < 0.001$).

Analysis of Tumor Samples

Tumors were isolated at sacrifice and sectioned for analysis. One section was

used to make tissue homogenate to check for the presence of viral RNA or infectious

virus. Homogenized tumor sections were prepared in DMEM using a tissue

homogenizer and then centrifuged at 13,000 rpm for 10 min at 4°C to remove large

cellular debris. RNA was extracted from the supernatant using the Quick-RNA

MiniPrep Kit (Zymo Research). RNA was reverse transcribed using random hexamers

and SmartScribe reverse transcriptase (Clontech). The resulting cDNA was PCR

amplified using the primers VG31, 5′-CCCAATCCATTCATCATGAGTTCC-3′, and

VG32, 5′-CACTTCATAGTGACGCGTAAACAG-3′, which bind part of the intergenic

region on either side of the VSV M gene. PCR was conducted for 35 or 40 cycles with

an annealing temperature of 55°C. PCR products were electrophoresed on a 2% agarose

gel stained with ethidium bromide and visualized using a GelDoc-It imager (UVP

Imaging, Upland, CA). A second tumor section was used to make tissue lysates for

Western blot analysis. Western blot detection was performed with tumor lysates, using

1:5,000 rabbit polyclonal anti-VSV antibodies (raised against VSV virions), 1:1,000

anti-VSV N antibodies, or 1:1,000 anti-VSV G antibodies. A third tumor section was

formalin fixed and paraffin embedded and analyzed by hematoxylin and eosin (H&E)

staining and by immunohistochemistry (IHC). IHC was performed to look for the

presence of VSV N and G proteins (antibody dilution, 1:50).

<div align="center">Statistical Analysis Software</div>

All statistical analyses were performed using GraphPad Prism, version 5.0c for

Mac OS X (GraphPad Software, San Diego, CA).

2.4 Results

<div align="center">Susceptibility of Murine PDAC cells to VSV</div>

The immunocompetent model of PDAC described in this study can be used with

various mouse PDAC cell lines either expressing human MUC1 or MUC1 null. VSV

has never been tested (*in vitro* or *in vivo*) against any mouse PDAC cells before. Our

previous study with human PDAC cells in athymic nude mice showed very good

correlation between the oncolytic efficacy of VSV-ΔM51-GFP *in vitro* and *in vivo*

(105). Therefore, we wanted to test first *in vitro* if VSV can infect and kill such PDAC

cell lines and whether oncolytic efficacy of VSV would be negatively affected by

MUC1 overexpression in PDAC cells. The first set of cell lines, KC, KCKO, and KCM

(Figure 7), originate from spontaneous PDACs expressing or lacking the human

(MUC1) and/or mouse (Muc1) mucin 1 gene (129, 130). KC cells express murine Muc1

while KCM cells express both murine Muc1 and human MUC1, and KCKO cells lack

mucin 1 expression from either species. MUC1 expression in KC, KCKO, and KCM

cells may not be the only difference between these cell lines, as an accumulation of

additional mutations is likely during spontaneous PDAC formation. Therefore, in

addition to these cell lines, we also tested two isogenic cell lines, Panc02-Neo and Panc02-MUC1, which should differ only in their human MUC1 expression profile and were previously characterized in detail (121, 131). The MUC1 expression phenotypes of these five cell lines were confirmed by Western blotting and immunofluorescence (Figure 9) as well as flow cytometry (data not shown).

The major focus of our study was the recombinant VSV-ΔM51-GFP retaining its oncolytic abilities without the neurotoxicity associated with WT-like VSV (132, 133). In addition, the insertion of a GFP gene at position 5 of the VSV-ΔM51-GFP genome allows for monitoring of virus replication and spread based on VSV-driven GFP expression (66). To examine if the ΔM51 or GFP insertion would have any effect on the oncolytic abilities of VSV-ΔM51-GFP, our initial *in vitro* experiments included the VSV-GFP recombinant (similar to VSV-ΔM51-GFP but encoding WT M) and VSV-rWT (lacking either modification) for comparison. To analyze the ability of viruses to infect and kill the described mouse PDAC cell lines *in vitro*, the cells were mock infected or infected at increasing MOIs: 0.001, 0.1, or 10 CIU/cell (MOI values were calculated based on the titration of viruses on KCKO cells, so the same amounts of infectious particles were added to each cell line). Virus replication was monitored by GFP fluorescence readings (for VSV-ΔM51-GFP and VSV-GFP) taken approximately every 12 h. Cell viability was determined using an MTT assay performed at 120 h p.i. As shown in figure 10, both VSV-rWT and VSV-GFP killed all cells by 120 h p.i. VSV-GFP behaved similarly to VSV-rWT, which is in agreement with previous reports indicating that insertion of the GFP gene into VSV-rWT produced a virus with similar oncolytic ability (134-136).

Both GFP expression and cell viability assay indicated that VSV-ΔM51-GFP

was less effective in KCM and Panc02-MUC1 at an MOI of 0.001 and in Panc02-Neo

at all tested MOIs (especially at MOIs of 0.001 and 1). This result could be
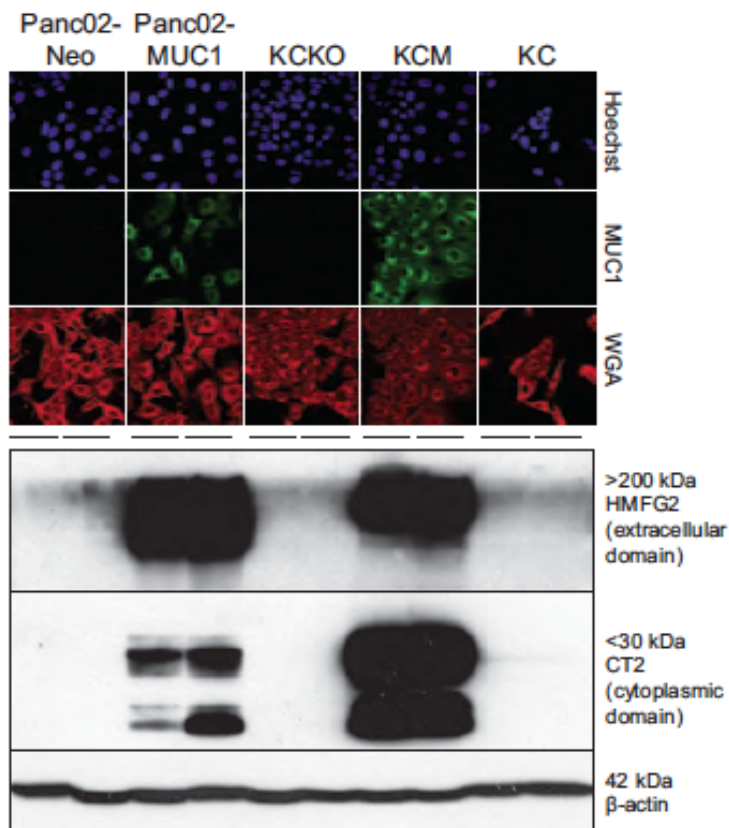
Figure 7: MUC1 expression profile of PDAC cell lines. For immunofluorescence (IF) analysis using confocal microscopy, cells were analyzed using HMFG2 antibody to detect the extracellular domain of human MUC1 and FITC-conjugated secondary antibody. Hoechst dye was used to stain for the nucleus, and wheat germ agglutinin (WGA) was used to stain the plasma membrane. For Western blot analysis, total cell lysates were separated by SDS-PAGE and then analyzed by Western blotting with HMFG2 antibody or CT2 antibody to detect the transmembrane domain of human MUC1. Western blotting using β-actin antibody was used as a loading control (119).
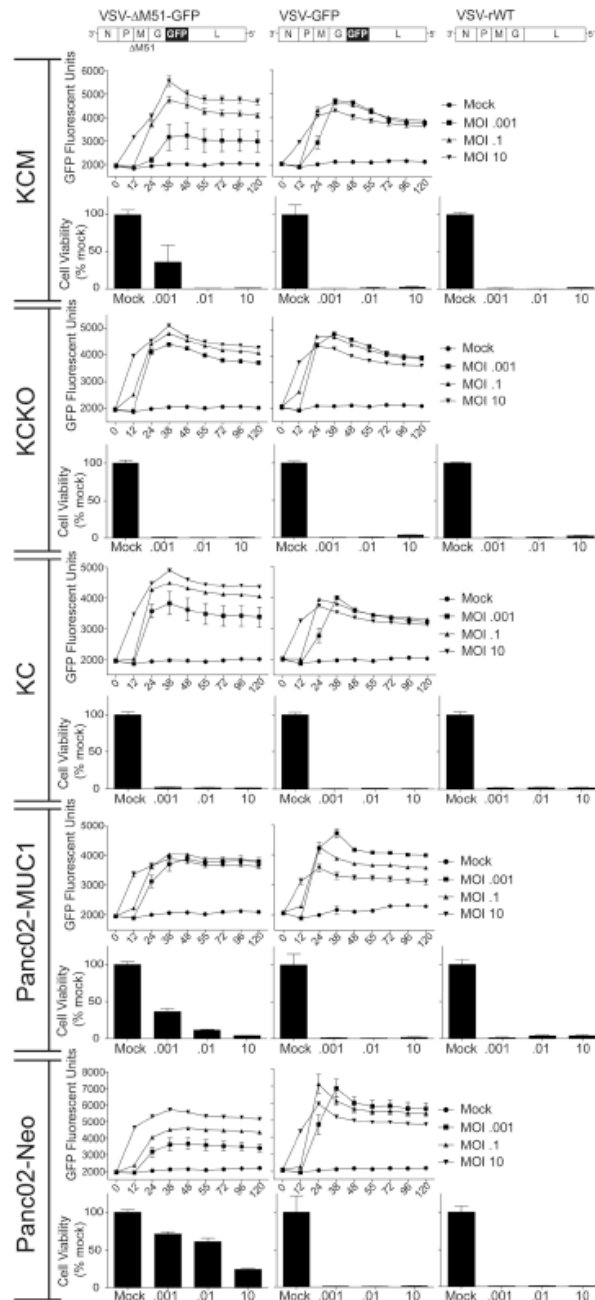
Figure 8: Mouse PDAC cell viability following infection with VSV recombinants. Cells were mock infected or infected with viruses at an MOI of 0.001, 0.1, or 10.0 CIU/cell based on their titration on KCKO cells. VSV-ΔM51-GFP and VSV-GFP replication-driven GFP expression was measured by CytoFluor GFP fluorescence readings at the indicated time points. Cell viability was analyzed 120 h p.i. by an MTT cell viability assay and is expressed as a percentage of mock-treated cells. All MTT assays were done in triplicate, and the data represent the means ± SEM (119).

explained by differences in the infectivity of this virus on these mouse PDAC cell lines. To test it, the titer of VSV-ΔM51-GFP stock was determined on all cell lines, and the oncolytic abilities of VSV-ΔM51-GFP correlated with its abilities to initiate infection in the tested cell lines (Figure 8). We hypothesized that if murine PDAC cells differ only in their initial susceptibility to infection, then virus replication would be different after the lower-MOI infection but similar when all cells are infected at a higher MOI. To test this hypothesis, multistep (MOI of 0.001 CIU/cell) and one-step (MOI of 5 CIU/cell) growth kinetics of virus replication were examined (Figure 9). As predicted, VSV-ΔM51-GFP was somewhat attenuated in KCM, Panc02-MUC1, and Panc02-Neo when cells were infected at the cell type-specific MOI of 0.001, but it replicated very similarly in all tested cell lines when they were infected at the cell type-specific MOI of 5 (Figure 9).

Type I IFN Signaling in Mouse PDAC Cell Lines

The observed attenuation of VSV-ΔM51-GFP (but not VSV-GFP) in KCM, Panc02-MUC1, and Panc02-Neo (at least at some tested MOIs) suggested that the M51 deletion in the M protein, rather than GFP insertion, was responsible for this attenuation. Because WT M protein prevents a robust innate antiviral response (the M51 deletion in M allows for nuclear export and translation of cellular mRNA), we hypothesized that intact (or residual) type I IFN signaling may play a role in the reduced susceptibility of KCM, Panc02-MUC1, and Panc02-Neo to VSV-ΔM51-GFP. This information is very important in predicting VSV success *in vivo*, as our recent analysis of a panel of human PDAC cell lines showed that responsiveness to IFN-α treatment and the expression of the IFN-stimulated gene (ISG) *MxA* could be predictive of

resistance to VSV-ΔM51-GFP *in vitro* as well as *in vivo* (104, 105). To test this hypothesis, all mouse PDAC cell lines were tested for their IFN responsiveness. Cells were mock treated or treated with three different concentrations of human IFN-α and analyzed for virus infectivity after the treatment. As controls, we used IFN-α-responsive BHK-21 and nonresponsive 4T1 cells. Unlike BHK-21 cells (which showed a 1,000-fold decrease in VSV-ΔM51-GFP infectivity following IFN treatment), none of the tested mouse PDAC cell lines mounted robust antiviral responses following IFN-α treatment (Figure 10). In addition, all cells were infected with VSV-ΔM51-GFP and cell lysates were collected at 4, 12, and 24 h p.i. Analysis of cell lysates indicated that the expression levels of Mx1, the murine version of human MxA, were similar for all cell lines and did not increase upon infection (Figure 10). However, while all of the cell lines were able to sense virus infection (as determined by phosphorylation of IRF3), phosphorylation of STAT1 was observed at 12 and 24 h p.i. in Panc02-MUC1 and Panc02-Neo only. Together, our results indicate that while none of the tested mouse PDAC cell lines have a robust type I IFN response, Panc02-MUC1 and Panc02-Neo demonstrated a limited antiviral response, which may explain their reduced susceptibility to VSV-ΔM51-GFP. A possible mechanism of VSV-ΔM51-GFP attenuation in KCM cells will be discussed below.

Efficacy of VSV-ΔM51-GFP *in vivo* in Immunocompetent Muc1.Tg Mice

Based on previous studies that demonstrated unacceptable neurotoxicity of VSV-rWT and VSV-GFP, we decided to conduct our *in vivo* experiments with VSV-ΔM51-GFP (59, 60, 137). We focused our initial experiment on mice bearing KCM tumors, given that MUC1-expressing tumors are more clinically relevant and more challenging.
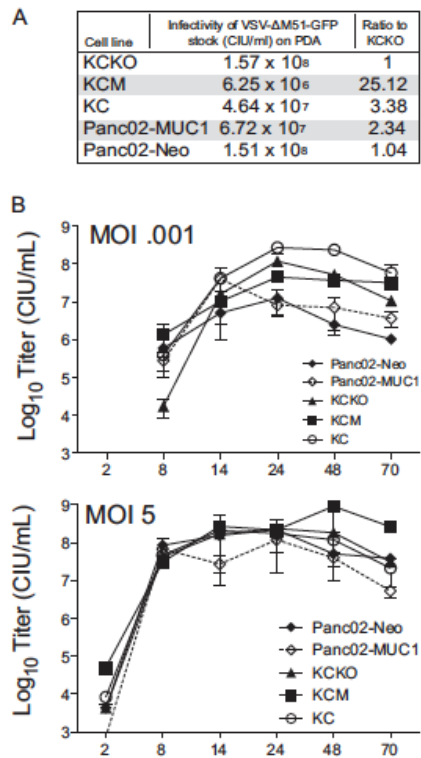
Figure 9: Infectivity and growth kinetics of VSV-ΔM51-GFP in mouse PDAC cells. (A) Serial dilutions of VSV-ΔM51-GFP were used to infect PDAC cell lines to calculate relative infectivity of this virus on tested cell lines. (B) For growth kinetics, cells were infected with VSV-ΔM51-GFP at a cell line-specific MOI of 0.001 or 5.0. At the times indicated, supernatant was collected, and virus titers were determined by plaque assay on BHK-21 cells. All infections were done in triplicate, and the data represent means ± SEM (119).

Previous comparative studies of KCM and KCKO cell lines *in vitro* and *in vivo*

demonstrated that KCM cells display a much more aggressive phenotype, evidenced by

an increase in invasiveness of KCM cells, an increase in proliferation, and deregulation

of the mitogen-activated protein kinase (MAPK) pathway (98). The efficacy of VSV-

ΔM51-GFP was compared to that of gemcitabine, the most common chemotherapeutic

used against pancreatic cancer (138). In addition, the efficacy of OV therapy alone was

also compared to combinational therapy ("chemovirotherapy") using both VSV-ΔM51-GFP and gemcitabine.

Subcutaneous injections of KCM cells were used to establish tumors in the flank of MUC1.Tg mice, which express human MUC1 under its own promoter and in a tissue-specific manner (128, 139). The MUC1.Tg mice exhibit T and B cell tolerance when immunized with human MUC1 antigen, making it a relevant model to study (128).

On day 5, when tumors were palpable, mice were treated i.p. with a single dose of gemcitabine (50 mg/kg in PBS) or PBS control. Depending on the group, tumors were injected i.t. with VSV-ΔM51-GFP, UV-killed VSV-ΔM51-GFP, or PBS on days 7, 9, and 11 (Figure 11). UV-killed virus was used as a control to determine whether viral replication was required for antitumor effects of VSV-ΔM51-GFP and if the presence of viral components alone without virus replication would affect tumor progression. Mice were monitored for signs of distress, and tumor size was measured daily for the first 8 days and then every other day afterward. Mice were sacrificed 18 days p.t.i., at which time the animals showed no clinical signs that would indicate severe morbidity. KCM tumors injected with PBS as a control continued to grow at a steady rate. In agreement with previously published data demonstrating resistance of KCM tumors to gemcitabine, tumor growth with gemcitabine alone was comparable to that observed with PBS treatment (140). Treatment with VSV-ΔM51-GFP alone and VSV-ΔM51-GFP plus gemcitabine showed a statistically significant reduction in tumor burden beginning on day 12 compared to PBS treatment (Figure 11). This significance was maintained until day 18, at which point the mice were sacrificed. The greatest
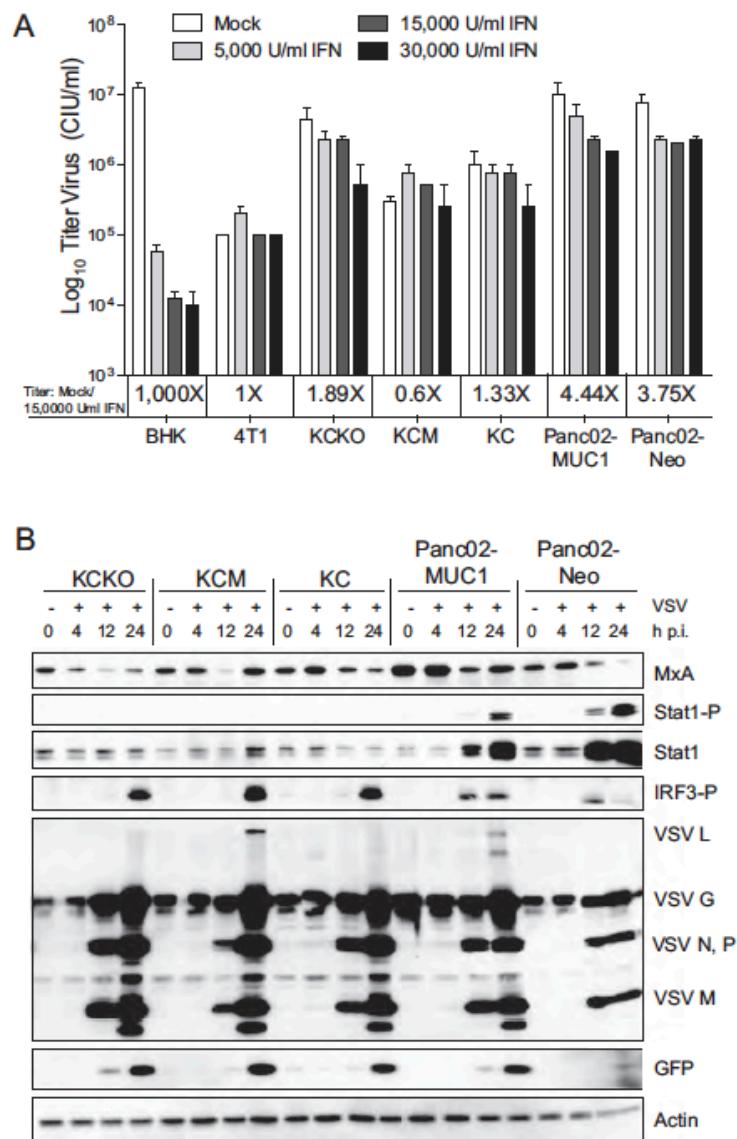
Figure 10: Type I IFN status of mouse PDAC cell lines. (A) Monolayer cultures of PDAC cells and control 4T1 and BHK-21 cell lines were mock treated or treated with 5,000, 15,000, or 30,000 U/ml human IFN-α in growth medium with 5% FBS. Twenty-four hours post treatment, the cells were infected with serial dilution of VSV-ΔM51-GFP, and the infectious foci were counted 12 h p.i. by fluorescence microscopy to calculate the virus titer. Treatments and infections were performed in duplicate; the data represent the means ± SEM. (B) Expression of cellular antiviral proteins and VSV-ΔM51-GFP proteins during infection. Monolayer cultures of cells were infected with VSV-ΔM51-GFP at a MOI[BHK-21] of 10.0. Total cell lysates were collected at the indicated time points. Lysates were separated by SDS-PAGE and then analyzed by Western blotting with antibodies to detect the indicated proteins. Western blotting using β-actin antibody was used as a loading control (119).

therapeutic effect was seen in the combinational therapy of VSV-ΔM51-GFP plus

gemcitabine, which showed a significant reduction in tumor burden compared to the use

of virus alone at day 18 (Figure 11). Surprisingly, KCM tumors injected with UV-killed

virus grew larger than the PBS control, with a significantly increased tumor burden on

days 16 and 18. It is unclear why UV-killed virus would result in enhanced tumor

growth, and we are planning to address this question in future studies.

Reduced tumor sizes in the groups containing infectious (but not inactivated)

VSV-ΔM51-GFP could be attributed to continued virus infection, replication, and

oncolytic action. Therefore, we hypothesized that if the virus was still replicating at the

endpoint within the tumor, then VSV infectious particles, proteins, or RNA could be

detectable. Tumor lysates were analyzed for the presence of infectious VSV-ΔM51-

GFP particles (using plaque assay on BHK-21 cells) and VSV RNA via RNA isolation,

cDNA synthesis, and PCR using VSV RNA-specific primers. In addition, a section of

each tumor was sliced and histologically stained for the presence of VSV proteins using

antibodies against VSV G and N proteins. In addition, another tumor section was used

to isolate total protein that was analyzed by Western blotting for antibodies against

different VSV proteins or GFP. Interestingly, despite the differences in the tumor

volumes in treatment groups, we were unable to detect VSV infectious particles by

plaque assay or VSV proteins by either IHC or Western blotting (data not shown). Only

when total RNA from tumor lysates was analyzed by reverse transcription (RT)-PCR

(35 or 40 cycles of PCR), 2 of the 6 VSV-ΔM51-GFP-treated mice and 4 of the 6 VSV-

ΔM51-GFP- plus gemcitabine-treated mice showed evidence of viral material in the

tumors (Figure 11). No viral RNA was detected in UV-killed VSV-ΔM51-GFP-treated

mice, suggesting that in the tumors treated with infectious virus, VSV replication took place at least at some point during treatment. Importantly, the products of RT-PCR, as shown in Figure 11, were sequenced, and all viral products retained the M51 deletion (data not shown).

While live VSV-ΔM51-GFP significantly reduced the KCM tumor burden up to 18 days following subcutaneous injections of cancer cells, OV therapy (alone or in combination with gemcitabine) did not abolish tumor growth (Figure 11). Therefore, we conducted a survival study to determine whether VSV-ΔM51-GFP treatment could result in a sustained antitumor effect (Figure 12). In this experiment, in addition to the more aggressive KCM-based model (MUC1 overexpression), we included KCKO-based tumors (MUC1 null). First, subcutaneous injections of KCM or KCKO cells were used to establish tumors in the flanks of MUC1.Tg mice. When tumors were palpable, mice were treated i.t. with PBS as a control or with VSV-ΔM51-GFP every other day for three treatments (days 8, 10, and 12) (Figure 12). Mice were monitored for signs of distress, and tumor size was measured every other day. Mice were sacrificed when tumor length reached 1.5 cm, tumors became ulcerated, or animals presented clinical signs indicative of morbidity. The results confirm that KCM is a more aggressive form of PDAC, with tumor growth greatly exceeding that of KCKO. VSV-ΔM51-GFP treatment of both cell lines temporarily delayed tumor growth compared to the control mice (Figure 12). For KCM, all control mice were sacrificed by day 20, with all animals being sacrificed by day 26. For KCKO, there was a significant decrease in tumor burden starting at day 12, which lasted through day 32, when significance could no longer be determined due to the need to sacrifice the control animals needed for comparison.

Figure 11: *In vivo* short-term efficacy of VSV-ΔM51-GFP against KCM tumors. (A) MUC1.Tg male mice, 16 to 18 weeks old, were subcutaneously (s.q.) injected with KCM cells in the right flank ($n = 30$). Tumors were established by day 5, and the mice were randomly divided into 5 groups ($n = 6$ per group). On day 5, mice were administered one dose of gemcitabine or PBS i.p. On day 7, treatments began with groups being administered 10^8 CIU VSV-ΔM51-GFP, UV-killed VSV-ΔM51-GFP, or PBS three times, on days 7, 9, and 11. Tumor size was monitored by caliper measurements, and tumor weight was calculated according to the standard ellipsoid formula: weight in grams = (length in cm × width^2)/2. Mice were sacrificed at day 18 p.t.i. Bonferroni *post hoc* tests compared all groups to PBS and VSV-ΔM51-GFP to VSV-ΔM51-GFP + gemcitabine (*, $P < 0.05$; **, $P < 0.01$; ***, $P < 0.001$; ##, $P < 0.01$). (B) At the endpoint (as indicated in panel A), tumor sections from each group were homogenized, and RNA was extracted from the supernatant. RNA was reverse transcribed, and the resulting cDNA was PCR amplified using the primers that bind part of the intergenic region on either side of the VSV M gene. PCR was conducted for 35 or 40 cycles, and samples were electrophoresed on a 2% agarose gel stained with ethidium bromide (119).

However, by day 34 control tumors and those treated with VSV-ΔM51-GFP reached similar sizes. Regardless of treatment, most KCKO tumors never grew as large as the KCM tumors. This observation is in agreement with previous studies in which mice bearing KCKO tumors present a less-challenging, more-stable form of PDAC disease as the cells grow at a lower rate than the more aggressive KCM cells (98).

Humoral Immune Response in Immunocompetent MUC1.Tg Mice at the Endpoint

While our *in vitro* and short-term *in vivo* results show promising oncolytic abilities of VSV-ΔM51-GFP against both KCM and KCKO cells, there is a clear indication that this treatment is not having a long-term, sustained anticancer effect. The design of our experiment did not allow us to look at early time points to assess intratumoral virus replication, oncolysis, and innate immune resources against VSV. However, premature inactivation of virus by the humoral immune response in an immunocompetent subject could negatively affect the efficacy of OV therapy. To determine the production of neutralizing antibodies against VSV-ΔM51-GFP, serum samples were examined from the KCM experiments in which all mice were sacrificed 18 days following KCM cell injection (Figure 13). Serial dilutions of mouse sera were first incubated with a known amount of VSV-ΔM51-GFP. The serum/VSV incubation was then used to infect BHK-21 cells for plaque assay analysis. In the VSV-ΔM51-GFP alone and VSV-ΔM51-GFP plus gemcitabine groups, it is evident that a strong humoral immune response was mounted against the virus (Figure 13). Importantly, much lower antibody levels were detected in sera from mice treated with UV-killed VSV-ΔM51-GFP, indicating that active virus replication was necessary for a robust humoral response.
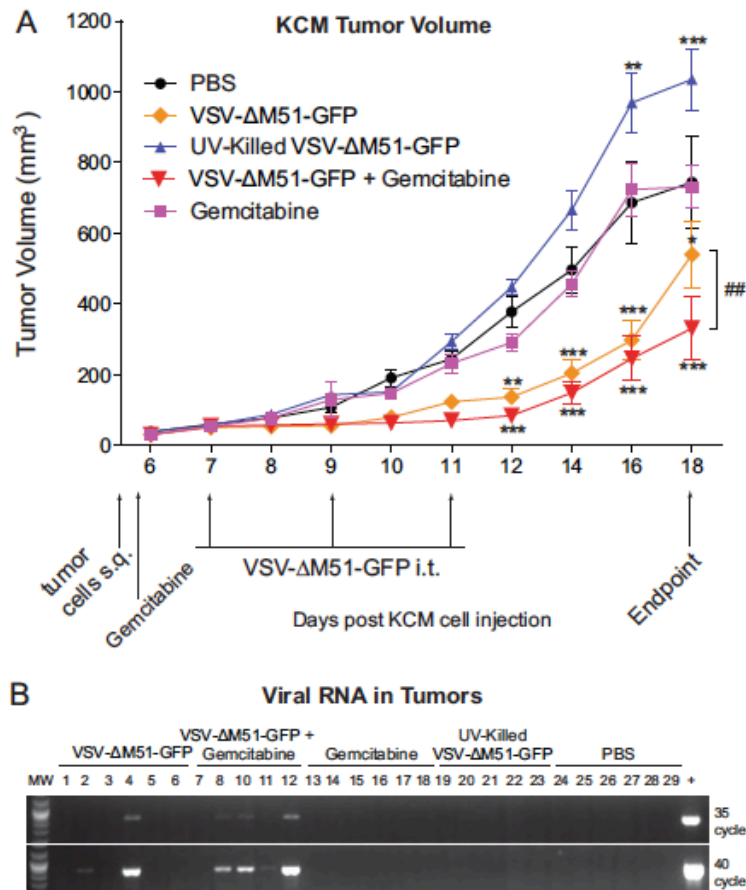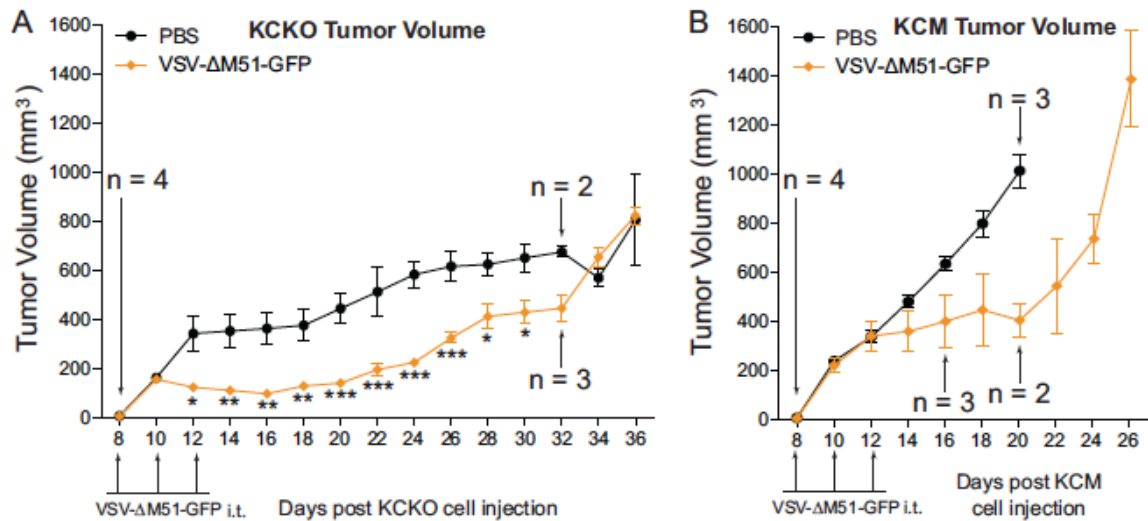
Figure 12: *In vivo* long-term efficacy of VSV-ΔM51-GFP against KCM and KCKO tumors. Male MUC1.Tg mice, 8 to 11 weeks old, were subcutaneously injected with KCM or KCKO cells in the right flank (*n* = 8 per group). Tumors were established by day 8, and then mice were randomly divided into 2 groups (*n* = 4 per group) per cell line. Mice were administered PBS or VSV-ΔM51-GFP i.t. on days 8, 10, and 12. Tumor size was monitored by caliper measurements, and tumor volume was calculated according to the standard ellipsoid formula: tumor volume = (length in cm × width^2)/2. Mice were sacrificed when the length of the tumor reached 1.5 cm, tumors became ulcerated, or mice presented clinical signs indicating morbidity. Comparison of groups was done using a 2-way ANOVA (time, treatment) only at the time points at which the groups had the same population (*, $P < 0.05$; **, $P < 0.01$; ***, $P < 0.001$) (119).
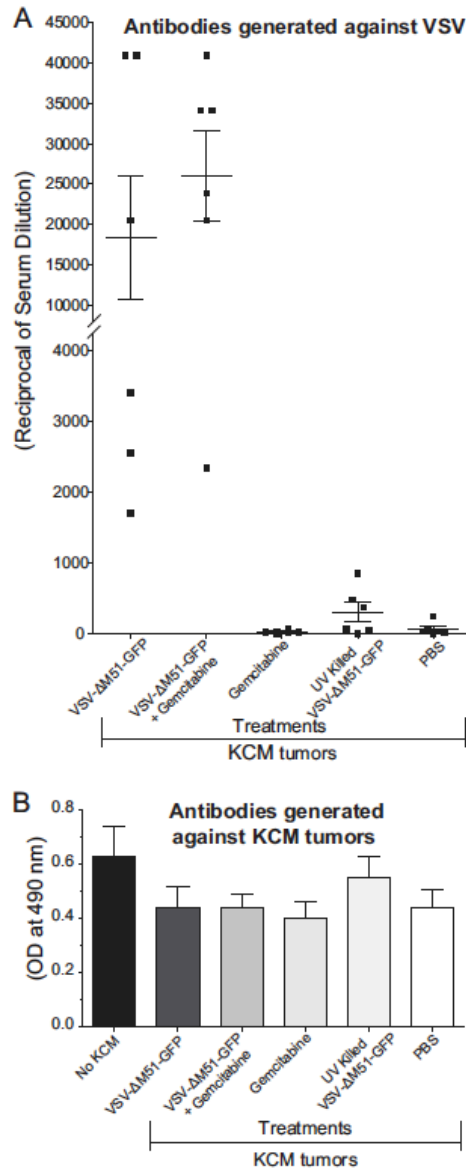
Figure 13: Humoral response against virus and cancer cells. (A) VSV-neutralizing antibody detection in mouse serum. Serum dilutions from all animals whose results are shown in Fig. 8 were incubated together with VSV-ΔM51-GFP and then added to BHK-21 cells. Infectious foci were counted by fluorescence microscopy at 16 h p.i. Antibody titers were determined to be the inverse of the dilution with one-half the number of plaques obtained with VSV-ΔM51-GFP alone. All serum samples were tested in triplicate. (B) KCM cell-specific antibody detection in serum. KCM cells were fixed, permeabilized, blocked in BSA, and incubated with dilutions of mouse sera. Detection was with HRP-conjugated secondary antibodies and the OPD substrate, and OD reading was done at 490 nm. All serum samples were repeated in triplicate, and the data represent means ± SEM (119).

The absence of a sustained antitumor response suggests that no effective humoral immune responses were mounted against the tumors following OV treatment. To test whether VSV-ΔM51-GFP treatment induced humoral responses against KCM tumors, mouse sera were analyzed for antibodies directed against KCM cells (Figure 13). KCM cells were fixed and permeabilized and then incubated with serial dilution of mouse sera from treated animals to detect KCM-specific antibodies. Results indicate that there was no significant difference in humoral response against KCM cells in any of the treatments compared to sera from mice that were never injected with KCM (Figure 13).

2.5 Conclusions

In the present study, for the first time, we tested VSV against mouse PDAC cells *in vitro* and *in vivo* and in a clinically relevant, immunocompetent mouse model of PDAC. VSV has never been tested in any immunocompetent model of pancreatic cancer. We have utilized a system that allows the study of oncolytic viruses (VSV or other OVs) in the context of MUC1 overexpression, as seen in approximately 80% of PDAC patients, or no expression (141, 142). Our data show that VSV can infect and kill all tested mouse PDAC cell lines *in vitro* and cause transient reduction of KCM and KCKO tumors *in vivo*.

Our study was focused on five mouse PDAC cell lines overexpressing MUC1 or MUC1 null, which could all be used in this immunocompetent model of PDAC. Although our main focus was on the performance of VSV *in vivo*, OV therapy success is generally dependent on the abilities of the virus to infect and kill cells, and our previous study with human PDAC cells in athymic nude mice showed very good

correlation between the oncolytic efficacy of VSV-ΔM51-GFP *in vitro* and *in vivo* (105). Therefore, in addition to *in vivo* experiments, we conducted a series of *in vitro* experiments to determine the abilities of VSV to infect, replicate, and kill these five mouse PDAC cell lines, as well as to examine cellular characteristics of these cell lines important for their susceptibility to OV therapy.

We were particularly interested in determining the ability of VSV to kill cancer cells overexpressing MUC1. MUC1 is overexpressed and aberrantly glycosylated in more than 80% of human PDACs and in 100% of metastatic lesions (96). It not only plays an important role in development and progression of PDAC and other cancers but also is a major marker of poor prognosis, and its expression often confers resistance of cancer cells to chemotherapeutics (98, 99, 101). In general, our data suggest that VSV is tolerant to the expression of MUC1, at least in the tested PDAC cell lines. The tolerance of VSV to MUC1 is a significant result. Although the role of MUC1 in oncolytic therapy has never been studied before, the *O*-linked carbohydrates of MUC1 purified from human breast milk can inhibit poxvirus (117), HIV (106, 107), and rotavirus (108), and MUC1 expression can block adeno-associated virus attachment (109). Although VSV-ΔM51-GFP was slightly less infectious in MUC1-expressing CM cells than in MUC1-null KCKO cells, the opposite could be seen in Panc02-based cell lines (Figure 10). Moreover, as VSV-rWT and VSV-GFP were not attenuated at all in KCM or Panc02-MUC1, our data suggest that VSV can successfully infect PDAC cells regardless of their MUC1 expression status.

We observed some variations in the susceptibility of different cell lines, specifically to VSV-ΔM51-GFP (but not VSV-rWT or VSV-GFP) infection and virus-

induced oncolysis. Specifically, VSV-ΔM51-GFP had reduced oncolytic ability in KCM, Panc02-MUC1, and Panc02Neo. The M51 deletion improves VSV oncoselectivity by preventing WT M protein's ability to shut down cellular gene expression (67-69). Therefore, VSV-ΔM51-GFP is unable to successfully replicate in healthy cells with intact type I IFN responses. Our recent analysis of a panel of human PDAC cell lines showed that responsiveness to IFN-α treatment and the expression of the IFN-stimulated genes could be predictive of resistance to VSV-ΔM51-GFP (104, 105). When cell lines were treated with type I IFN for 24 h prior to infection, some reduction, though modest, in virus infectivity was seen in Panc02-MUC1 and Panc02-Neo. Also, all cell lines were able to sense virus infection (as determined by phosphorylation of IRF3); however, where KCKO, KC, and KCM cell lines showed IRF3 phosphorylation at 24 h p.i., Panc02-MUC1 and Panc02Neo cells showed IRF3 phosphorylation as early as 12 h p.i. Additionally, only Panc02-MUC1 and Panc02Neo cells showed any detectable phosphorylation of STAT1 following VSV infection (indicative of type I IFN signaling). Together, our results indicate that while none of the tested mouse PDAC cell lines have robust type I IFN responses, Panc02-MUC1 and Panc02-Neo have limited antiviral signaling, which may explain their reduced susceptibility specifically to VSV-ΔM51-GFP.

At present, we cannot determine a mechanism for the somewhat low *in vitro* susceptibility of KCM cells to VSV-ΔM51-GFP compared to that of KCKO cells. However, it should be noted that MUC1 expression in KC, KCKO, and KCM might not be the only difference between these cell lines, as an accumulation of additional mutations is likely during spontaneous PDAC formation. Some of these mutations could

confer resistance of KCM cells to VSV-ΔM51-GFP (but not VSV-rWT or VSV-GFP) independently of MUC1 or type I IFN signaling.

We focused on KCM cells for our *in vivo* experiments because xenografts of KCM lead to more aggressive tumors than KCKO or KC and because most human PDAC patients exhibit MUC1 overexpression (96). Our *in vivo* data demonstrated that VSV-ΔM51-GFP significantly reduced the tumor burden in mice with subcutaneous KCM xenografts after 18 days. However, this effect was not sustained when mice were monitored for survival. Furthermore, a similar result was shown even for KCKO-derived tumors, which exhibit much slower tumor growth than do KCM-derived tumors (98).

Our previous *in vivo* study with human PDAC cells in athymic nude mice showed that cell lines that were susceptible to VSV-ΔM51-GFP-mediated oncolysis *in vitro* also showed a sustained antitumor response *in vivo* (105). Similarly, many other immunocompromised models using cell lines susceptible to VSV *in vitro* demonstrated a sustained oncolytic effect *in vivo*, including subcutaneous G62 glioblastoma tumors (143), SMT-91-01 rhabdoid tumors (144), and KU-7 orthotopic bladder tumors (145). Here, however, VSV-ΔM51-GFP demonstrated very good oncolytic activities against KCM and especially KCKO cells *in vitro*, but no long-term, sustained anticancer effect *in vivo*. The major difference between these studies is possible premature clearance of virus by the adaptive immune response in immunocompetent mice that could negatively affect the efficacy of OV therapy. Mice treated with "live" replicative virus (but not UV-killed virus) developed a robust antibody response directed at VSV-ΔM51-GFP. Previous studies also showed an immune response to VSV with an M mutation (VSV-

rM51R-M), with antibody titers being comparable to those seen against WT VSV (132). In the context of oncolytic therapy, one study showed a transient reduction of multiple myeloma and a significant antibody response generated against virus (146). Additionally, transient reduction of melanoma tumor burden and robust antibody response against VSV was seen even in a model where VSV was capable of only a single-cycle replication (145).

In addition to a humoral response to VSV (which peaks a week after infection), a negative role for innate immune responses to VSV has been demonstrated, with neutrophils (peak response at 36 h p.i.) (137) and natural killer (NK) cells (peak response, 3 to 4 days p.i.) (147) responsible for early-stage virus clearance (136, 147-149). A limitation of our study is that our experimental design did not allow for analysis of early time points, so we cannot rule out that these innate immune responses contributed to a limited efficacy of VSV-ΔM51-GFP *in vivo*.

Several approaches to inhibit host responses to VSV have been reported. Neutrophil and NK cell depletion as well as inhibitors of NK cell-activating chemokines greatly increased VSV spread and animal survival (136, 148, 149). Cell-based delivery seeks to use infected "Trojan horse" carrier cells, i.e., T cells that home to the tumor and deliver VSV without initial immune detection (150, 151). Additional methods to hide virus employ DNA aptamer technology (152) or pegylation of VSV (153) to shield the virus from neutralizing antibodies. Even more, a putative cotherapeutic like cyclophosphamide (CPA) was shown to suppress an immune response to virus (154), but one oncolytic study with mesothelioma showed reduced therapeutic efficacy of the VSV and CPA co-therapy (155).

In addition to premature immune clearance of virus, limited penetration and spread within the tumor mass were noted in several previous studies using VSV and other OVs, and this may also contribute to the limited antitumor effect of VSV in this study. While we did not conduct a time course analysis of VSV infection within tumors in mice, we were unable to detect VSV infectious particles or VSV proteins at the endpoint. Only when total RNA from tumor lysates was analyzed by RT-PCR was viral RNA detected in 2 of the 6 VSV-ΔM51-GFP-treated mice and 4 of the 6 VSV-ΔM51-GFP plus gemcitabine-treated mice (no viral RNA was detected in UV-killed VSV-ΔM51-GFP-treated mice). These results suggest possible limited replication and spread of the virus within tumor (in addition to immune clearance of VSV). Future studies will focus on the analysis of VSV replication following various VSV-ΔM51-GFP doses and administration protocols to determine the contributions of various factors to the limited antitumor effect of VSV in this study. Several approaches could be employed to address such limitations. For example, using VSV encoding suicide genes like HSV thymidine kinase (135) or cytosine deaminase (156, 157) enhanced the bystander effect and increased tumor regression compared to parental virus treatment. Penetration and spread of VSV within the tumor mass also were shown to be improved by incorporation of fusogenic proteins from Newcastle disease virus (158, 159) or simian parainfluenza virus (160) and resulted in enhanced tumor killing and prolonged survival compared to parental virus. Also, prolonged tumor exposure to virus and increased survival were reported when tumor vasculature was targeted, either by blocking arterial flow with starch microspheres (161) or reducing angiogenesis (162). Future experiments will test whether these approaches can improve tumor reduction and prolong survival as well as

allow us to assess intra-tumoral replication, virus spread, and direct oncolysis at earlier time points, which we were unable to address in this study.

Importantly, in this study, no humoral immune responses against tumor cells could be detected in any treatment group. This is consistent with the previous results that indicate tolerance of MUC1.Tg mice toward MUC1-expressing cells (128). It should be noted that a lack of antibody production against the tumor does not rule out that other antitumor immune responses were generated. Virus-induced long-term antitumor responses include increase in inflammatory cytokines, dendritic cell migration to lymph nodes, NK cell activation, and antitumor cytotoxic T lymphocytes (CTLs) (163). Specifically for VSV, increased infiltration of CTLs generated against virus and tumor epitopes, increased infiltration of B cells, interleukin-28 (IL-28) induction to promote NK cell activation, and downregulation of regulatory T cells were reported (164-171). As our study was limited only to antitumor antibody analysis (no detectable response), we cannot rule out activation of those other antitumor immune responses. However, even if such responses were generated, they were not potent enough to induce long-term antitumor effects.

Overall, the immunocompetent murine system described here is a clinically relevant model of PDAC to study oncolytic virotherapy against PDAC tumors (MUC1 positive or null) using OVs as a monotherapy or in combination with other treatments.

CHAPTER 3: ENGINEERING ONCOLYTIC VESICULAR STOMATITIS VIRUS
TO RESTORE P53 IN PANCREATIC CANCER CELLS

3.1 Abstract

Vesicular stomatitis virus (VSV, a rhabdovirus) has an inherent oncotropism and is being developed for clinical application against many malignancies. Human pancreatic ductal adenocarcinoma (PDAC) cell lines are highly heterogeneous in their susceptibility to VSV-mediated oncolysis. To identify cellular pathways where targeting may improve VSV oncotoxicity, we analyzed 11 human PDAC cell lines for mutations to 50 cancer-associated genes. All PDAC cell lines showed mutations in the tumor suppressor TP53, resulting in either absence of p53 protein expression or expression of a mutant p53. As the promise of clinical success using exogenous delivery of WT p53 has been limited, we engineered recombinant VSVs (rVSVs) to express human p53 or the novel p53-CC, which evades the dominant-negative activity of endogenous, mutant p53. Even more, we fused the p53 transgenes to a far-red fluorescent protein, eqFP650, to improve visualization. As p53 is known to enhance type I IFN antiviral responses in addition to cancer killing, it was important to determine if the transgene would attenuate VSV. Surprisingly, the oncolytic efficacy of VSV expressing p53 against 11 human PDAC cell lines *in vitro* is similar to the parental strain in all cell lines. Analysis of global gene expression suggests that the p53 transgene may inhibit type I IFN antiviral responses in cancer cells thereby preventing attenuation and making the virus a viable option for therapeutic use.

3.2 Introduction

We sought to generate a recombinant VSV expressing a transgene with enhanced oncolytic efficacy against PDAC. Analysis of genomic DNA of an array of 11 human PDAC cell lines for 50 common oncogenes and tumor suppressors identified several targets. Not surprisingly, mutations to the Kirsten Rat Sarcoma (KRAS) and TP53 genes were prevalent (Table 4). As p53 is a known tumor suppressor and other viral-based cancer therapies that restore WT p53 show promise, we chose to insert human TP53 into VSV-ΔM51 (115, 175-182). Specific to PDAC, mutations occur to the TP53 gene in more than 75% of patients and are shown to contribute to proliferation and even drive metastasis through gain of function activity (183) (184). Restoration of WT p53 activity has been reviewed extensively and is canonically known to induce cell-cycle arrest, apoptosis, and senescence. Additionally, more recently identified functions include regulation of metabolism and promotion of enhanced antiviral and antitumor immunity (112-114). What, if any, combination of these pathways in PDAC may be modified by the expression of human p53 from oncolytic VSV remains to be explored.

Previously murine p53 was inserted into the VSV genome and *in vivo* treatment of murine mammary adenocarcinoma metastases resulted in enhanced oncolytic efficacy in tandem with an increased antiviral response (115). However, this study did not look at global gene expression profiles to fully characterize a role for p53 in regard to VSV infection and did not consider improvements to therapy visualization. Importantly, to emphasize the need to study human p53 in oncolytic VSV, analysis of murine and human p53 response element consensus sequences suggests using caution

when generalizing about the similarity of regulation of the p53 pathway between

humans and rodents (185). Building on the work of (115), we inserted human p53 fused

to a far-red fluorescent protein into the VSV genome containing the ΔM51 mutation

(68, 186). Of note, most of the PDAC cell lines examined here are reported to express

p53 with dominant negative activity against WT p53 (IARC: http://p53.iarc.fr/) (Table

4). Because of this we also generated a recombinant VSV expressing the recently

described p53-CC (Figure 17) that replaces 216 nucleotides of the p53 C-terminus with

the coiled coil (CC) domain of the breakpoint cluster region (BCR) protein and evades

the dominant negative effect of endogenous mutant p53 (116), presumably providing a

stronger tumor suppressive response in the presence of mutant p53. As p53 expression

is known to be upregulated by type I IFN and in turn acts to enhance the antiviral

response (187), we analyzed the effect of virally expressed human p53 transgene

activity on PDAC cell lines, looked at global mRNA expression as well as determined if

any attenuation of virus replication impaired the oncolytic efficacy of the rVSVs.
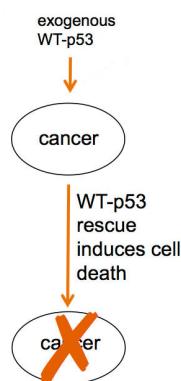
Figure 14: Scheme of p53 therapy. Addition of wild type p53 to a cancer cell is known to induce cell death through a variety of mechanisms. This illustration was created by Eric Hastie.
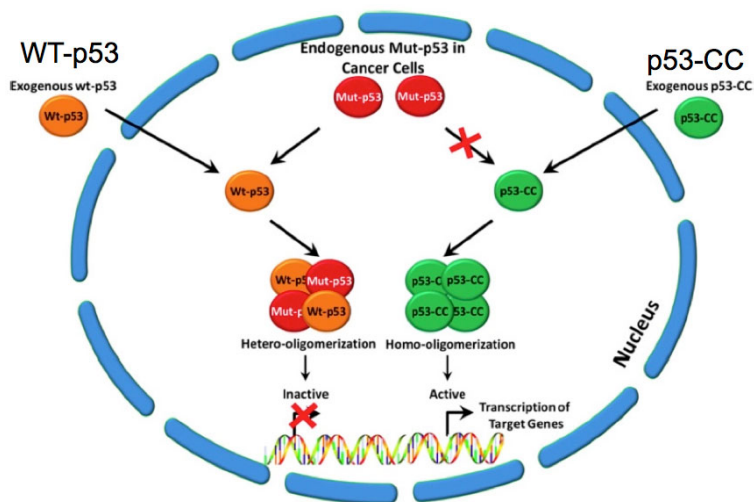
Figure 15: Scheme of p53-CC based therapy. The newly generated p53-CC by the Lim lab is able to evade the dominant negative, inhibitory action of endogenous, mutant p53. (Adapted from Okal, *et al*. 2013)

3.3 Materials and Methods

Cell Lines and Culture

The human PDAC cell lines used in this study were: AsPC-1 (ATCC CRL-1682), Capan-1 (ATCC HTB-79), Capan-2 (ATCC HTB- 80), CFPAC-1 (ATCC CRL-1918), HPAC (ATCC CRL-2119), HPAF-II (ATCC CRL-1997), Hs766T (ATCC HTB-134), MIA PaCa-2 (ATCC CRL-1420), Panc-1 (ATCC CRL-1469), Suit2 (188) and T3M4 (189). A non-malignant human pancreatic duct epithelial (HPDE) cell line (190) was used and maintained in Keratinocyte-SFM (K-SFM, Gibco). This cell line was generated by introduction of the E6 and E7 genes of human papillomavirus 16 into normal adult pancreas epithelium, retains a genotype similar to pancreatic duct epithelium and is non-tumorigenic in nude mice (190). In addition, the non-malignant

human pancreatic Nestin-expressing hTERT-HPNE (ATCC CRL-4023) was a gift from

Dr. Anirban Maitra (Johns Hopkins) and maintained in ATCC complete media (191).

The baby hamster kidney BHK-21 fibroblasts (ATCC CCL-10) were used to grow

viruses. Capan-1, CFPAC-1, HPAC, Hs766T MIA PaCa-2, Panc-1, and Suit2 cells were

maintained in Dulbecco's modified Eagle's medium (DMEM, Cellgro). AsPC-1,

Capan-2, and T3M4 cells were maintained in RPMI 1640 (HyClone). HPAF-II and

BHK-21 cells were maintained in modified Eagle's medium (MEM, Cellgro). All cell

growth media were supplemented with 9% fetal bovine serum (FBS, Gibco), 3.4 mM L-

glutamine, 900 U/ml penicillin and 900 mg/ml streptomycin (HyClone). MEM was

further supplemented with 0.3% glucose (w/v). K-SFM was never supplemented with

serum. Cells were kept in a 5% CO_2 atmosphere at 37^0C. PDAC cell lines were

passaged no more than 10 times.

Cell Line Oncogene Profiling by Next Generation Sequencing

The Ion AmpliSeq™ Cancer Hotspot Panel v2 Kit (Life Technologies) containing 207

primer pairs was used to perform multiplex PCR for the preparation of amplicon

libraries from genomic hot spot regions that are frequently mutated in human cancer

genes, including approximately 2800 Catalogue of Somatic Mutations in Cancer

(COSMIC) mutations of 50 oncogenes and tumor suppressor genes. Sequencing

libraries were prepared using an Ion AmpliSeq Library Kit (Life Technologies) per

manufacturer's instructions. Briefly, amplicons were ligated to Ion−compatible

adapters, followed by nick repair to complete the linkage between adapters and DNA

inserts. The libraries were clonally amplified by emulsion PCR on Ion Sphere Particles

(ISPs) using the Ion OneTouch 200 Template Kit (Life Technologies) as directed.

Following amplification, the template-positive ISPs were enriched to maximize the

number of sequencing reads produced using the Ion PGM Sequencing 200 Kit (Life

Technologies) on an Ion PGM™ Sequencer (Life Technologies) and Ion 314™ Chips

(Life Technologies). Raw data was transferred to the Ion PGM™ Torrent Server for

base calling, preprocessing 3' trimming, quality control and assessment, and mapping.

Variant calling and annotation was performed using Ion Reporter™ Software (Life

Technologies) and Ingenuity® Variant Analysis™ Knowledge Module (Ingenuity

Systems, Inc.) for Ion Reporter™.

Recombinant VSV Generation

Plasmids encoding VSV-XN2-ΔM51 (VSV-ΔM51, Indiana serotype) (126)

were kindly provided by Jack Rose (Yale University). A pUC57 plasmid encoding

eqFP650 (accession HQ148301; (192)) was ordered from Genscript with a T7 promoter,

N-terminal XhoI site, and Kozak sequence upstream of the eqFP650 start site

(TAATACGACTCACTATAGGGAGACTCGAGCCACCATG) and a modified C-

terminus that includes a BspEI site, two stop sites, and a NheI site

(CAGCTCCGGATAATAGCTAGC). Plasmids encoding GFP-p53 (12091 (193)) and

HA-tagged BCR (38189) were purchased from Addgene, Inc. Plasmids were amplified

in chemically competent JM109 Escherichia coli. Selection for colonies containing

VSV-rWT, VSV-ΔM51, or HA-tagged BCR plasmids was done with 50 μg/ml of

ampicillin and the GFP-p53 plasmid with 50 μg/ml of kanamycin. To generate VSV-

ΔM51-eqFP650, plasmids encoding VSV-ΔM51, and pUC57-eqFP650 were double

digested using XhoI and NheI restriction enzymes from New England Biolabs Inc.

(NEB) and gel purified (QIAGEN, gel extraction kit (28706)). The eqFP650 insert was

ligated into the VSV-ΔM51 plasmid using T4 DNA ligase (Promega, M180A). To

generate the p53 insert, the p53 sequence from the GFP-p53 plasmid was PCR

amplified using primers VG 283 and 284 (Table 2). To generate the TP53ΔODRD

insert, the TP53ΔODRD sequence from the GFP-p53 plasmid was PCR amplified using

primers VG 283 and 285. To generate the CC insert, the CC sequence from the HA-

tagged BCR plasmid was PCR amplified using primers VG 286 and 292. To generate

TP53-CC, the TP53ΔODRD sequence from the GFP-p53 plasmid was PCR amplified

using primers VG 283 and 293 and the CC sequence from the HA-tagged BCR plasmid

was PCR amplified using primers VG 288 and 292. The TP53ΔODRD and CC PCR

products were used for overlapping PCR along with primers VG 283 and 292. All

forward and reverse primers, except those used for overlap PCR contained a N-terminal

BspEI site and a C-terminal NheI site. The pUC57-eqFP650 plasmid and all PCR

products were digested sequentially with NheI and BspEI and ligated into the pUC57-

eqFP650 plasmid to generate pUC57-eqFP650-TP53wt, pUC57-eqFP650-

TP53ΔODRD, pUC57-eqFP650-CC, pUC57-eqFP650-TP53-CC. To create the pUC57-

eqFP650-TP53-CC/fs, the pUC57-eqFP650-TP53-CC plasmid was BspEI digested,

filled in with T4 DNA polymerase (NEB, MO203S), and ligated. All plasmids

containing the eqFP650-fusion genes were double digested with XhoI and NheI and

ligated into the VSV-XN2-ΔM51 plasmid using T4 DNA ligase. All plasmids were

sequenced to confirm the ΔM51 deletion and all gene insertions (Table 3). Recombinant

VSVs were rescued as was previously described (Lawson et al., 1995). Following virus

rescue, amplification, and purification, RNA was isolated and sequenced to confirm the

ΔM51 deletion and all gene insertions (Figure 17).

Table 2: Plasmids or oligonucleotides used to generate viruses in the p53 study

Plasmid /Primer name	Description / Nucleotide Sequence (5' to 3') [a]
pVSV-XN2-ΔM51	Full length VSV genome with ΔM51 mutation and XhoI and NheI cut sites
pT7-eqFP650	Custom order from Genscript: eqFP650 gene in pUC57 plasmid
pGFP-p53	Ordered from Addgene (12091) to clone the p53 gene (Boyd et al., 2000)
pHA-tagged Bcr	Ordered from Addgene (38189) to clone the CC domain of BCR
pEGFP-N3	Used for mammalian cell transfection; contains XhoI and XbaI cut sites
VG 283	(+) GAGATCCGGAATGGAGGAGCCGCAGTCA
VG 284	(-) GAGAGCTAGCTATTAGTCTGAGTCAGGCCCTTCTGT
VG 285	(-) GAGAGCTAGCTATTATGGTTTCTTCTTTGGCTGGGG
VG 286	(+) GAGATCCGGAATGGTGGACCCGGTGG
VG 292	(-) AGAAGCTAGCTATTACCGGTCATAGCTCTTCTTTTCCTTGG
VG 288	(+) TCGGGACTCAGGTCTCGTGTGATGGTGGACCCGGTGGGC
VG 293	(-) CACACGAGACCTGAGTCCCGATGGTTTCTTCTTTGGCTGGGG

Plasmid / PCR products(s)	Primer pairs	Used to generate [b]
pGFP-p53	VG 283 / VG 284	p53 PCR product
pGFP-p53	VG 283 / VG 285	p53ΔODRD PCR product
pHA-tagged Bcr	VG 286 / VG 292	CC PCR product
pGFP-p53	VG 283 / VG 293	p53ΔODRD overlap PCR product
pHA-tagged Bcr	VG 288 / VG 292	CC overlap PCR product
p53ΔODRD overlap / CC overlap PCR products	VG 283 / VG 292	p53-CC fusion PCR product

[a] (+) indicates primer has mRNA polarity, (-) indicates primer is complimentary to mRNA.

[b] PT7-eqFP650 and all PCR products were digested with BspEI / NheI then ligated together for amplification. All resulting plasmids were XhoI / NheI digested and ligated into the VSV-ΔM51-XN2 plasmid. All resulting plasmids were also ligated into XhoI / XbaI digested pEGFP-N3.

Table 3: Oligonucleotides to sequence TP53 and eq-FP650-fusion constructs

Gene name	Primer name	Nucleotide Sequence (5' to 3')[a]	Product size, bp	NIH GenBank accession number
Genomic p53	VG 268	(+) GGTTGCAGGAGGTGCTTAC	1900	NM_000546.5
	VG 269	(-) TGCCCCCTGATGGCAAATG		
Flanking VSV insert	VG 245	(+) CTCCGAGTTGGTATCCATCTTTGC	Construct dependent	N/A
	VG 246	(-) CAAGTACGTCATGCGCTCATCGGG		
eqFP650-p53 fusion (N terminus)	VG 245	(+) CTCCGAGTTGGTATCCATCTTTGC	Construct dependent	N/A
	VG 297	(-) CCGTCATGTGCTGTGACT		
eqFP650-p53 fusion (C terminus)	VG 296	(+) CGCTGCTCAGATAGCGAT	Construct dependent	N/A
	VG 246	(-) CAAGTACGTCATGCGCTCATCGGG		

[a] (+) indicates primer has mRNA polarity, (-) indicates primer is complimentary to mRNA.

Viruses Amplification

VSV stocks were prepared using BHK-21 cells infected at a multiplicity of infection (MOI) of 0.005 CIU (cell infectious units) and incubated at 37°C in MEM-based medium containing 5% FBS. Virus-containing medium was collected at 24 h post infection (h p.i.) and centrifuged at $4,000 \times g$ for 10 min at 40C to remove large cellular debris. Virus was purified by the method of Kalvodova et al. (194) with slight modifications. In brief, clarified supernatants were underlaid with 5 ml 20% (wt/vol) sucrose in HEN buffer (10 mM HEPES [pH 7.4], 1 mM EDTA, 100 mM NaCl) and centrifuged at 28,000 rpm for 3.5 h at 4°C in a Beckman SW32 Ti rotor. The resulting viral pellet was resuspended in HEPES buffered saline (HBS) (pH 7.5) (21 mM HEPES, 140 mM NaCl, 45 mM KCl, 0.75 mM Na_2HPO_4, 0.1% [wt/vol] dextrose) at 4°C overnight and then centrifuged in a 7.5 to 27.5% continuous gradient of Optiprep (Axis Shield) in HBS at 26.5×10^3 rpm for 30 min at 4°C using a Beckman SW40 Ti

rotor. The virus-containing band was collected from the gradient, diluted with ET buffer (1 mM Tris-HCl, pH 7.5, 1 mM EDTA), pelleted by centrifugation at 27,000 rpm for 1.5 h at 4°C using a Beckman SW40 Ti rotor, and then resuspended in PBS. Cell specific viral titers were obtained using the standard plaque assay.

Confocal Imaging for Virus-Expressed Transgene Localization

Cells were seeded in borosilicate glass chamber slides (Labtek, Cat. No. 155411) to be approximately 80% confluent in 24 h. Cells were infected with VSV at BHK MOI 15 CIU/cell or mock infected in growth medium without FBS. Virus-containing medium was aspirated 1 h post infection and replaced with growth medium containing 5% FBS. At 8 and 24 h p.i., growth media was aspirated and cells were stained with 1 μM Hoechst dye and HCS CellMaskTM (Life Technologies, H32714), 30 minutes. Growth media was aspirated, cells were washed 2x with PBS, then media with 5% FBS was added and cells were used for confocal imaging (Olympus FluoView 1000) using filters for DAPI (blue), FITC (green), and Alexa Fluor 568 (red).

Cell Viability Assay

Cells (in triplicate) were seeded in 96-well plates so that they reached approximately 80% confluence at 24 h. Cells were infected with VSV at BHK MOI of .001, 0.01, 0.1 or 1.0 CIU/cell or mock infected. Virus replication was measured by RFP fluorescence readings approximately every 12 h p.i. for 5 days (Cyto-Fluor Series 4000, with excitation filter of 590/20 nm, emission filter of 645/40 nm, and gain of 63; Perseptive Biosystems). Cell viability was analyzed at 24, 48, 72, or 96 h p.i. by a 3-(4,5-dimethyl-2-thiazolyl)-2,5-diphenyl-2H-tetrazolium bromide (MTT) cell viability assay (Cat. No. M2128, Sigma).

Gene Array Studies, RNA isolation, and Microarray Hybridization

Cells (in five repeats) were seeded in 6-well plates so that they reached approximately 80% confluence at 24 h. Cells were infected with cell line specific MOI 5 or mock infected. Cellular RNA was extracted with TRIzol^{TM} (Life Technologies) per the manufacturer protocol with slight modification. In brief, following the first phase separation, the aqueous layer was transferred to a new tube and 500 μl of TRIzol and 100 μl of chloroform were added and phase separation was repeated. Isolated RNA was run on a Bioanalyzer 2100 (Agilent) to check for purity (RIN values were >= 7). Three samples from each group were selected for microarray analysis. RNA samples were reverse transcribed, amplified and labeled using GeneAtlas® 3' IVT Express Kit (Affymetrix Inc). The resultant labeled complementary RNA (cRNA) was purified and fragmented as per vendor's instructions. The cRNA samples together with probe array controls were hybridized onto Affymetrix Human Genome U133+ Plus PM array strips which cover more than 47,000 transcripts and variants selected from GenBank®, dbEST, and RefSeq. Hybridization controls were spiked into the cRNA samples in order to monitor and troubleshoot the hybridization process. Probes for housekeeping genes were used to assess sample integrity. Hybridization, washing, staining and scanning were performed using Affymetrix GeneChip® system instruments. Affymetrix GeneAtlas® instrument control software version 1.0.5.267 was used to analyze microarray image data and to compute intensity values. Affymetrix .CEL files containing raw, probe-level signal intensities were analyzed using Partek Genomics Suite version 6.6.12.0713 (Partek). Robust multichip averaging (RMA) was used for background correction, quantile normalization and probeset summarization with median

polish (195). Statistical difference was calculated by two-way ANOVA analysis with a false discovery rate (FDR) rate of 0.05. Pathway analysis was performed using differentially expressed data 2-fold or higher with Ingenuity Pathway Analysis software (Ingenuity Systems Inc., Redwood City, CA, USA).

Western Blotting

Cells were seeded in 6-well plates so that they reached approximately 80% confluence at 24 h. Cells were infected with VSV at cell specific MOI 1 CIU/cell or mock infected. At 8 or 18 h p.i., protein was collected with cellular lysis buffer (0.0625 M Tris-HCl pH 6.8, 10% glycerol, 2% SDS, 5% 2-mercaptoethanol, 0.02% (w/v) Bromophenol blue). Ten μl of protein lysate was separated by electrophoresis on 10% or 14% SDS PAGE gels and electroblotted to polyvinylidene difluoride membranes. Membranes were blocked using 5% non-fat powdered milk in TBS-T [0.5M NaCl, 20 mM Tris (pH7.5), 0.1% Tween20]. The following antibodies from Cell Signaling Technology, Inc. were used: p53 (1:2,000; #2524) and Phospho-p53 (1:500; #2521). The following antibodies from Santa Cruz Biotechnology, Inc. were used: PARP-1 (1:500; #sc-25780), p21 (1:500, #sc-397), and MDM2 (1:500, #sc-965). In addition, the following primary antibodies were used in TBS-T with 5% BSA and 1% of 2% sodium azide: 1:5,000 rabbit polyclonal anti-VSV antibodies (REF?). The following horseradish peroxidase (HRP)-conjugated secondary antibodies in TBS-T with 5% milk antibodies were used: 1:4,000 goat anti-mouse and 1:2,000 goat anti-rabbit (catalog no. 115-035-003 and 111-035-003, respectively; Jackson-ImmunoResearch Laboratories, Inc.). The Amersham ECL Western Blotting Detection kit (catalog no. RPN2106; GE Healthcare) was used for detection.

3.4 Results

Genomic Analysis of PDAC Cell Lines Highlights PDAC Target Genes

Using an Ion AmpliseqTM Hotspot cancer panel, we analyzed an array of 11 PDAC

cell lines for common mutations to 50 oncogenes and tumor suppressors that may serve

as therapeutic target genes (Table 4). Mutant KRAS protein, a known initiation factor

for PDAC oncogenesis (196), was confirmed mutated in 10 of 11 cell lines.

Additionally, we identified mutations to the tumor suppressor TP53 in 8 of 11 cell lines.

PCR using primers complementary to introns flanking genomic TP53 exons 5 to 9

found that three cell lines (ASPC-1, HS766T, or HPAC) reported as having WT p53 by

the Ion Ampliseq^{TM} Hotspot cancer panel in fact had a TP53 frameshift, genomic

deletion, or uncommon TP53 mutation, respectively. This confirmed TP53 mutations in

11 of our 11 PDAC cell lines. These findings were compared to the International

Agency for Research on Cancer (IARC) TP53 Database (http://p53.iarc.fr/) database

and to literature describing the same cell lines (Table 4)(197-199). Though some of the

cell lines were identified as having TP53 mutations different from those the literature

reports, it remains the case that TP53 mutations exist in more than 75% of PDAC

patients as well as being prevalent in a majority of other cancers (183). Western blotting

also was done to look for p53 protein expression in the PDAC cell lines (Table 4).

Protein expression was not seen in PDAC cells with a TP53 frameshift or genomic

deletion, but was seen at varying levels in the remaining PDAC cell lines that are

known to have dominant negative or gain of function p53 mutants. Additional oncogene

or tumor suppressor mutations were identified, but none were as ubiquitous as KRAS

and TP53. As various methods of exogenous delivery of p53 result in reduction of

tumor burden (reviewed in (113), including oncolytic viruses (175) (177) (176) (178) (179) (180) (181) (115) (182), we focused on the TP53 gene in generating rVSVs.

Table 4: Next generation sequencing of PDAC cell line genomic DNA and TP53 profiling.

CELL LINE	FBXW7	KRAS	SMAD4	MET	ALK	BRAF	RBI	TP53
AsPC-1	x	x	x					
Hs766T		x						
HPAC		x						
T3M4		x						x
CFPAC		x						x
HPAF-II		x						x
Capan-1		x						x
MIA PaCa2		x						x
Capan-2					x	x		x
Panc-1		x					x	x
Suit2		x						x
HPDE			x					
HPNE								

CELL LINE	Ion Ampliseq	Sequencing PCR products	Reported*	Dominant Negative*	Transactivation Class*	Protein Expression
ASPC1	-	-	p.C135fs	p.R273H	-	-	-
HS766T	-	-	-	WT, pR181H	-	-	-
HPAC	p.G187R	p. P72R	p.G187R	WT	NA	Functional	-
T3M4	p.Y220C	p. P72R	p.Y220C	p.Y220C	Moderate	Non-functional	++
CFPAC	p.C242R	p. P72R	p.C242R	p.C242R	NA	Non-functional	+
HPAF-II	p.P151S	p. P72R	p.P151S	p.P151L	Moderate	Non-functional	-
Capan-1	p.R248W	-	p.R248W	p.A159V	Yes	Non-functional	+++
Mia-Paca 2	p.R248W	-	p.R248W	p.R248W, p.R273H	Yes	Non-functional	+++
Capan-2	p.R273H	-	p.R273H	WT, p.R273H	Yes	Non-functional	+++
Panc-1	p.R273H	p. P72R	p.R273H	p.R273H, p.V272A	Yes	Non-functional	+++
Suit2	p.R273H	p. P72R	p.R273H	p.R273H	Yes	Non-functional	++
HPDE	-	p. P72R	WT	NA	-	-	NA
HPNE	-	p. P72R	WT	NA	-	-	NA

*Data from IARC p53 Database (http://p53.iarc.fr/)

Table 4: Next generation sequencing of PDAC cell line genomic DNA and TP53 profiling. Genomic DNA was isolated from an array of pancreatic ductal adenocarcinoma (PDAC) cell lines and analyzed for mutations to 50 common oncogenes and/or tumor suppressors. TP53 was identified as a commonly mutated gene in PDAC and PCR analysis was done to confirm these findings. PCR products were sequenced and identified mutations not determined with next generation sequencing. These findings were compared to the http://p53.iarc.fr/ database, PDAC literature, and western blot was done to look for endogenous p53 expression in PDAC cell lines.

Generation of a new VSV recombinant for *in vivo* Visualization

Imaging of infection using current VSV-GFP or VSV-luciferase constructs is common in rodent models, but requires levels of expression that may not be attainable in human clinical studies (66, 135). To address a need for improved visualization of virus replication *in vivo*, we introduced a recently characterized far-red fluorescent

protein, eqFP650, into the VSV genome (192, 200). EqFP650 offers an improved *in vivo* fluorescent signal compared to current GFP, potentially providing better sensitivity of infection in a living system. We designed and rescued the recombinant VSV-ΔM51-eqFP650 (herein called M51-RFP) expressing the eqFP650 fluorescent protein (Figure 16). The M51-RFP virus was used as a parental genome to the recombinant VSVs described in the next section.
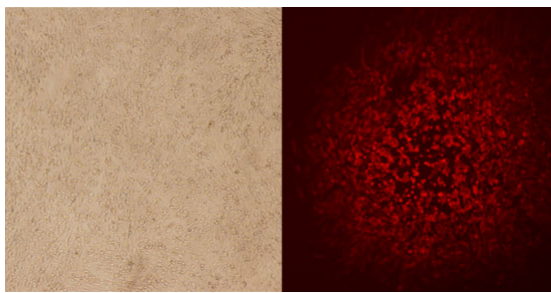
Figure 16. Generation of VSV expression eqFP650. Shcherbo et al. 2007 generated the eqFP650 far red fluorescent protein to improve whole-body imaging (left) (192). The eqFP650 protein was inserted into the VSV genome rescued viruses express RFP in infected cells, light and fluorescent microscopy (right).

Recombinant VSVs Express p53 Transgenes

Based on our genomic data and extensive literature that shows the therapeutic potential of rescuing WT p53 activity in cancer cells we chose to generate rVSVs expressing p53 proteins. However, exogenous delivery of p53 faces a major hurdle for use. Endogenous, mutant p53 in cancer cells can function as a dominant-negative to abrogate any therapeutic effect. To address this issue, we designed the recombinant VSV-ΔM51-eqFP650-TP53-CC (herein called M51-RFP-P53-CC) expressing the eqFP650-p53-CC fusion gene (Figure 17). This recombinant virus was based on work

by (116) that describes a chimeric p53-CC protein that evades endogenous dominant-

negative p53 and restores WT p53 activity better than WT p53 *in vitro* in human ductal

breast epithelial, human breast adenocarcinoma, human epithelial cervical

Figure 17. Engineering recombinant VSV and sequencing rescued viruses. Recombinant viruses were engineered using the VSV-ΔM51-XN2 backbone, with the transgenes inserted between the VSV G and L protein sequences using XhoI and NheI restriction sites. Virus genomes were amplified using JM109 E. Coli. then rescued in BHK cells using a reverse genetics system (Lawson et al., 1995). Viral genomes were purified and cDNA was made and sequenced to confirm the ΔM51 deletion and transgene insertion.

adenocarcinoma, and human non-small cell lung carcinoma cell lines. We designed all

of our constructs with the same parental genome, VSV-ΔM51-XN2, with the transgene

inserted between the VSV G and L protein sequences (Figure 17). As controls we,

designed viruses: 1) VSV-ΔM51-eqFP650-TP53WT (herein called M51-RFP-p53wt)

for comparison to M51-RFP-p53-CC, 2) VSV-ΔM51-eqFP650-TP53-CC/frameshift (fs)

(herein called M51-RFP-p53-CC/fs) where a frameshift creates an early termination to

prevent transcription of the p53-CC protein but allows for monitoring of any VSV

attenuation caused by the length of the inserted transgene, 3) VSV-ΔM51-eqFP650-

TP53ΔODRD (herein called M51-RFP-p53ΔODRD) that expresses p53, but without the

WT C terminus, and 4) VSV-ΔM51-eqFP650-CC (herein called M51-RFP-CC) that

expresses the CC domain of BCR alone. Viruses were rescued, amplified, and

sequenced to confirm the ΔM51 deletion as well as transgene insertion (Figure 17).

Protein profiles of purified virions were examined with a Coomassie blue-stained gel

and all viruses showed similar banding patterns to the parental virus (Figure 17).

Moreover, RT-PCR was used to confirm transgene inserts (Figure 18) and cellular

expression of the p53 transgenes. Viral proteins expression of p53 transgenes was

examined using Western blots (Figure 18).

<div style="text-align:center">Virally Expressed p53 Transgenes Localize to the Nucleus</div>

Previously Okal et al. showed nuclear localization of their novel p53-CC protein, but it

was unknown if this localization would occur when the protein was fused to eqFP650

and expressed from the VSV genome (116). The full length WT p53 contains three

nuclear localization signals (NLS) in the C terminus: amino acids 305-322, 370-376,

and 380-386. As p53-CC, generated by truncating WT p53 (removal of amino acids 323

to 393), still contains one NLS, fluorescent microscopy was used to confirm nuclear localization in Suit2 cells (Figure 18) as well as ASPC-1 and Mia-PaCa-2 (data not shown). Similar nuclear localization was seen for M51-RFP-p53wt, M51-RFP-p53-CC, and M51-RFP-p53ΔODRD in all cell lines examined. In the viruses encoding transgenes without any NLS, M51-RFP and M51-RFP-p53-CC/fs, localization remained cytoplasmic. Interestingly M51-RFP-CC showed punctate localization in the cytoplasm and may be of interest for future studies in regard to the function of the CC domain originating from the BCR gene.

<center>Efficacy of Virally Expressed p53 on VSV Replication in vitro</center>

As VSV with the M51 deletion is extremely sensitive to intact type I IFN signaling (201), (69, 202) and p53 is known to enhance the type I IFN response (187), it was important to determine if rescued p53 activity would attenuate VSV infection. Results based on infection at MOIs 0.1 and 0.001 (based on titer on BHK) for 4 PDAC cell lines, are: Mia-Paca 2 (highly susceptible), AsPC-1 and Suit2 (intermediate susceptibility), and Hs766T (highly resistant, not shown) and followed with MTT analysis. Thus, we did not see significant attenuation of any of the rVSVs generated for this study (Figure 19). Interestingly, while previous rVSVs used GFP expression as a correlative marker for virus replication and cell death (203), here, RFP readings did not parallel MTT results. Potentially, the nuclear localization of the p53 transgenes concentrates the RFP signal, making signal from RFP fused to p53 an inaccurate indicator of cell death (Figure 19). Importantly, based on MTT, in Suit2 and Mia-Paca 2 cells there is significantly more oncolysis by the rVSVs expressing p53 at 48 and 24 h p.i., respectively, compared to the parental strain that expresses eqFP650 only.

Moreover, when we focused on rVSVs expressing p53 or p53-CC in an expanded set of 11 PDAC cell lines, there was no significant virus attenuation in any of the cell lines (Figures 20). Additionally, we examined virus kinetics in Suit2 and Mia-Paca 2 and
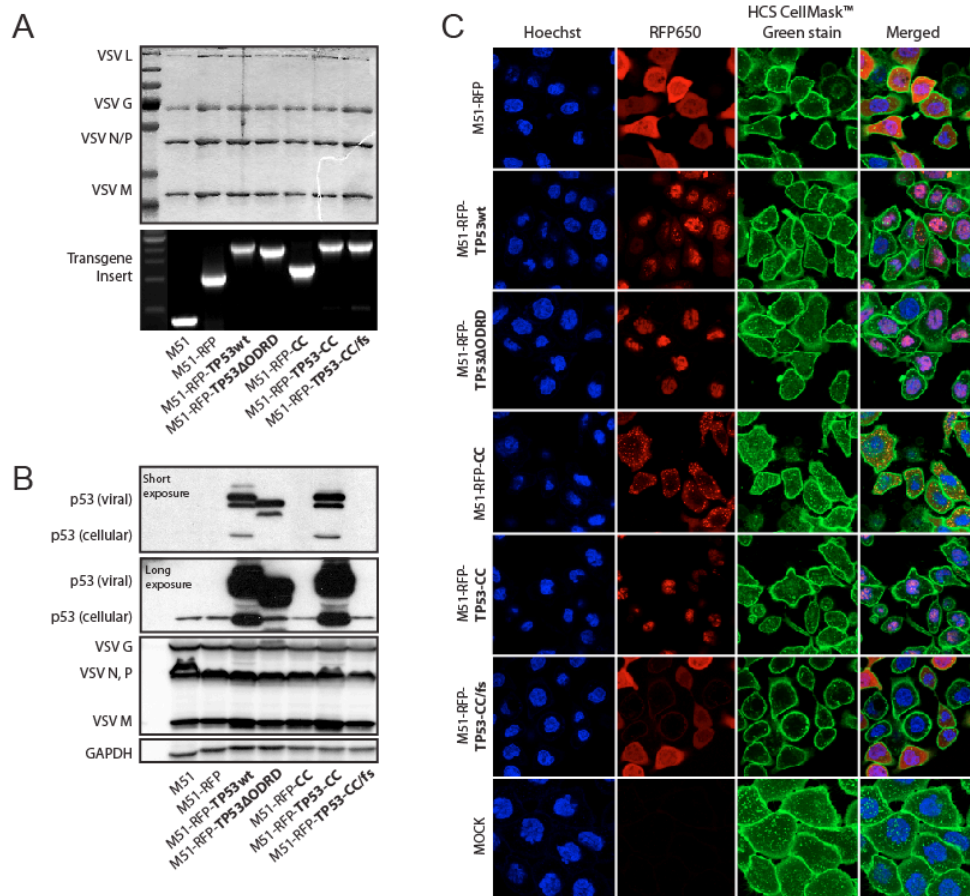
Figure 18. Recombinant virus protein profile and transgene expression and localization. (A) Recombinant viruses were amplified, purified, and run on an acrylamide gel and Coomassie stained to compare viral protein profiles. RNA was extracted from purified virus stocks and reverse transcribed into cDNA. Viral cDNA was PCR amplified using primer VG245 and VG246 to confirm transgene inserts. (B) Suit2 cells were infected at cell specific MOI 5 and lysed 8 h p.i. to look for expression of viral proteins as well as p53 transgenes. Long exposure of p53 blot shows endogenous p53 as well as virally expressed p53. (C) Suit2 cells were infected at cell-specific MOI 5 and stained with Hoechst nuclear stain (blue) and HCS CellMaskTM membrane stain (green) 8 h p.i. then used for fluorescent microscopy to detect transgene localization (red).

found no significant difference between viruses (Figure 21). This is in agreement with

the Heiber and Barber (115) results in murine mammary adenocarcinoma cells *in vitro*.

Importantly, the Heiber and Barber (115) study did show attenuation of VSV expressing

murine p53, but only *in vivo*, suggesting that VSV expressing p53 may infect differently

in an animal model.

<p align="center">Virally Expressed p53 Transgenes are Transcriptionally Active</p>

As no dramatic differences were seen between rVSVs in different cell lines, it was

unclear if the p53 transgenes were functional as transcription factors for p53 targeted

genes. Previously it was shown, on a murine p53 signaling pathway-specific DNA

microarray that VSV expressing murine p53 activates transcription of target genes

MDM-2 and p21 in mouse embryonic fibroblasts and murine mammary

adenocarcinoma TS/A cell lines (115). Our results, using human transcriptome mRNA

analysis, show that in Suit2 cells infected with M51-RFP-p53wt, upregulation of MDM-

2 and p21 transcripts compared to mock infections were 6.22-fold and 7.15-fold,

respectively, while in M51-RFP-p53-CC, upregulation of MDM-2 and p21 transcripts

compared to mock were 5.27-fold and 6.41-fold, respectively. Further, using the

Ingenuity p53 pathway analysis module, we examined changes in expression of many

additional p53 target genes associated with canonical p53 activity, including: apoptosis,

glycolysis, angiogenesis, autophagy, DNA repair, and the cell cycle. We identified up

regulation and repression (204) of many known p53 target genes summarized in Table

5. This data is suggests that p53 is functional, but interestingly not as part of an

infection-attenuating process *in vitro*.
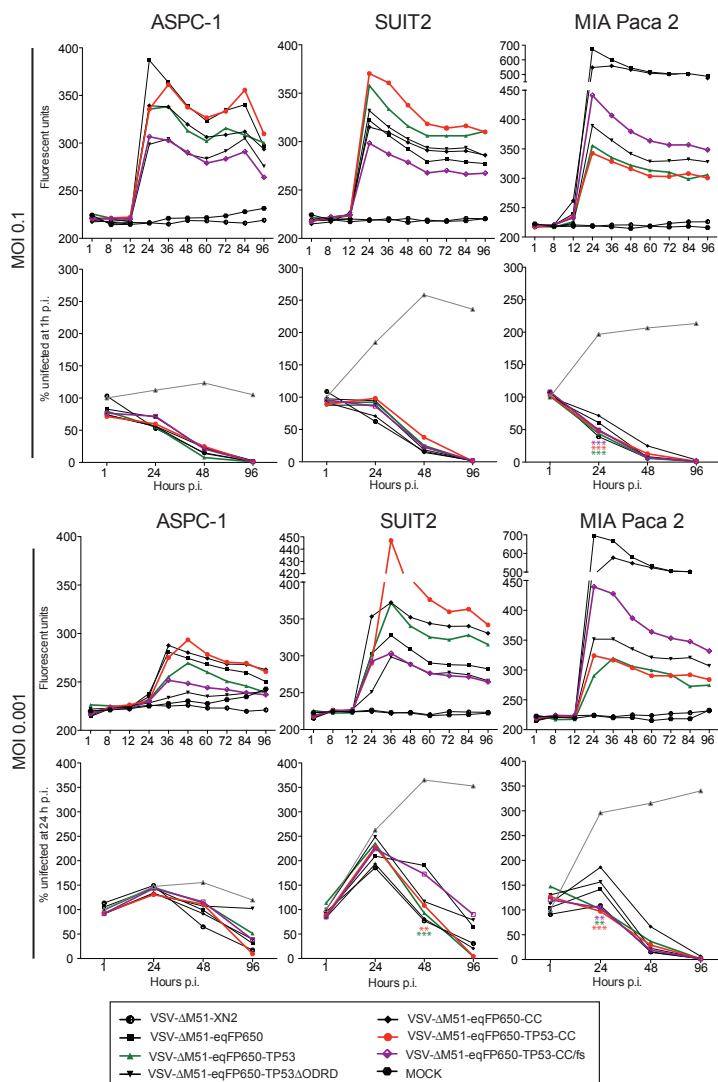
Figure 19. PDAC cells viability following infection with VSV recombinants. Cells were mock-infected or infected with viruses at MOIs 0.1 or 0.001 CIU/cell based on titration on BHK-21 cells. Virus driven RFP expression was measured by CytoFluor fluorescence readings at the indicated time points. Cell viability was analyzed every 12 h p.i. for 96 h using MTT cell viability assays and is expressed as a percentage of mock-treated cells. All MTT assays were done in triplicate and the data represent the mean ± SEM.
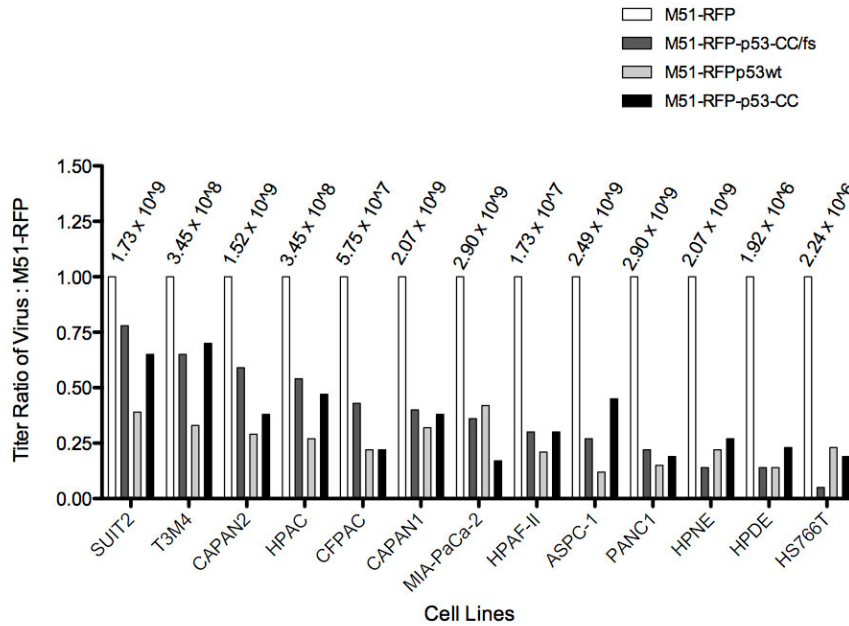
Figure 20. Permissiveness of PDAC cell lines to VSV recombinants. PDAC cell lines and HPDE and HPNE cells were incubated with serial dilutions of viruses. The infectious foci of M51-RFP, M51-RFP-p53wt, M51-RFP-p53-CC, or M51-RFP-p53-CC/fs were analyzed by fluorescence microscopy 24 h p.i. Virus permissiveness (relative yield) is expressed as ratio to M51-RFP on the same cell line.
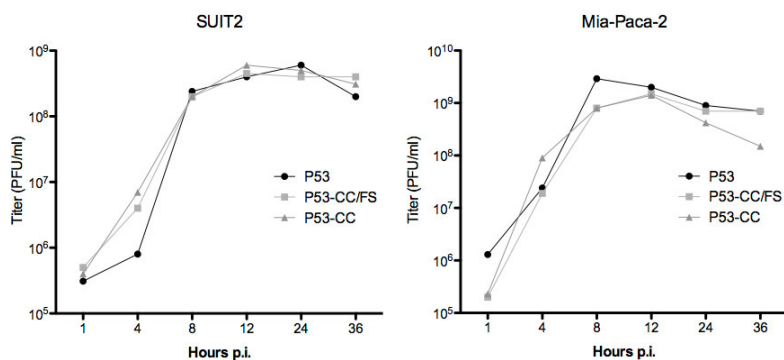
Figure 21. One-step growth kinetics of VSV recombinants in PDAC cell lines. PDAC cells were infected with M51-RFP-p53wt, M51-RFP-p53-CC, or M51-RFP-p53-CC/fs at a cell-specific MOI of 1 CIU/cell. At 1 h p.i., the virus was aspirated and the cells were washed and overlaid with 5% growth medium. At 1, 4, 8, 12, 24, and 36 h p.i., the supernatant was collected, and virus titers were determined by plaque assay on BHK-21 cells. All infections were done in duplicate and the data represent means.
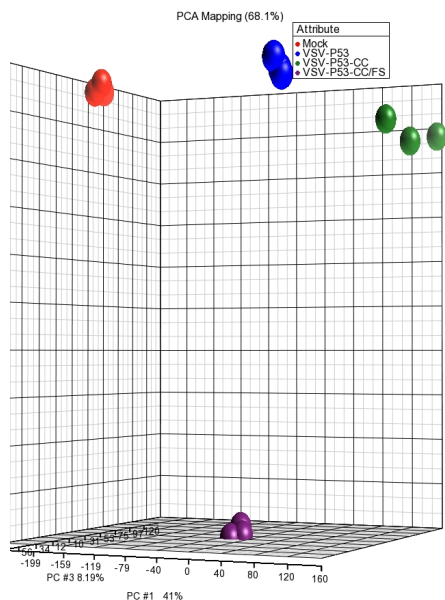
Figure 22. Affymetrix microarray data, analyzed for principle component analysis (PCA). Suit2 cells were mock-infected or infected with M51-p53wt, M51-p53-CC/fs, or M51-p53-CC at cell-specific MOI 5 CIU/cell. Total RNA was extracted and processed, then subjected to microarray analysis using a 2-fold cut-off for significance: mock (top left, red), M51-p53wt (top middle, blue), M51-p53-CC/fs (bottom, purple), and M51-p53-CC (top right, green).

Table 5: Regulation of Gene Expression of the p53 Pathway

Symbol	Entrez Gene #	Fold Induction (compared to mock)			Fold Induction		
		VSV-p53-CC/fs	VSV-p53wt	VSV-p53-CC	VSV-p53wt toVSV-p53-CC/fs	VSV-p53-CC to VSV-p53-CC/fs	VSV-p53-CC to VSV-p53wt
CHEK2 (CHK2)	11200	7.36	-	-	-5.47	-9.31	-
CHEK1 (CHK1)	1111	-	-3.50	-3.03	-	-2.05	-
PIK3CA (PI3K)	5290	-	-	-2.17	-	-2.48	-
CTNNB1 (B-CATENIN)	1499	-3.11	-3.75	-2.87	-	2.26	-
MDM2	4193	2.03	6.22	5.27	3.07	2.67	-
MDM4	4194	-	-3.89	-2.58	-2.22	-2.04	-
PML	5371	4.34	2.25	2.09	-2.69	-2.10	-
HIPK2	28996	-	-2.25	-2.17	-2.06	-	-
Tumor suppressor genes							
PTEN	5728	2.01	3.62	3.69	2.46	2.34	-
Proapoptotic genes							
APAF1	317	-3.42	3.08	2.09	10.54	6.17	-
LRDD (PIDD)	55367	3.08	5.05	5.22	2.49	2.19	-
NOXA (PMAIP1)	5366	25.42	17.52	16.68	-	-	-
PIG3 (TP53I3)	9540	-2.06	17.61	10.82	36.32	22.32	-
TEAP (TP53INP1)	94241	-	33.44	18.51	49.87	27.61	-
PUMA (BBC3)	27113	3.43	2.04	-	-	-	-
BAX	581	-	2.46	-	4.11	3.24	-
PPP1R151B	84919	-	-3.24	-3.88	-4.02	-4.81	-
MED1 (TRAP220)	5469	-	-3.35	-3.59	-2.53	-	-
EP300 (p300)	2033	-	-3.63	-4.43	-2.94	-3.72	-
JMY	133746	-	-	-2.08	-	-2.84	-
FAS	355	6.40	3.72	-	-	-3.74	-2.01
TNFRSF10A (DR4)	8797	-	2.55	-	5.07	2.13	-2.38
TNFRSF10B (DR4)	8795	5.09	-	-	-2.31	-3.85	-
CASP6	839	-4.96	2.04	-	6.00	2.30	-2.14
ADCK3 (CABC1)	56997	-	3.85	2.28	3.61	2.14	-2.50
PLAGL1 (ZAC1)	5325	-	2.17	-	2.47	-	-
Antiapoptotic genes							
TRIM29	23650	-	2.76	2.95	2.55	2.73	-
HDAC9	9734	8.93	-	-	-12.51	-14.43	-
SLUG (SNAI1)	6591	-	13.81	6.63	24.61	11.82	-2.08
BCL2	596	-	-	2.61	-	3.30	2.05
Glycolysis							
TIGAR (C12orf5)	57103	-2.75	3.34	2.44	9.20	6.71	-
Cell cycle							
GADD45	1647	-	3.22	3.47	3.82	4.12	-
CDKN1A (p21)	1026	2.75	7.15	6.41	2.60	2.33	-
PIAS1	8554	-	-3.46	-3.38	-2.78	-2.79	-
TOPBP1	11073	-	-3.61	-3.42	-2.91	-2.75	-
JUN (C-JUN)	3725	8.08	-2.96	-2.46	-6.32	-4.71	-
KAT2b (PCAF)	8850	-	3.71	3.17	6.38	5.44	-
CCND1 (Cyclin D)	595	-2.65	-2.22	-2.69	-	-	-
CDK2	1017	-2.21	-	-2.49	2.25	-	-
SFN (14-3-3 SIGMA)	2810	-3.84	4.73	3.57	15.80	11.75	-
Angiogenesis							
THBS1	7057	-	-	2.51	-	2.64	2.52
SERPINE1 (PAI-1)	5054	2.48	5.76	20.69	2.33	8.36	4.11
Autophagy							
DRAM	55332	2.07	4.36	4.08	2.11	-	-
DNA repair							
RRM2B (P53R2)	50484	-	2.23	2.09	2.48	2.32	-
PCNA	5111	-3.28	-	-	2.80	2.81	-

Table 6: Regulation of Gene Expression of IFN Signaling

Symbol	Entrez Gene	Fold Induction (compared to mock)			Fold Induction		
		VSV-p53-CC/fs	VSV-p53wt	VSV-p53-CC	VSV-p53wt to VSV-p53-CC/fs	VSV-p53-CC to VSV-p53-CC/fs	VSV-p53-CC to VSV-p53wt
Interferon signaling							
IFNB1	3456	291.10	25.24	4.56	-11.53	-63.80	-5.53
IFN Gamma (IL28A)	282616	476.72	173.02	62.15	-2.76	-7.67	-2.78
IFNAR1	3454	-2.07	-3.36	-3.87	-2.18	-2.51	-
IFNAR2	3455	2.74	-2.96	-3.21	-5.12	-3.22	-
IFNGR1	3459	-5.90	-7.13	-10.35	-3.98	-5.54	-
IFNGR2	3460	2.16	-2.24	-2.14	-4.84	-4.61	-
JAK2	3717	22.74	5.30	3.26	-5.55	-6.98	-
STAT1	6772	23.33	7.92	4.35	-2.18	-7.30	-
STAT2	6773	8.08	2.59	-	-3.11	-3.79	-
IRF9	10379	6.08	2.84	2.05	-2.14	-2.96	-
Inhibitor of Jak/Stat signaling							
SOCS1	8651	2.24	10.34	13.74	9.32	12.38	
PTPN2 (TCPTP)	5771	-2.03	-4.35	-4.61	-2.14	-2.27	
PIAS1	8554	-	-3.46	-3.38	-2.78	-2.79	
Interferon B/gamma Stimulated Genes							
MX1	4599	71.99	37.77	27.59	-	-2.61	-
OASL	8638	170.50	59.90	29.63	-2.85	-5.73	-2.02
IRF1	3659	21.52	7.83	4.21	-3.39	-7.51	-2.21
IFI35	3430	8.03	3.74	2.43	-2.15	-3.30	-
IFIT1	3434	71.80	19.34	9.30	-3.71	-7.72	-2.08
IFIT3	3437	74.99	24.06	26.15	-3.12	-2.87	-
PSMB8	5696	3.40	2.56	-	-	-2.49	-
Downstream of IRF1							
BAX	581	-	2.46	-	4.11	3.24	-
BAK1	578	-	2.64	-	2.50	-	-2.94
BCL2	596	-	-	2.61	-	3.30	2.05
RELA	5970	-	-2.17	-2.66	-2.91	-2.62	

Virally Expressed p53 Transgenes Suppress the Type I IFN Response

The transcriptome mRNA profile of Suit2 cells following infection with the three viruses: M51-RFP-p53-CC/fs, M51-RFP-p53wt, and M51-RFP-p53-CC allowed us to analyze expression levels over many pathways using the Ingenuity software (Figure 22). Surprisingly in the Suit2 cells infected with rVSV expressing p53 or p53-CC, the type I IFN signaling was dramatically attenuated (Table 6). Specifically, there was a 291.10-fold increase in IFN-β transcripts by M51-RFP-p53-CC/fs compared to mock-infected cells; the recombinant does not express functional p53. This can be

compared to increases of 25.24-fold and 4.56-fold in IFN-β transcripts by M51-RFP-p53 and M51-RFP-p53-CC, respectively, that do express functional p53. These results were confirmed in five additional cell lines, where both M51-p53wt and M51-p53-CC reduce expression of the IFN-β mRNA 8 h p.i. (Figure 23). Reduction in IFN-β expression results in reduced antiviral responses by cells by inhibiting expression of interferon stimulated genes (ISGs) like MX1 and OASL and allows for improved virus replication. Importantly, there was no inhibition of IFN-β signaling in HPDE, a non-malignant pancreatic cell line, adding additional evidence to studies that suggest that rVSVs expressing p53 are safe for use (Figure 23). Inhibition of Stat-1 phosphorylation and signaling was demonstrated at the protein level using Western blot analysis (Figure 24).

Many rVSVs have been generated to improve virus efficacy as an oncolytic vector, reviewed in Hastie and Grdzelishvili (51). Here, for the first, time, we have generated rVSVs expressing human p53 and the chimeric p53-CC (116). Replacing the C-terminus of WT p53 with the CC domain of human BCR creates a chimeric p53 that is not inhibited by the dominant negative effect of endogenous mutant p53 that is often found in cancers (116). Here, our data demonstrate functionality and oncolytic success of the virally expressed p53 transgenes.

Importantly, while murine p53 has been tested in the context of global expression changes due to VSV, the human form of p53 has never been tested; here we tested it specifically against PDAC cell lines. Previously, Heiber et al. (115) demonstrated that VSV expressing murine p53 is not significantly attenuated *in vitro*. We see the same lack of attenuation in our rVSVs against PDAC. However, VSV

expressing murine p53 is highly attenuated *in vivo*, but treatment still results in

enhanced tumor killing through stimulated antitumor immunity (115). Interestingly, a

clinical trial of VV expressing p53 has shown enhanced oncolytic efficacy in clinical

trials (175) through stimulation of an antitumor immune response.
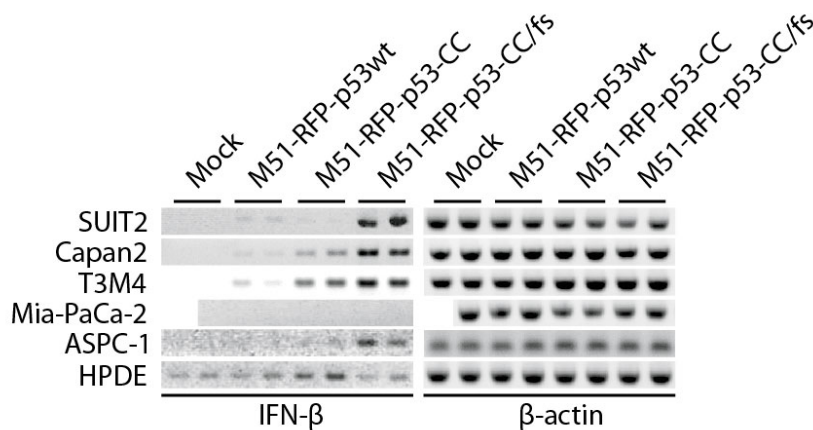
Figure 23: PCR confirmation of IFN-β expression. Cells were mock-infected or infected with M51-p53wt, M51-p53-CC, or M51-p53-CC/fs, at Suit2-specific MOI 5 CIU/cell. Total RNA was extracted and subjected to reverse transcription and cDNA synthesis. PCR was run for IFN-β.
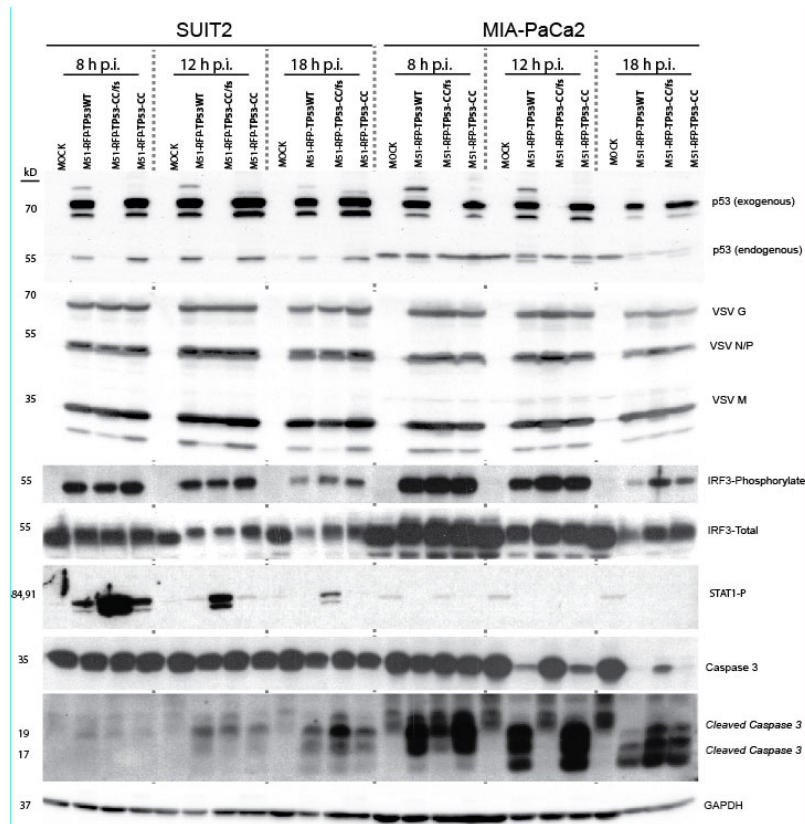
Figure 24: Expression of cellular antiviral proteins during infection timecourse. Monolayer cultures of cells were mock-infected or infected with M51-p53wt, M51-p53-CC, or M51-p53-CC/fs, at Suit2-specific MOI 5 CIU/cell. Total cell lysates were collected at the indicated time points. Lysates were separated by SDS-PAGE and then analyzed by Western blotting with antibodies to detect the indicated proteins. Western blotting using β-actin antibody was used as a loading control

3.5 Conclusions

Future *in vivo* studies with rVSVs expressing human p53 in animal models will

need to be done to see if the same phenotype is seen as we observed in PDAC cell lines.

The described above study is the first to date to examine global PDAC mRNA

expression following infection with VSV expressing a human p53 transgene and may

highlight the potential mechanism for this enhanced oncolytic efficacy of virus

expressing p53 in an *in vivo* setting.

Even more, continued research is generating additional modifications in the p53 protein for cancer therapy that may have improved efficacy when expressed from viral vectors. For example, there is evidence (205) that a specific polymorphism at p53 codon 72 may skew the immune response by affecting inflammation. P72 and R72 are common alleles for p53: the transgene in previous studies and our study encodes the R72 polymorphism. The authors demonstrate that p53 with P72 interacts with NF-Kb to cause an enhanced inflammatory response (205). It is not known whether this change would promote enhanced oncolytic efficacy *in vitro* or generation of improved tumor specific immunity *in vivo* in a PDAC model. Another example is ongoing work using the p53-CC construct. The creators of p53-CC (116) have continued to engineer the protein, including a reengineered p53-CC chimera, with a modified CC homo-oligomerization domain, that evades interacting with endogenous mutant p53 and endogenous BCR (206). While it is unclear if interaction with endogenous BCR can inhibit treatment efficacy, evading interaction with endogenous BCR sets up a system for p53 therapy without unknown side effects. Additionally, shorter p53 peptides were fused to mitochondrial localization signals from the proapoptotic proteins Bak or Bax; these constructs led to enhanced apoptotic responses in cell lines derived from multiple malignancies (207).

CHAPTER 4: DISSERTATION SUMMARY

4.1 Introduction

In summary, the aim of this dissertation was to strengthen vesicular stomatitis virus (VSV) as an OV therapy against PDAC. Previous work in our lab identified MUC1 as a host protein potentially inhibiting VSV efficacy against PDAC. This was addressed by research described in the second chapter, which describes *in vitro* and *in vivo* techniques, including the first study of VSV efficacy against PDAC xenografts in an immunocompetent mouse model, to explore a role for MUC1 in inhibiting VSV as an OV. Our findings demonstrate that the presence of MUC1 does not appear to have a significant effect on VSV efficacy and that the transient reduction in tumor burden is likely attributed to premature clearance of virus and lack of an immune response toward the tumor. In chapter 3 we examine human p53, a known tumor suppressor and therapeutic agent, expanding on known conditions where delivery of exogenous WT p53 from viral vectors causes enhanced cancer cell killing. Work from the Barber lab (115) identified VSV expressing murine p53 as an enhanced oncolytic virus in murine mammary adenocarcinoma. We generated rVSVs expressing human p53, as well as a re-engineered form called p53-CC (116) that has been shown to evade the dominant negative activity of endogenous p53 mutants, and examined the efficacy of both viruses against an array of human PDAC cell lines. As the p53 expressing rVSVs were not attenuated *in vitro*, future *in vivo* studies will need to demonstrate their efficacy against

PDAC. Both of these studies suggest there will be a benefit to continued investigation of VSV as an OV therapy for PDAC. The next three sections will detail potential methods to alter VSV tropism at different points of its life cycle, enhance VSVs oncolytic efficacy, and discuss future directions for this work.

4.2 Altering VSV Tropism

Altering VSV Tropism by Targeting Virus Entry

While the broad tropism of VSV is beneficial in many applications, others could be improved by specific targeting. VSV G protein modification by molecular and genetic engineering is an effective strategy for generating enhanced targeting of VSV particles. A site on VSV G protein is exposed on the protein's surface and has been shown to be tolerant to foreign epitope insertion was identified (208). The feasibility of this approach was demonstrated by (209), who constructed a chimeric VSV G protein by linking a large (253 aa) cell-directing single-chain variable fragment (scFv) antibody to the N-terminus of VSV G. HIV-1 particles pseudotyped with VSV G linked to a scFv against human major histocompatibility complex class I (MHC-I) bound strongly and specifically to human cells. However, the fusogenicity of the novel protein was diminished, resulting in a reduced infectivity.

Another approach is to replace VSV G with a heterologous glycoprotein from another virus. Detargeting of VSV from neurons was accomplished by pseudotyping the virus with the non-neurotropic envelope glycoprotein of the lymphocytic choriomeningitis virus (LCMV) (210). In a combination of approaches, VSV G was replaced with Sindbis virus G protein fused to a single-chain antibody against the Her2 receptor, commonly overexpressed on breast cancer cells (211, 212).

Several serial passages generated an adapted recombinant VSV that successfully targeted and eliminated Her2-expressing tumors in mice *in vivo*. Using a similar strategy, replication defective VSV particles were pseudotyped with measles virus envelope glycoproteins displaying single chain antibodies meant to target cancer cells expressing epidermal growth factor receptor, folate receptor or prostate membrane-specific antigen. These retargeted VSV infected only cells expressing the targeted receptor *in vitro* and *in vivo* in subcutaneous tumors established in mice (213). A different strategy entails the modification of the cellular and/or viral environment to non-specifically alter the viral tropism. For instance, repetitive administration of viral vectors (e.g., in OV therapy) provokes the generation of neutralizing antibodies that can diminish virus efficacy by depleting the amount of virions free to infect the host. One approach extends circulation time by conjugating polyethylene glycol to a VSV G in pseudotyped lentiviral particles, preventing virion inactivation in serum (214). Also, DNA aptamers against the antigen-binding fragment of polyclonal antibodies against VSV are used to shield the virus from neutralizing antibodies and enhances *in vivo* survival of VSV (152, 215). In a novel approach, nanotechnology was used to generate an encapsulated VSV G-pseudotyped lentiviral vector by crosslinking a polymer shell to reduce non-specific targeting. Acrylamide-tailored cyclic RGD peptide was also introduced to the shell to target this "nanovirus" specifically to HeLa cells (216). The resulting targeting nanovirus had similar titers to non-crosslinked pseudotypes, specifically transduced HeLa cells with high transduction efficiency, and did not change

Table 7: VSV Recombinants with Altered Tropism

VSV	Description and how tropism is affected	References
Parental recombinant "WT" VSV		
VSV-WT ("Rose Lab")	The parental rWT VSV. The L gene and the N-terminal 49 residues of the N gene are derived from the Mudd-Summers strain, the rest is from the San Juan strain (both Indiana serotype).	Lawson et al. (1995)
VSV-WT ("Wertz Lab")	An alternative rWT VSV. The N, P, M, and L genes originated from the San Juan strain; G gene from the Orsay strain (both Indiana serotype).	Whelan et al. (1995)
VSV-WT-XN2 (or XN1)	A derivative of VSV-WT ("Rose Lab") commonly used to make recombinant VSVs. Generated using pVSV-XN2 (or pVSV-XN1), a full-length VSV plasmid containing unique XhoI and NheI sites flanked by VSV transcription start and stop signals between G and L genes.	Schnell et al. (1996)
Attachment Modification		
VSV-DV/F(L289A) (*same as rVSV-F*)	VSV expressing the Newcastle disease virus (NDV) fusion protein gene between G and L. The L289A mutation in this protein targets VSV to cells with sialic acid-containing receptors and allows it to induce syncytia alone (without NDV HN protein).	Ebert et al. (2004)
VSV-S-GP	Pseudotyped VSV with a Sindbis virus (SV) glycoprotein. Targets VSV to cells with the Her2 receptor.	Bergman et al. (2007)
VSV-FAST, VSV-(ΔM51)-FAST	VSV or VSV-MΔ51 expressing the p14 FAST protein of reptilian reovirus (between VSV G and L) demonstrates enhanced fusogenic ability and induces extensive neuropathology.	Brown et al. (2009)
VSV-CT9-M51	Cytoplasmic tail of VSV-G was reduced from 29 to 9 amino acids in combination with the ΔM51 mutation. Attenuated neurotoxicity.	Ozduman et al. (2009), Wollmann et al. (2010)
VSV-CT1	Cytoplasmic tail of the G protein was truncated from 29 amino acids to 1 amino acid. Attenuated neurotoxicity.	Ozduman et al. (2009), Wollmann et al. (2010)
VSV-ΔG-SV5-F	Pseudotyped VSV with the fusogenic simian parainfluenza virus 5 fusion protein (SV5-F). Shows increased syncytial formation and apoptosis.	Chang et al. (2010)
VSV-LCMV-GP (Replication-defective)	Pseudotyped VSV with the lymphocytic choriomeningitis virus (LCMV) glycoprotein. Allows for infection of brain cancer cells while decreasing neurotoxicity.	Muik et al. (2011)
VSV-G5, -G5R, -G6, -G6R	VSV with a mutant G protein (aa substitutions at various positions between residues 100 and 471). Triggers type I IFN secretion that promotes infection/replication in IFN defective cells and provides alternate antigen epitopes.	Janelle et al. (2011)
VSV-H/F, - αEGFR, -αFR, -αPSMA (Replication-defective)	Pseudotyped VSV with the measles virus (MV) F and H displaying single-chain antibodies (scFv). Targets VSV to cells that express epidermal growth factor receptor, folate receptor, or prostate membrane-specific antigen.	Ayala-Breton et al. (2012)
VSV G protein (S162 T, T230 N and T368A mutations enhanced serum resistance)	VSV could be passaged in the presence of polyclonal antiserum resulting in the selection of antibody-escape mutants.	Hwang and Schaffer (2013)
Replication Modification		
VSV N1G4(WT), G1N2, G3N4, or G1N4	Changes to the gene order of VSV can attenuate the virus.	Flanagan et al. (2001)
VSV-12′GFP	Placement of two reporter GFP genes at position 1 and 2 attenuates VSV replication by moving viral genes downward, to positions 3 to 7.	van den Pol and Davis (2013)
VSV-G/GFP	Fusing a GFP sequence to the VSV G gene, inserted between the WT G and L genes, in addition to WT G. Phenotype is similar to WT VSV.	Dalton and Rose (2001)
VSV-p1-GFP, VSV-p1-RFP	Placement of a GFP or red fluorescent protein (RFP or dsRed) reporter gene at position 1 attenuates VSV replication by moving viral genes downward, to positions 2 to 6.	Wollmann et al. (2010)
VSV-WT-GFP, -RFP, -Luc, -LacZ	Insertion of reporter genes between G and L. Mild attenuation.	Fernandez et al. (2002), Wu et al. (2008)
VSV-ΔM51, VSV-ΔM51-GFP, - RFP, -FLuc, -Luc, - LacZ	Deletion of VSV M methionine at position 51 (ΔM51) mutation prevents WT VSV M from inhibiting the host cell antiviral response. Additionally, some variants encode a reporter gene between the G and L	Stojdl (2003), Power and Bell (2007), Wu et al. (2008)
VSV-M51R	The M51R mutation was introduced into M. This mutation prevents WT VSV M from inhibiting the host cell antiviral response.	Kopecky et al. (2001)

Table 7: (continued) VSV recombinants with altered tropism

VSV	Description and how tropism is affected	References
VSV-M6PY> A4-R34E and other M mutants	Mutation of aa M51R or the PSAP motif (residues 37–40) of VSV M prevents the protein from inhibiting nuclear export of cellular mRNA to reduce cellular antiviral response.	Irie et al. (2007)
VSV-*M_{mut}	Single mutations to VSV M or combination of mutations at VSV M aa positions M33A, M51R, V221F and S226R reduce the ability of VSV to prevent an antiviral response.	Hoffmann et al. (2010)
VSV-M(mut)	Mutation to VSV M residues 52 to 54 from DTY to AAA M(mut) prevents the ability of WT M to block nuclear mRNA export.	Heiber and Barber (2011)
VSV-mIFNβ, VSV-hIFNβ, VSV-rIFNβ	Addition of the mouse, rat, or human IFN-β gene in VSV enhances the antiviral state of normal cells, but retains oncolytic abilities against cancer cells with defective IFN responses.	Obuchi et al. (2003), Jenks et al. (2010)
VSV-let-7wt	Addition of let-7 microRNA target into the 3'-UTR of VSV M of the VSV genome limits replication only to cancer cells.	Edge et al. (2008)
VSV-124, -125, -128, -134 (M or L mRNA)	Addition of neuron-specific microRNA (miR-124, 125, 128, or 134) targets inserted in the 3'-UTR of VSV M or L mRNA result in reduced neurotoxicity.	Kelly et al. (2010)
VSV-IRESFMDV-GFP and VSV-IRESHRV-GFP	Internal ribosomal entry sites (IRES) from human rhinovirus 2 and foot and mouth disease virus were incorporated to control the translation of VSV M and attenuate neurovirulence.	Ammayappan et al. (2013)
VSV-rp30	Positive selection of VSV-G/GFP (see above) on glioblastoma cells results in a virus with two silent mutations and two missense mutations, one in P and one in L (rp30– 30 times repeated passaging). Better growth on glioblastoma cells.	Wollmann et al. (2005)
VSV-ΔP, -ΔL, -ΔG, (Semireplication-competent)	Three replication defective VSV variants, upon coinfection, show good replication, safety, and oncolysis (especially the combination of VSVΔG/VSVΔL).	Muik et al. (2012)
VSV-dG-GFP (or RFP) (Replication-defective)	Similar to VSV-p1-GFP or VSV-p1-RFP, above, but with a deleted VSV G that prevents a second round of infection.	Wollmann et al. (2010)

the viral entry pathway. Importantly, the polymer shell provided the targeting nanovirus with enhanced stability in the presence of human serum, protecting the nanovirus from human serum complement inactivation. Alternatively, VSV could be passaged in the presence of polyclonal antiserum resulting in the selection of antibody-escape mutants. Recently, directed evolution was used to select for VSV G mutants displaying increased resistance to human serum neutralization (217). Numerous common mutations were found which exhibited higher *in vitro* resistance to human serum as well as thermostability when introduced to pseudotyped lentiviral vectors. Finally, VSV can also infect human lymphocytes, dendritic cells, and natural killer (NK) cells and these cells have been exploited as delivery vehicles to prevent premature virus clearance prior to therapeutic effect (164, 218).

Altering VSV Tropism by Targeting Virus Replication

VSV tropism can be effectively changed by modifying the viral genome and/or

the cellular environment to make it more or less hospitable for viral replication. While

experimental adaptation of VSV to a particular cell type *in vitro* is still used in some

studies (219), most approaches are based on rational designs of VSV-based

recombinants generated using a reverse genetic system (126, 220). A hallmark of VSV

is its rapid replication. Any strategy that attenuates VSV replication (e.g., inhibiting

viral polymerase activities, VSV mRNA stability and/or translatability, virus abilities to

evade antiviral responses) has the potential to alter VSV cell tropism. Non-specific

attenuation via rearrangement of the highly conserved VSV gene order (221, 222) may

change the cell tropism of VSV as cell types less permissive to wild type WT VSV may

become resistant to the attenuated VSV-recombinant. Similar results can be achieved by

mutation of individual proteins. For example, single amino acid changes in VSV L can

abolish its mRNA cap methylation ability, resulting in a so-called host range phenotype

characterized by the ability of the VSV mutants to replicate only in some permissive

cell lines (20, 21). More rational strategies employ VSV recombinants with mutations

diminishing VSV's abilities to evade cellular antiviral responses. VSV M protein

localizes to the nuclear membrane where it interacts with cellular Rae1 complexes to

thwart antiviral response by inhibition of cellular mRNA trafficking and possibly

mRNA synthesis through interaction with transcription factor II D (223-226). The well-

studied VSV M51 mutation, either a mutation or deletion of the methionine codon at

position 51 of the M protein, abrogates M protein's ability to inhibit nuclear exit of host

mRNAs (69, 201, 202). As a result, VSV-M51 recombinants are more attenuated in

normal cell types, but are still very effective in cells with defective antiviral responses (51, 84). VSV recombinants are also designed to express host molecules modulating the cellular environment to make it more or less hospitable to virus. VSV encoding IFN-β is being used in a clinical trial against hepatocellular carcinoma (trial NCT01628640). VSV-IFNβ is highly attenuated in normal tissues, as increased secretion of IFN-β stimulates a protective antiviral response in surrounding cells (118). Instead, VSV-IFNβ specifically targets cancer cells, which are frequently defective in type I IFN signaling (84). Cell-specific micro-RNA expression can also be used to target VSV to a particular cell type. A VSV with a let-7 micro-RNA target sequence demonstrated increased tropism for cells, like cancer cells, that express lower levels of the let-7 micro-RNA (227). Beyond direct virus modification, VSV tropism can be altered through drug treatments that modulate the cellular environment, for example by inhibiting the type I IFN response. Treatment with JAK inhibitor 1 was shown to dramatically improve VSV cancer killing in resistant cancer cells with intact IFN response (104, 228, 229). A recombinant VSV encoding miRNA-4661 was able to repress IFN expression to inhibit host antiviral response (230). As mentioned above, co-infection of VSV with VV can be used to evade type I IFN response, thus enhancing VSV infection and replication (231).

4.3 Improving VSV Oncolytic Ability

<div align="center">Improving VSV Oncoselectivity and Safety</div>

As described in the chapter one, WT VSV can cause severe neurotoxicity in rodents, especially when administered intracranially or intranasally. Therefore, the development of any clinical application involving replication-competent VSV vectors requires understanding of potential VSV neuropathogenesis in humans and appropriate

attenuation of VSV to remove it. Many relevant studies analyzed WT VSV and rVSVs with regard to their potential as vaccine vectors, and these studies are relevant to the applications of VSV recombinants as oncolytic agents. In fact, many oncolytic rVSVs were originally developed as vaccine vectors. Some approaches, such as the rearrangement of VSV resulting in its attenuation, have yet to be applied to OV therapy, but will probably be explored in the future (221).

In non-human primate (NHP) infection models, which resemble human disease pathogenesis more closely, intranasal or intramuscular injection of WT VSV and rVSVs caused no clinically adverse signs (133, 232, 233). However, intrathalamic administration can result in severe neurological disease (133). In this study, when WT VSV, rWT VSV and two rVSV-HIV (human immunodeficiency virus) vectors were administered intranasally to NHPs, there was no evidence of VSV spread to CNS tissues. However, macaques inoculated intrathalamically with WT VSV developed severe neurological disease. Interestingly, rWT VSV was attenuated significantly compared with WT VSV, and all of the macaques in the rVSV-HIV vector groups showed no clinical signs of disease. The attenuation of rWT VSV (compared with WT VSV) was probably due to spontaneous mutations generated during the reverse genetics process or due to sequence differences between WT VSV and rWT VSV (Table 1). The attenuation of rVSV-HIV (compared with rWT VSV) was probably due to the presence of the additional gene (HIV Gag) and the CT1 mutation. With regard to OV therapy, a recent study tested VSV-IFNβ on rhesus macaques via intrahepatic injection; no neurological signs were observed at any time point (234). As a result, a phase I clinical trial using VSV-IFNβ is currently in progress to evaluate the safety of intratumoral

administration of VSV-IFNβ to human patients with hepatocellular carcinoma (trial NCT01628640).

Currently, at least eight approaches have been shown to improve VSV oncoselectivity and neurotropism safety without compromising its oncolytic abilities: (i) mutating the VSV M protein; (ii) VSV-directed IFN-β expression; (iii) attenuation of VSV through disruption of normal gene order; (iv) mutating the VSV G protein; (v) introducing targets for microRNA from normal cells into the VSV genome; (vi) pseudotyping VSV; (vii) experimental adaptation of VSV to cancer cells; and (viii) using semi-replicative VSV.

Employing VSVs encoding a mutated M protein, which are unable to evade antiviral innate responses in normal cells, is possibly the most common approach to improve both oncoselectivity and safety of VSV (Table 8). Such VSV mutants retain their oncotoxicity in cancer cells defective in their antiviral responses. Most studies use VSV M recombinants containing a mutation or deletion of the methionine residue at position 51 of the M protein (201) (202). Alternatively, an M mutant with residues 52–54 mutated from DTY to AAA has been used (115). These mutations prevent the M protein from binding to the Rae1–Nup98 mRNA export complex and inhibiting cellular gene expression in normal cells, and thus provide enhanced safety, including no neurotoxicity *in vivo*. Even safer VSVs have been generated by additional M modifications within the PSAP region (residues 33–44) (235). It is important to note that inactivation of the ability of the M protein to inhibit cellular gene expression is a strategic advantage not only for safety reasons (e.g. normal cells can produce type I IFN and ISGs), but also when cellular gene expression is desirable (e.g. for tumor antigen

presentation).

The oncoselectivity and safety of VSV are greatly improved in VSVs encoding mouse, rat or human IFNβ (which are species-specific), and one is being used in an ongoing clinical trial to evaluate VSV-IFNβ in human patients with hepatocellular carcinoma (trial NCT01628640). IFNβ stimulates innate immune responses in normal cells, but not in cancers with defective type I IFN signaling (234) (118) (86). In addition to enhanced oncoselectivity and safety, VSV-directed IFNβ expression also generates desirable immunostimulation of the tumor microenvironment. Theoretically, any significant attenuation of VSV can improve oncoselectivity and safety. This approach has been used to generate VSV-p1-GFP and similar recombinants with a foreign gene inserted in position 1 of the VSV genome (before the N gene). While a typical insertion of a foreign gene between the VSV G and L genes affects VSV replication only marginally (L polymerase mRNA can be downregulated without dramatic consequences for VSV fitness), insertions at position 1 negatively affect expression of all VSV genes. The resulting VSV-p1-GFP lacks neurotoxicity, but retains good oncolytic abilities in an intracranial human glioblastoma tumor xenograft mouse model (66).

WT VSV can also be attenuated by mutations in the G protein (Table 7). CT1 and CT9 mutants have the cytoplasmic tail of G truncated by removal of residues 1–29 and 9–29, respectively (Ozduman et al. , 2009). The best oncolytic ability and safety was shown for VSV-CT9-M51, which combined the CT9 and M51 mutations in a mouse model of human neuroblastoma (66, 236). Another study, examining four VSVs with point mutations in the G protein against a variety of cancer cell lines, showed that

Table 8: VSV recombinants used as oncolytic agents against cancer

Recombinant VSV	Virus description	Reference(s)	Designed to improve: Oncoselectivity	Safety	Oncotoxicity	VSV survival	Tumour immunity
WT and miscellaneous							
WT VSV ('Rose lab')	The parental rWT VSV for most VSV-based OVs. The L gene and the N-terminal 49 residues of the N gene are derived from the Mudd-Summers strain, the rest is from the San Juan strain (both Indiana serotype)	Lawson et al. (1995)					
VSV-WT-XN2 (or XN1)	Derivative of rWT VSV ('Rose lab'). Generated using pVSV-XN2 (or pVSV-XN1), a full-length VSV plasmid containing unique XhoI and NheI sites flanked by VSV transcription start and stop signals between G and L genes. pVSV-XN2 (or pVSV-XN1) is commonly used to generate recombinant VSVs encoding an extra gene	Schnell et al. (1996)					
WT VSV ('Wertz lab')	Alternative rWT VSV. The N, P, M and L genes originate from the San Juan strain; G gene from the Orsay strain (both Indiana serotype). Rarely used in OV studies	Whelan et al. (1995)					
VSV-WT-GFP, -RFP, -Luc, -LacZ	WT VSV encoding reporter genes (between G and L) to track virus infection. Based on pVSV-XN2. Toxicity similar to VSV-WT	Fernandez et al. (2002), Wu et al (2008)					
VSV-G/GFP	GFP sequence fused to VSV G gene is inserted between the WT G and L genes (in addition to WT G). Toxicity similar to that of VSV-WT	Dalton & Rose (2001)					
VSV-rp30	Derivative of VSV-G/GFP. Generated by positive selection on glioblastoma cells and contains two silent mutations and two missense mutations, one in P and one in L. 'rp30' indicates 30 repeated passages	Wollmann et al. (2005)	X	X	X		
VSV-p1-GFP, VSV-p1-RFP	VSV expressing GFP or red fluorescent protein (RFP or dsRed) reporter gene at position 1. Attenuated because all VSV genes are moved downward, to positions 2–6. Safe and still effective as an OV	Wollmann et al. (2010)	X	X			
VSV-dG-GFP (or RFP) (replication-defective)	Similar to VSV-p1-GFP or VSV-p1-RFP described above, but with the G gene deleted. Cannot generate a second round of infection. Poor ability to kill tumour cells	Wollmann et al. (2010)	X	X			
VSV-ΔP, -ΔL, -ΔG (semi-replication-competent)	Each virus cannot replicate alone because of one VSV gene deleted, but when viruses co-infect, they show good replication, safety and oncolysis (especially the combination of VSVΔG/VSVΔL). VSVΔP and VSVΔL contain dsRed in place of the corresponding viral gene. VSVΔG contains GFP gene in place of G	Muik et al. (2012)	X	X			
M mutants							
VSV-M51R	The M51R mutation was introduced into M	Kopecky et al. (2001), Stojdl et al. (2003), Power & Bell (2007), Wu et al (2008)	X	X			
VSV-ΔM51, VSV-ΔM51-GFP, - RFP, -Fluc, -Luc, - LacZ	The ΔM51 mutation was introduced into M. In addition, some recombinants encode a reporter gene between the G and L		X	X			
VSV-'Mmut	VSV with a single mutation or combination of mutations at the following M positions: M33A, M51R, V221F and S226R	Hoffmann et al. (2010)	X	X			

Table 8: (continued) VSV recombinants used as oncolytic agents against cancer

Recombinant VSV	Virus description	Reference(s)	Oncoselectivity	Safety	Oncotoxicity	VSV survival	Tumour immunity
VSV-M6PY >A4-R34E and other M mutants	The M51R mutation was introduced into the M gene, and, in addition, the mutations in the PSAP motif (residues 37–40) of M	Irie et al. (2007)	X	X			
VSV-M(mut)	VSV M residues 52–54 are mutated from DTY to AAA. M(mut) cannot block nuclear mRNA export	Heiber & Barber (2011)	X	X			
G mutants							
VSV-G5, -G5R, -G6, -G6R	VSV-expressing mutant G with amino acid substitutions at various positions (between residues 100 and 471). Triggers type I IFN secretion as the M51R, but inhibits cellular transcription and host protein translation like WT	Janelle et al. (2011)	X	X			
VSV-CT1	The cytoplasmic tail of the G protein was truncated from 29 to 1 aa. Decreased neuropathology, but marginal oncolytic efficacy	Ozduman et al. (2009), Wollmann et al. (2010)	X	X			
VSV-CT9-M51	The cytoplasmic tail of VSV-G was reduced from 29 to 9 aa, also has ΔM51 mutation. Attenuated neurotoxicity and good OV abilities	Ozduman et al. (2009), Wollmann et al. (2010)	X	X			
Foreign glycoproteins							
VSV-DV/F(L289A) (same as rVSV-F)	VSV expressing the NDV fusion protein gene between G and L. The L289A mutation in this protein allows it to induce syncytia alone (without NDV HN protein)	Ebert et al. (2004)	X	X	X		
VSV-S-GP	VSV with the native G gene deleted and replaced with a modified glycoprotein protein (GP) from Sindbis virus (SV). Also expressing mouse GM-CSF and GFP (between SV GP and VSV L). The modified GP protein recognizes the Her2 receptor, which is overexpressed on many breast cancer cells	Bergman et al. (2007)	X		X		
VSV-ΔG-SV5-F	VSV G gene is replaced with the fusogenic simian parainfluenza virus 5 fusion protein (SV5-F) gene	Chang et al (2010)		X	X		
VSV-FAST, VSV-(ΔM51)-FAST	VSV or VSV-MΔ51 expressing the p14 FAST protein of reptilian reovirus (between VSV G and L)	Brown et al. (2009)	X	X	X		
VSV-LCMV-GP (replication-defective)	VSV lacking the G gene was pseudotyped with the non-neurotropic glycoprotein of LMCV	Muik et al. (2011)		X			
VSV-H/F, -αEGFR, -αFR, -αPSMA (replication-defective)	VSV lacking the G gene was pseudotyped with the MV F and H displaying single-chain antibodies (scFv) specific for epidermal growth factor receptor, folate receptor, or prostate membrane-specific antigen. Retargeted VSV to cells that expressed the targeted receptor	Ayala-Breton et al. (2012)	X		X		X
microRNA targets							
VSV-let-7wt	The let-7 microRNA targets are inserted into the 3'-UTR of VSV M	Edge et al. (2008)	X	X			

Table 8: (continued) VSV recombinants used as oncolytic agents against cancer

Recombinant VSV	Virus description	Reference(s)	Designed to improve:				
			Oncoselectivity	Safety	Oncotoxicity	VSV survival	Tumour immunity
VSV-124, -125, -128, -134 (M or L mRNA)	VSV recombinants with neuron-specific microRNA (miR-124, 125, 128 or 134) targets inserted in the 3'-UTR of VSV M or L mRNA	Kelly et al (2010)	X	X			X
Cancer suppressors							
VSV-mp53, VSV-M(mut)-mp53	VSV [WT or M(mut)] expressing the murine p53 gene. M(mut) has residues 52–54 of the M protein changed from DTY to AAA	Heiber & Barber (2011)	X	X	X		X
Suicide genes							
VSV-C:U	VSV expressing E. coli CD/UPRT, catalysing the modification of 5-fluorocytosine into chemotherapeutic 5-FU	Porosnicu et al (2003)	X		X		
VSV-C	VSV-MΔ51 expressing CD/UPRT	Leveille et al. (2011b)	X	X	X		
VSV-(MΔ51)-NIS	VSV-MΔ51 expressing the human NIS gene (for 'radiovirotherapy' with ^{131}I)	Goel et al. (2007)	X	X	X		
VSV-TK	VSV expressing TK; can improve oncolysis if used with non-toxic prodrug ganciclovir	Fernandez et al. (2002)	X	X	X		X
Immunomodulation							
VSV-mIFNβ, -hIFNβ, VSV-rIFNβ	VSV expressing the murine (m), human (h) or rat (r) IFN-β gene	Obuchi et al. (2003), Jenks et al. (2010)	X	X	X		X
VSV-IL4	VSV expressing IL-4	Fernandez et al. (2002)			X		X
VSV-IL12	VSV expressing IL-12	Shin et al. (2007a)			X		X
VSV-IL23	VSV expressing IL-23. Significantly attenuated in the CNS, but effective OV	Miller et al (2010)	X	X	X		X
VSV-IL28	VSV expressing IL-28, a member of the type III IFN (IFN-λ) family	Wongthida et al. (2010)	X	X	X		X
VSV-opt.hIL-15	VSV-MΔ51 expressing a highly secreted version of human IL-15	Stephenson et al. (2012)	X	X	X		X
VSV-CD40L	VSV expressing CD40L, a member of the tumour necrosis factor (TNF) family of cell-surface molecules	Galivo et al. (2010)	X		X		X
VSV-Flt3L	VSV-MΔ51 expressing the soluble form of the human Flt3L, a growth factor activating DCs	Leveille et al. (2011a)	X	X	X		X
VSV/hDCT	VSV-MΔ51 expressing hDCT	Boudreau et al. (2009)	X	X	X		X
VSV-hgp100	VSV expressing hgp100, an altered self-TAA against which tolerance is well-established in C57BL/6 mice	Wongthida et al. (2011b)			X		X
VSV-ova	VSV expressing chicken ovalbumin (for B16ova cancer model)	Diaz et al (2007)	X		X		X
VSV-gG	VSV expressing EHV-1 glycoprotein G, a broad-spectrum viral chemokine-binding protein	Altomonte et al. (2008b)	X		X	X	
VSV-UL141	VSV expressing a secreted form of the human cytomegalovirus UL141 protein, known to inhibit the function of NK cells by blocking the ligand of NK cell-activating receptors	Altomonte et al. (2009)	X		X	X	
VSV-(Δ51)-M3	VSV-MΔ51 expressing the murine gammaherpesvirus-68 chemokine-binding protein M3	Wu et al. (2008)	X		X	X	

mutant VSV-G6R (E238G substitution in the G protein) is as efficient as WT VSV at cell killing and inhibition of cellular transcription and host protein translation. Surprisingly, VSV-G6R triggers type I IFN secretion as efficiently as a VSV M51 mutant (237).

Altered expression of microRNAs in cancer cells can also be exploited to increase oncoselectivity and safety of VSV. A recombinant containing the highly conserved let-7 micro-RNA target sequence in the M mRNA 39-UTR resulted in attenuation via lower M expression in normal cells that express high levels of let-7, but not in cancer cells that express low levels of let-7 *in vitro* and *in vivo*, and caused no neurotoxicity after intranasal virus infection of mice (238). Insertion of neuronal miR125 targets into VSV, particularly the L mRNA 3' -UTR, reduced neurotoxicity even when virus was injected intracranially into mice, while retaining oncolytic abilities (227).

VSV neurotropism can also be inhibited through a pseudotyping approach (Table 7). Pseudotyped VSV-LCMV-GP virions, containing the non-neurotropic envelope glycoprotein of lymphocytic choriomeningitis virus instead of the VSV G protein, showed enhanced infectivity of malignant glioma cells while sparing primary human and rat neurons (210). Although only replication-defective viruses were used, this proof-of principle study demonstrated that VSV-LCMV-GP has a longer lasting therapeutic outcomes than VSV, especially for clinical applications targeting brain cancers.

While the approaches described above were designed to prevent VSV replication in normal cells, several studies designed VSVs specifically to target cancer

cells. One approach used VSV-S-GP, where a modified glycoprotein from Sindbis virus replaced VSV G (211, 212). The modified glycoprotein was designed to specifically recognize the Her2 receptor, which is overexpressed on many breast cancer cells. This approach successfully targeted and eliminated Her2-expressing tumors in mice *in vivo*. In a separate study, replication defective VSV was pseudotyped with measles virus fusion and haemagglutinin glycoproteins displaying single chain antibodies to target and infect cells expressing epidermal growth factor receptor, folate receptor or prostate membrane-specific antigen (213) in human tumor xenografts in mice.

VSV oncoselectivity can be increased via adaptation to cancer cells using serial passages. This approach successfully adapted VSV-S-GP to a murine mammary tumor cell line expressing the Her2 receptor (212). In a separate study, VSV-rp30 was generated by repeated passaging (rp) VSV-G/GFP (Table 8) 30 times on glioblastoma cells (219). VSV-rp30 contains two silent mutations and two missense mutations, one in P and one in L.

While oncolytic virotherapy is based predominantly on replication-competent viruses, some studies have examined replication-defective viruses, which do not produce infectious progeny, similar to those employed in most standard gene-therapy studies (167). While it is unlikely that replication-defective recombinants could be as effective as replicative VSVs (unless used mainly to deliver anticancer genes, induce adaptive immunity, etc.), so-called semi-replicative viruses have been generated and tested. Two *trans*-complementing recombinants, VSV*ΔG and VSVΔLdsRed, lack the VSV G and L genes, respectively, and are non-replicative alone (Muik et al., 2012). However, coinfection of a cell with the two recombinants results in production and

spread of non-replicative progeny. The VSVΔG/VSVΔL-dsRed combination was as potent as WT VSV *in vitro* and induced long-term glioblastoma tumor regression in mice *in vivo* without neurotoxicity.

There are several options for treating VSV-resistant cancer cells. Pre-screening cells against an array of VSVs or other OVs could identify the best OV for treating a particular tumor. OV therapy can also be combined with chemical inhibitors to overcome VSV resistance. For example, the mammalian target of rapamycin stimulates type I IFN production via phosphorylation of its effectors. Using rapamycin, the inhibitor of this protein, in combination with VSVΔM51 increased survival of immunocompetent rats with malignant gliomas (239). Histone deacetylase inhibitors influence epigenetic changes within cells, ultimately altering gene expression and affecting antiviral responses. Indeed, these inhibitors reversibly compromise host antiviral responses in multiple cancer cell lines and allow enhanced spread of VSV that correlates with inhibited IFN responses and VSV-mediated oncolysis in cancer cells (240).

The resistance of cancer cells to VSV can also be overcome using a combination of VSV with other OVs, e.g. the double deleted VV. The deletions restrict VV to cells that overexpress transcription factor E2F and have activated epithelial growth factor receptor pathways, a common cancer cell signature. Expression of the VV-encoded B18R protein antagonizes the innate cellular antiviral response to allow more robust VSVΔM51 replication in colon cancer xenografts in mice (241). Furthermore, a recent analysis showed that previous infection of cervical carcinoma cancer cells with human papillomavirus (HPV) improved VSV infection and killing, compared with cervical

carcinomas not infected with HPV (242). HPV can inhibit IFN signaling, possibly creating a more hospitable environment for VSV.

<div align="center">Increased Oncotoxicity</div>

The ultimate goal of any successful OV therapy is the selective killing of cancer cells. There are at least seven approaches that have been shown to improve the oncolytic abilities ('oncotoxicity') of VSV independent of the immune system (as discussed in the last section): (i) combination of VSV with chemical agents; (ii) viral expression of tumor suppressor genes; (iii) viral expression of 'suicide genes'; (iv) syncytium induction; (v) radiovirotherapy; (vi) combining VSV with tumor embolization; and (vii) combining VSV with anti-angiogenic agents.

VSV kills infected cells by inducing apoptosis via the mitochondrial (intrinsic) or death receptor (extrinsic) pathway, or both (70) (71, 243) (244). The mechanisms of induction can be cell-type-specific, and many cancer cells inhibit apoptosis to allow prolonged proliferation (245, 246). WT VSV induces apoptosis primarily via the intrinsic pathway, while recombinants with an M51 mutation induce apoptosis primarily via the extrinsic pathway, although this is not absolute (70, 71). Understanding the interplay between VSV and cellular apoptotic mechanisms may be critical for developing and selecting OV treatment. Overexpression of the anti-apoptotic B-cell lymphoma 2 (BCL-2) protein was shown to impair VSV-mediated oncolysis, while this resistance was reversed when VSV was combined with obatoclax, a small-molecule BCL-2 inhibitor (247). Another BCL-2 inhibitor, EM20-25, rendered apoptosis-resistant cancer cells susceptible to VSV induced apoptosis (248). In another study, infection by WT VSV (but not VSV with the M51 mutation) increased degradation of

an anti-apoptotic myeloid cell leukemia 1 protein (Mcl-1) that contributes to chemotherapy resistance (249). This VSV-mediated Mcl-1 degradation sensitized apoptosis-resistant cancer cells to doxorubicin, an approved chemotherapeutic. This combined chemovirotherapy had an enhanced therapeutic effect compared with each treatment alone in mice (249).

The oncotoxicity of VSV can be enhanced by the expression of functional tumor-suppressor genes in cancer cells, e.g. VSV-M(mut)-mp53, which encodes p53 in addition to the mutated M protein and induces potent anti-tumor responses in mice (115). This study showed that VSV-M(mut)-mp53 retained the selective ability to lyse cancer cells and also directed expression of high levels of functional p53. Importantly, VSV-M(mut)-mp53 showed improved safety when attenuated *in vivo* due to the activation of innate immune genes (such as type I IFNs) by p53, and induced enhanced adaptive tumor specific immune responses.

One limitation of a standard OV therapy is that oncotoxicity is normally limited to virus-infected cancer cells. To address this issue, several approaches aim to increase the bystander effect and to kill uninfected cancer cells. One approach uses VSV expressing so-called 'suicide genes'. These genes catalyse conversion of a non-toxic prodrug into a toxic form that, in addition to its toxicity in infected cancer cells, can diffuse to neighboring uninfected cancer cells through gap junctions. Administration of VSV expressing the herpesvirus thymidine kinase (TK) protein to mice in combination with the prodrug ganciclovir exerted a great oncolytic effect through TK/ganciclovir-mediated apoptosis, enhanced the bystander effect and induced tumor-specific immune responses in breast or melanoma tumors in mice (135). Cytosine deaminase (CD)

catalyses the conversion of 5-fluorocytosine (5-FC) to the commonly used

chemotherapeutic drug 5-fluorouracil (5-FU), while uracil phosphoribosyltransferase

(UPRT) converts 5-FU into the active 5-fluoro-UMP form. Intratumoral inoculation

with VSV expressing these two proteins (VSV-C:U) followed by 5-FC administration

improved tumor regression significantly compared with VSV or 5-FU alone, and

activated tumor-specific immune responses against lymphoma or mammary carcinoma

in mice (157). This approach was further optimized by combining the M51 mutation

with CD/UPRT expression (VSV-C) (156).

One critical limitation of OVs is their relatively poor penetration and spread

within tumor masses. Several studies have attempted to address this problem through

the generation of VSVs that spread by forming giant, multinuclear cells called syncytia.

While VSV is generally not fusogenic, several fusogenic recombinants have been

generated and showed promising results in different cancer models. VSV-NDV/F

(L289A) (designated rVSV-F) encodes the Newcastle disease virus (NDV) fusion

protein gene with an L289A mutation to allow syncytium formation in the absence of

the NDV haemagglutinin–neuraminidase protein (149, 158) (159). VSV-ΔG-SV5-F

expresses the simian parainfluenza virus F protein (160) and VSV/FAST virus

expresses the p14 FAST protein of reptilian reovirus (250). Adding fusogenic genes to

the VSV genome should be done with caution as VSV/FAST with WT M showed

dramatically increased neuropathology in mice, although VSV M51 expressing p14

remained attenuated (250).

One of the most elegant approaches to increase VSV oncotoxicity is based on a

combination of viro- and radiotherapy ('radiovirotherapy'). VSV-ΔM51-NIS expresses

a human sodium iodide symporter (NIS) protein that mediates high-concentration iodide uptake and, in mice, has a synergistic effect with iodine. VSV-NIS in combination with iodine-123 allows sensitive monitoring of infection, while iodine-131 is used for treatment of radiosensitive tumors (251, 252).

VSV-based OV therapy of liver cancers can be improved significantly when combined with tumor embolization ('viroembolization'), the blocking of arterial blood flow in the liver, thereby prolonging exposure of tumor cells to the therapeutic agent. When VSV was administered to rats in combination with degradable starch microspheres, an embolic agent currently used clinically for liver tumors, massive tumor necrosis and substantially prolonged survival were observed in test animals compared with monotherapy with either VSV or the embolic agent alone (253).

Finally, VSV oncotoxicity can be improved by targeting tumor vasculature. VSV has the ability to target tumor vasculature and angiogenesis when administered subcutaneously to mice with colon adenocarcinoma (162). The use of antiangiogenic vascular endothelial growth factor 165 inhibitor combined with VSV led to increased tumor regression and improved virus titer and dissemination, even within tumors that previously supported poor VSV replication (254).

<div align="center">Preventing Premature Clearance of VSV</div>

Safe virotherapy ultimately requires clearance of the OV from the body. Unfortunately, those same mechanisms can eliminate the OVs prematurely, before they complete their task. Prior to initiation of infection, circulating antibodies (Abs), non-specific host proteins or complement proteins can neutralize virus particles. Virus sequestration to certain organs can also result in ineffective OV therapy. Several

approaches have been developed to protect VSV-based OVs from premature clearance, including: (i) physical delivery methods hiding/masking virus from Abs, other host components or immune cells; (ii) VSVs expressing genes favoring VSV survival; and (iii) combination of VSV with chemicals favoring VSV survival.

Various cell-based methods to deliver OVs to tumors via carrier cells have been reviewed by (255) and (256). With regard to VSV, murine OT-I CD8+ T-cells, specific for an epitope of the ovalbumin antigen, were infected *ex vivo* with VSV and delivered to B16-OVA melanoma tumors in the lungs of immunocompetent mice (150, 151). These virus 'Trojan horses' demonstrated significantly improved therapy compared with VSV or T-cells alone. Importantly, this therapy was effective even in mice with pre-existing Abs against VSV, indicating that therapy with virus-loaded T-cells may be useful even in patients with pre-existing immunity to VSV (150). A new approach called aptamer-facilitated virus immunoshielding (AptaVISH) uses aptamer technology to mask OVs from their respective neutralizing Abs, and is currently in development for several OVs, including VSV (152).

While these studies physically hide or mask VSV from the immune system, other approaches have attempted to modulate the immune system environment to favor virus survival. For instance, VSV-gG expresses the equine herpesvirus-1 glycoprotein G, a broad-spectrum chemokine-binding protein. Addition of EHV-1 G increases the oncolytic potency of VSV due to substantial suppression of host antiviral inflammatory responses in rats (253). Similarly, VSV-M51-M3 expresses the murine gammaherpesvirus-68 M3 protein, which binds a broad range of chemokines and reduces the inflammatory response and NK and neutrophil accumulation in lesions in

rats (136). Further, recombinant VSV-UL141 downregulates NK cell-activating ligand CD155 to inhibit NK-cell recruitment in rats (149).

Additional studies investigated the prevention of Ab mediated VSV neutralization by combined administration of VSV and cyclophosphamide (CPA). CPA enhances delivery of OVs through reductions in levels of neutralizing Abs, suppression of innate immune effectors (257, 258), depletion of number of Tregs (168) and activation of immune cells (259). While a single dose of CPA has been shown to be insufficient to control primary anti-VSV immune responses in animal models, a clinically approved multi-dose CPA regimen suppressed antiviral Ab responses against VSV, even in mice with pre-existing Abs against VSV (154). However, a recent study surprisingly showed that the combination of CPA and VSV was less effective than CPA alone, despite increased intratumoral VSV titers (155). This study suggests that CPA-mediated therapy is dependent upon both CD4 T-cell and NK-cell activation, which are suppressed upon VSV infection, and serves as a warning of unforeseen consequences of experimental therapies involving immune modulation

<center>Inducing Tumor-specific Immunity</center>

Fully effective OV therapy may require the activation of tumor-specific adaptive immune responses (163). Although all VSVs have immunostimulatory abilities, in this section we focus on VSV-based OVs designed specifically to induce tumor-specific immune responses.

A number of tested VSVs encode immunostimulatory host genes (Table 8), including interleukin (IL)-4 (135), IL-12 (260), IL-15 (261), IL-23 (262, 263), type III IFN-l (also called IL-28) (171), Fms-like tyrosine kinase 3 ligand (Flt3L) (264) and

CD40L (167) (Table 8). Interestingly, a study utilizing VSV-CD40L with or without

VSV G indicated that therapeutic success may not depend on progressive rounds of

VSV replication, as non-replicative VSV-CD40LΔ-G was equally as effective as fully

replication-competent VSV-CD40L in mice. This result illustrates that tumor specific

immune responses could play a dominant role, at least in the employed experimental

system (167). Some interleukins provide not only immunostimulation but also improved

safety. For example, the incorporation of IL-23 into the VSV genome stimulated NK

and CD4 cells and enhanced nitric oxide production in the CNS, aiding viral clearance

from neurons (262, 263).

While these approaches stimulated the immune system and often resulted in

tumor-specific memory responses, several studies investigated whether VSV can be

designed specifically to facilitate the presentation of tumor-associated antigen (TAA) to

immune cells. In a proof-of principle study, the VSV-OVA virus was generated to

express the chicken ovalbumin (ova) gene (166). Injection of VSV-OVA into

established B16-OVA tumors increased the number of ova-specific T-cells significantly

compared with VSV-GFP (265). VSV expressing an altered version of the murine self-

TAA gp100 was able to stimulate gp100-specific T-cells despite pre-existing immune

tolerance. Although tumor reduction was not improved significantly compared with

VSV-GFP, combining VSV-hgp100 infection with adoptive transfer of naive gp100-

specific T-cells improved efficacy greatly, suggesting the potential of this treatment

strategy (265).

Dendritic cells (DCs) have the ability to activate Ag-specific T-cells and NK

cells. While DCs do not support robust VSV replication, they can be infected ex vivo,

then used to mount a specific anti-tumor response. DCs infected with VSV encoding human melanoma-associated Ag dopachrome tautomerase (hDCT) endogenously expressed by B16-OVA cells, or luciferase tagged with the immunodominant class-I epitope SIINFEKL, were able to mature and produce pro-inflammatory cytokines (164). When mice with metastatic tumors received DCVSV/hDCT, tumor growth was controlled by both NK and CD8+ T-cells (164). In an even more sophisticated approach, a combination of an adenovirus and VSV both expressing hDCT were used sequentially. The adenovirus pre-immunization of *in vivo* murine DCT tumors did not prevent intratumoral VSV infection. Furthermore, this treatment resulted in reduced VSV replication in normal cells and a shift in immune activation from viral Ags to TAAs (266).

These approaches may be useful if a specific TAA is stably expressed, but in most cancer types TAA expression is variable, transient, and often unknown for individual tumors. In a new approach, a VSV-cDNA library was used to identify TAAs capable of inducing enhanced tumor specific immunity (267). The screen identified three viruses encoding putative TAAs, and their therapeutic effect against B16 murine melanoma tumors was reconstituted *in vivo* when these viruses were used together.

A fine balance between antiviral and anti-cancer responses is probably needed for effective OV therapy using VSV. For example, TLR signaling through myeloid differentiation primary response gene 88 (MyD88) activates specific antiviral immune responses that inhibit virus replication within the tumor, but also induces critical anti-cancer responses; a recent study has shown that VSV anti-tumor therapy in the B16-OVA mouse model depends on antiviral signaling through MyD88 (268).

Finally, while the majority of studies have demonstrated the desirable immunomodulation of the tumor microenvironment following VSV infection to favor tumor rejection, the opposite situation can also occur. A recent study demonstrated that VSV infection can negatively affect surface expression of immunostimulatory NKG2D-ligand, allowing viruses to escape immune recognition by NK cells, but negatively affecting anti-tumor immune responses (269).

4.4 Future Directions

With applications ranging from gene therapy to cancer targeting, a better understanding of the biological basis for VSV tropism is paramount. Recent identification of LDLR as a potential receptor for VSV is exciting (11), but additional studies confirming these results are necessary to explain the host range of VSV and also provide a means to predict and/or direct its tropism via receptor manipulation. Although the wide range tropism of VSV is a plus in many applications, other applications would benefit from more specific cell targeting. It is likely that more rationally designed VSV-based recombinants expressing foreign attachment genes will be generated to limit VSV tropism. Biosafety of such chimeras is an important issue as VSV expressing the p14 FAST reptilian reovirus virus fusion-associated protein demonstrated enhanced neurotoxicity in mice (250). Tropism and safety of VSV are greatly controlled by cellular IFN responses, which can be exploited to target and kill IFN defective cancer cells without damaging healthy tissues. However, new approaches are needed to specifically target cancer cells retaining functional IFN signaling. While WT VSV is not acceptable as a clinical vector, there are some conflicting reports even in regard to the safety of VSV recombinants depending on the route of administration (133). This is

particularly important for oncolytic applications of VSV in immunocompromised cancer patients. Potential evolution of VSV used in clinical applications should be more seriously studied. With more VSV recombinants likely to begin clinical trials, we expect to see an increased focus on preventing premature clearance of therapeutic VSV by host immune responses. VSV will continue to be one of the most popular viruses and because of its unique qualities it remains an essential tool for discovery of basic biological research and will play an important role in vaccine development, gene and oncolytic therapies.

To provide the best virus for clinical use, the 'perfect' therapeutic oncolytic VSV should cause no neurotoxicity, retain oncolytic ability, be easily adaptable to target specific cancer types, and induce immune memory toward the tumor. Based on these criteria, and the fact that host proteins can influence the VSV life cycle (Table 9), chapters two and three have provided informative groundwork with which to design and test potential methods to improve VSV OV therapy against PDAC.

Forecasting from the results shown in chapters two and three, future studies need to look at VSV's ability to stimulate the immune response toward cancer cells. VSV engineered to express a relevant tumor-associated antigen (TAA) such as MUC1 could be created. Studies with other tumor types utilized recombinant VSVs encoding TAAs like human melanoma-associated antigen (Ag) dopachrome tautomerase (164) or chicken ovalbumin (166, 268) demonstrated improved antitumor efficacy of VSV associated with the ability to generate increased numbers of TAA-specific T cells (166, 265). Also, other rVSVs expressing immune system-modulating cytokines or cancer suppressor proteins could be tested and compared to

Table 9: Host proteins potentially determining VSV tropism.

Common Protein name	Uniprot gene Name	Potential role in VSV life cycle	Selected References
Attachment			
Low Density Lipoprotein Receptor	LDLR	Proposed VSV cell surface receptor.	Finkelshtein et al. (2013)
Toll-like receptor 4	TLR4	Detects VSV G protein.	Georgel et al. (2007)
Toll-like receptor 13	TLR13	Detects VSV, but ligand is unknown.	Shi et al. (2011)
Heat Shock Protein 90 kDa Beta	HSP90B1 (Gp96)	Facilitates the correct folding of either a protein receptor or an enzyme required for the synthesis of a VSV receptor(s). May promote the stable configuration of VSV L multimers and facilitate the L-P interaction.	Bloor et al. (2010)
Entry			
Clathrin heavy chain	CLTC	Required for VSV endocytosis.	Sun et al. (2005)
Dynamin-1/2	DNM2-1/2	Binds VSV M to facilitate for virus assembly and budding.	Cureton et al. (2009), Raux et al. (2010)
Toll-like receptor 3	TLR3	Detects double-stranded RNA in endosomes.	Alexopoulou et al. (2001)
Toll-like receptor 7	TLR7	Detects single-stranded RNA in endosomes.	Diebold et al. (2004), Lund et al. (2004)
Toll-like receptor 8	TLR8	Detects single stranded RNA.	Heil et al. (2004)
Replication			
Peptidylprolyl Isomerase A (Cyclophilin A)	CYPA	Interacts with VSV N and is found bound to viral RNP in progeny. Required for VSV NJ replication, but not VSV IN.	Bose et al. (2003)
Casein kinase II	CSNK2A1	Phosphorylates VSV P to facilitate transcription.	Barik and Banerjee (1992)
Elongation factor 1-alpha 1	EEF1A1	Associates with VSV L to facilitate transcription.	Das et al. (1998)
Ubiquitin-60S ribosomal protein L40	UBA52	Required for VSV cap-dependent translation.	Lee et al. (2013)
Serrate RNA effector molecule homolog	SRRT/ARS2	Modulates antiviral responses to inhibit VSV infection.	Sabin et al. (2009)
Poly (RC) binding protein 1/2	PCBP-1/2	Interact with VSV P to inhibit viral mRNA synthesis.	Dinh et al. (2011)
Tubulin beta chain	TUBB	Facilitates transcription and may associate directly with VSV L.	Moyer et al. (1986)
60 kDa heat shock protein	HSPD1	Found to be bound to the transcriptase complex and in purified virions.	Qanungo et al. (2004)
mRNA-capping enzyme	RNGTT	Found to be bound to the transcriptase complex and in purified virions.	Qanungo et al. (2004)
Interferon-induced protein with tetratricopeptide repeats 2	IFIT2	Inhibits VSV replication as VSV titers rose several hundred folds higher in knockout mice compared to wt mice.	Fensterl et al. (2012)
Interferon induced transmembrane protein 3	IFITM3	Inhibits a post endocytosis event of VSV entry.	Weidner et al. (2010)
Interferon-induced GTP-binding protein Mx1	MX1	Inhibits VSV RNA synthesis.	Schwemmle et al. (1995)
2'-5'-Oligoadenylate Synthetase 1	OAS1	Detects single and double-stranded RNA with secondary structure and activates RNAseL, which degrades cellular mRNA.	Kumar et al. (1988)
Ubiquitin-like protein ISG15	ISG15	Regulator of antiviral proteins.	Zhao et al. (2005)
Probable ATP-dependent RNA helicase DDX58	DDX58/RIG-I	Detects uncapped 5'-triphosphate RNA and signals type I IFN production.	Hornung et al. (2006), Kato et al. (2006)
Interferon-induced, double-stranded RNA-activated protein kinase	EIF2AK2/PKR	Detects double-stranded RNA and inhibits translation of viral mRNAs through phosphorylation of eukaryotic translation initiation factor 2α.	Balachandran et al. (2000)
Interferon-induced helicase C domain-containing protein 1	IFIH1/MDA5	Recognizes dsRNA to facilitate antiviral signaling.	Kato et al. (2006)
TATA-box-binding protein	TBP/TFIID	VSV inhibits cellular host transcription by inactivation of TFIID.	Yuan et al. (1998)
tumor susceptibility gene 101	TSG101	Plays a role in nucleocapsid release from endosomes to the cytoplasm	Luyet et al. (2008)
Interferon alpha-1/13/Interferon beta	IFNA1/IFNB1	Key cytokine responsible for promoting upregulation of antiviral genes.	Gresser et al. (1979)
Interferon regulatory factor 3 and 7	IRF3, IRF7	VSV infection causes results in activation and upregulations of this transcription factor that upregulates type I IFN production for antiviral response.	Stojdl (2003)
Signal transducer and activator of transcription 1-alpha/beta	STAT1	Activation of STAT1 via IFN signaling results in this transcription factor causing upregulation of antiviral genes.	Wong et al. (2001)
Lupus La protein	SSB/La	Binds to VSV leader RNAs and may influence transcription of full-length genome.	Wilusz et al. (1983)
Assembly and Exit			
Actin			Cureton et al. (2009)
E3 ubiquitin-protein ligase NEDD4	NEDD4	A role in VSV budding.	Irie et al. (2004)
78 kDa glucose-regulated protein	HSPA5/GRP78	A role in folding of VSV G.	Hammond and Helenius (1994)
Common Protein name	Uniprot gene Name	Potential role in VSV life cycle	Selected References
Calnexin	CANX	A role in folding of VSV G.	Hammond and Helenius (1994)
Dynamin-1/2	DNM2-1/2	Binds VSV M to facilitate for virus assembly and budding.	Cureton et al. (2009), Raux et al. (2010)
Bone marrow stromal antigen 2/Tetherin	BST2	May impair VSV release.	Sarojini et al. (2011), Weidner et al. (2010)

VSV-ΔM51-GFP (51).

There is evidence that VSV expressing p53 has such a function, but this will need to be tested *in vivo*. Interestingly, the outcome of treatment may be dependent on the amount of virus used. At lower concentration, for an oncolytic VSV recombinant, antitumor effects were improved compared to higher concentrations (115), suggesting that the increased viral presence biases the immune response against viral antigens rather than tumor cell antigens. However, recently it was shown with a VSV vaccine vector that robust replication of VSV could be required for efficient adaptive immune responses against non-VSV antigen (270). Therefore, future experiments should study dose-dependent efficacy of VSV against PDAC tumors.

Additional strategies seek to use combinational therapies to improve oncolysis. A recombinant virus expressing a sodium iodide symporter, when coupled with iodine-131 radiation therapy, resulted in an enhanced oncolytic effect in radiation-sensitive tumors (251). Finally, OV therapy has been tested in combination with chemotherapeutics like obatoclax (248) or EM20-25 (247) (inhibitors of BCL-2) or doxorubin (intercalates DNA) (249), with all showing enhanced oncolysis compared to VSV monotherapy. When we tested a combinational treatment of VSV-ΔM51-GFP and a commonly used PDAC chemotherapeutic, gemcitabine, significant improvement was observed compared to use of VSV-ΔM51-GFP alone. In addition to its role as a chemotherapeutic, gemcitabine was shown to deplete B cells (271). While the antibody response was similar in the VSV-ΔM51-GFP alone and VSV-ΔM51-GFP plus gemcitabine groups at the endpoint, it is possible that gemcitabine contributed to the prolonged tumor reduction in this group. It should also be noted that gemcitabine had

no effect on VSV-ΔM51-GFP replication *in vitro* (data not shown). Future experiments will study the potential of VSV with gemcitabine (or other drugs) using additional concentrations and treatment schedules in different model systems.

Common to both studies, MUC1 and p53, and relevant to clinical investigation are the models being used for study in addition to the method of virus manufacturing. Use of spontaneous PDAC tumor models would prove more physiologically relevant and allow for a better means of monitoring of systemic virus infection and spread than we see in subcutaneous xenograft models. Regarding the p53 study, use of immunocompetent mice will be important to monitor the effect of p53 transgene activity on any potential tumor specific immune response. Specifically, recently described humanized mice may provide the best system for this task so that human-derived cancers can be studied in an animal context.

Finally, the development of good manufacturing practices (GMP) for virus production needs to be explored in more detail. Importantly, the cell line used for VSV amplification is necessary to ensure that the virus used for therapy is free of contaminants and optimized for clinical use (272, 273). Interestingly, in a pilot study, we demonstrated that VSV grown in murine cells expressing human MUC1 has enhanced oncolytic efficacy against PDAC compared to VSV grown in the standard BHK cell line (data not shown). It is unclear if cell-line specific membrane proteins incorporated into the virus envelope reduce premature clearance of virus from the system. Future work will need to explore human cell lines for production of virus used to treat human malignancy and determine if different cancer types will need to be treated most effectively with virus grown in different cell lines.

REFERENCES

1.	Russell SJ, Peng KW. 2007. Viruses as anticancer drugs. Trends Pharmacol Sci 28:326-333.

2.	Hammill AM, Conner J, Cripe TP. 2010. Oncolytic virotherapy reaches adolescence. Pediatric blood & cancer 55:1253-1263.

3.	Lyles DS R, CE. 2007. Rhabdoviridae, p. 1363-1408. *In* In: DM Knipe and PM Howley e (ed.), Fields Virology. Lippincott Williams & Wilkins, Philadelphia, 5th edition.

4.	Drolet BS, Stuart MA, Derner JD. 2009. Infection of Melanoplus sanguinipes grasshoppers following ingestion of rangeland plant species harboring vesicular stomatitis virus. Appl Environ Microbiol 75:3029-3033.

5.	Hansen DE, Thurmond MC, Thorburn M. 1985. Factors associated with the spread of clinical vesicular stomatitis in California dairy cattle. Am J Vet Res 46:789-795.

6.	Ge P, Tsao J, Schein S, Green TJ, Luo M, Zhou ZH. 2010. Cryo-EM model of the bullet-shaped vesicular stomatitis virus. Science 327:689-693.

7.	Roche S, Albertini AA, Lepault J, Bressanelli S, Gaudin Y. 2008. Structures of vesicular stomatitis virus glycoprotein: membrane fusion revisited. Cell Mol Life Sci 65:1716-1728.

8.	Gillies S, Stollar V. 1980. The production of high yields of infectious vesicular stomatitis virus in A. albopictus cells and comparisons with replication in BHK-21 cells. Virology 107:509-513.

9.	Mudd JA, Leavitt RW, Kingsbury DT, Holland JJ. 1973. Natural selection of mutants of vesicular stomatitis virus by cultured cells of Drosophila melanogaster. The Journal of general virology 20:341-351.

10.	Seganti L, Superti F, Girmenia C, Melucci L, Orsi N. 1986. Study of receptors for vesicular stomatitis virus in vertebrate and invertebrate cells. Microbiologica 9:259-267.

11.	Finkelshtein D, Werman A, Novick D, Barak S, Rubinstein M. 2013. LDL receptor and its family members serve as the cellular receptors for vesicular stomatitis virus. Proc Natl Acad Sci USA 110:7306-7311.

12.	Superti F, Seganti L, Ruggeri FM, Tinari A, Donelli G, Orsi N. 1987. Entry pathway of vesicular stomatitis virus into different host cells. The Journal of general virology 68 (Pt 2):387-399.

13.   Johannsdottir HK, Mancini R, Kartenbeck J, Amato L, Helenius A. 2009. Host cell factors and functions involved in vesicular stomatitis virus entry. J Virol 83:440-453.

14.   Cureton DK, Massol RH, Saffarian S, Kirchhausen TL, Whelan SP. 2009. Vesicular stomatitis virus enters cells through vesicles incompletely coated with clathrin that depend upon actin for internalization. PLoS pathogens 5:e1000394.

15.   Le Blanc I, Luyet PP, Pons V, Ferguson C, Emans N, Petiot A, Mayran N, Demaurex N, Faure J, Sadoul R, Parton RG, Gruenberg J. 2005. Endosome-to-cytosol transport of viral nucleocapsids. Nat Cell Biol 7:653-664.

16.   Roth SL, Whittaker GR. 2011. Promotion of vesicular stomatitis virus fusion by the endosome-specific phospholipid bis(monoacylglycero)phosphate (BMP). FEBS Lett 585:865-869.

17.   Gao Y, Lenard J. 1995. Cooperative binding of multimeric phosphoprotein (P) of vesicular stomatitis virus to polymerase (L) and template: pathways of assembly. J Virol 69:7718-7723.

18.   Green TJ, Luo M. 2009. Structure of the vesicular stomatitis virus nucleocapsid in complex with the nucleocapsid-binding domain of the small polymerase cofactor, P. Proc Natl Acad Sci USA 106:11713-11718.

19.   Emerson SU, Wagner RR. 1973. L protein requirement for in vitro RNA synthesis by vesicular stomatitis virus. J Virol 12:1325-1335.

20.   Grdzelishvili VZ, Smallwood S, Tower D, Hall RL, Hunt DM, Moyer SA. 2005. A single amino acid change in the L-polymerase protein of vesicular stomatitis virus completely abolishes viral mRNA cap methylation. J Virol 79:7327-7337.

21.   Grdzelishvili VZ, Smallwood S, Tower D, Hall RL, Hunt DM, Moyer SA. 2006. Identification of a new region in the vesicular stomatitis virus L polymerase protein which is essential for mRNA cap methylation. Virology 350:394-405.

22.   Hercyk N, Horikami SM, Moyer SA. 1988. The vesicular stomatitis virus L protein possesses the mRNA methyltransferase activities. Virology 163:222-225.

23.   Hunt DM. 1983. Vesicular stomatitis virus mutant with altered polyadenylic acid polymerase activity in vitro. J Virol 46:788-799.

24.   Hunt DM. 1989. Effect of analogues of S-adenosylmethionine on in vitro polyadenylation by vesicular stomatitis virus. The Journal of general virology 70 (Pt 3):535-542.

25. Li J, Fontaine-Rodriguez EC, Whelan SP. 2005. Amino acid residues within conserved domain VI of the vesicular stomatitis virus large polymerase protein essential for mRNA cap methyltransferase activity. J Virol 79:13373-13384.

26. Li J, Rahmeh A, Morelli M, Whelan SP. 2008. A conserved motif in region v of the large polymerase proteins of nonsegmented negative-sense RNA viruses that is essential for mRNA capping. J Virol 82:775-784.

27. Ogino T, Banerjee AK. 2007. Unconventional mechanism of mRNA capping by the RNA-dependent RNA polymerase of vesicular stomatitis virus. Mol Cell 25:85-97.

28. Sleat DE, Banerjee AK. 1993. Transcriptional activity and mutational analysis of recombinant vesicular stomatitis virus RNA polymerase. J Virol 67:1334-1339.

29. Hastie E, Cataldi M, Marriott I, Grdzelishvili VZ. 2013. Understanding and altering cell tropism of vesicular stomatitis virus. Virus Res 176:16-32.

30. Connor JH, Lyles DS. 2002. Vesicular stomatitis virus infection alters the eIF4F translation initiation complex and causes dephosphorylation of the eIF4E binding protein 4E-BP1. J Virol 76:10177-10187.

31. Mire CE, Whitt MA. 2011. The protease-sensitive loop of the vesicular stomatitis virus matrix protein is involved in virus assembly and protein translation. Virology 416:16-25.

32. Whitlow ZW, Connor JH, Lyles DS. 2006. Preferential translation of vesicular stomatitis virus mRNAs is conferred by transcription from the viral genome. J Virol 80:11733-11742.

33. Whitlow ZW, Connor JH, Lyles DS. 2008. New mRNAs are preferentially translated during vesicular stomatitis virus infection. J Virol 82:2286-2294.

34. Masters PS, Banerjee AK. 1988. Resolution of multiple complexes of phosphoprotein NS with nucleocapsid protein N of vesicular stomatitis virus. J.Virol. 62:2651-2657.

35. Peluso RW, Moyer SA. 1988. Viral proteins required for the in vitro replication of vesicular stomatitis virus defective interfering particle genome RNA. Virology 162:369-376.

36. Qanungo KR, Shaji D, Mathur M, Banerjee AK. 2004. Two RNA polymerase complexes from vesicular stomatitis virus-infected cells that carry out transcription and replication of genome RNA. Proc Natl Acad Sci USA 101:5952-5957.

37. Dinh PX, Beura LK, Panda D, Das A, Pattnaik AK. 2011. Antagonistic effects of cellular poly(c) binding proteins on vesicular stomatitis virus gene expression. J Virol 85:9459-9471.

38. Heinrich BS, Cureton DK, Rahmeh AA, Whelan SP. 2010. Protein expression redirects vesicular stomatitis virus RNA synthesis to cytoplasmic inclusions. PLoS pathogens 6.

39. Holland JJ, Domingo E, de la Torre JC, Steinhauer DA. 1990. Mutation frequencies at defined single codon sites in vesicular stomatitis virus and poliovirus can be increased only slightly by chemical mutagenesis. J Virol 64:3960-3962.

40. Steinhauer DA, de la Torre JC, Holland JJ. 1989. High nucleotide substitution error frequencies in clonal pools of vesicular stomatitis virus. J Virol 63:2063-2071.

41. Steinhauer DA, Holland JJ. 1986. Direct method for quantitation of extreme polymerase error frequencies at selected single base sites in viral RNA. J Virol 57:219-228.

42. Colonno RJ, Lazzarini RA, Keene JD, Banerjee AK. 1977. In vitro synthesis of messenger RNA by a defective interfering particle of vesicular stomatitis virus. Proc Natl Acad Sci USA 74:1884-1888.

43. Perrault J, Leavitt RW. 1978. Inverted complementary terminal sequences in single-stranded RNAs and snap-back RNAs from vesicular stomatitis defective interfering particles. The Journal of general virology 38:35-50.

44. Swinteck BD, Lyles DS. 2008. Plasma membrane microdomains containing vesicular stomatitis virus M protein are separate from microdomains containing G protein and nucleocapsids. J Virol 82:5536-5547.

45. Das SC, Nayak D, Zhou Y, Pattnaik AK. 2006. Visualization of intracellular transport of vesicular stomatitis virus nucleocapsids in living cells. J Virol 80:6368-6377.

46. Harty RN, Paragas J, Sudol M, Palese P. 1999. A proline-rich motif within the matrix protein of vesicular stomatitis virus and rabies virus interacts with WW domains of cellular proteins: implications for viral budding. J Virol 73:2921-2929.

47. Raux H, Obiang L, Richard N, Harper F, Blondel D, Gaudin Y. 2010. The matrix protein of vesicular stomatitis virus binds dynamin for efficient viral assembly. J Virol 84:12609-12618.

48.   Harty RN, Brown ME, McGettigan JP, Wang G, Jayakar HR, Huibregtse JM, Whitt MA, Schnell MJ. 2001. Rhabdoviruses and the cellular ubiquitin-proteasome system: a budding interaction. J Virol 75:10623-10629.

49.   Moerdyk-Schauwecker M, Hwang SI, Grdzelishvili VZ. 2009. Analysis of virion associated host proteins in vesicular stomatitis virus using a proteomics approach. Virol J 6:166.

50.   Moerdyk-Schauwecker M, Hwang SI, Grdzelishvili VZ. 2014. Cellular proteins associated with the interior and exterior of vesicular stomatitis virus virions. PloS one 9:e104688.

51.   Hastie E, Grdzelishvili VZ. 2012. Vesicular stomatitis virus as a flexible platform for oncolytic virotherapy against cancer. The Journal of general virology 93:2529-2545.

52.   Garber K. 2006. China approves world's first oncolytic virus therapy for cancer treatment. J Natl Cancer Inst 98:298-300.

53.   Quiroz E, Moreno N, Peralta PH, and Tesh RB. 1988. A human case of encephalitis associated with vesicular stomatitis virus (Indiana serotype) infection. Am J Trop Med Hyg 39:312-314.

54.   Dal Canto MC, Rabinowitz SG, Johnson TC. 1976. Status spongiousus resulting from intracerebral infection of mice with temperature-sensitive mutants of vesicular stomatitis virus. Br J Exp Pathol 57:321-330.

55.   Plakhov IV, Arlund EE, Aoki C, Reiss CS. 1995. The earliest events in vesicular stomatitis virus infection of the murine olfactory neuroepithelium and entry of the central nervous system. Virology 209:257-262.

56.   Shinozaki K, Ebert O, Woo SL. 2005. Treatment of multi-focal colorectal carcinoma metastatic to the liver of immune-competent and syngeneic rats by hepatic artery infusion of oncolytic vesicular stomatitis virus. International journal of cancer. Journal international du cancer 114:659-664.

57.   Schellekens H, Smiers-de Vreede E, de Reus A, Dijkema R. 1984. Antiviral activity of interferon in rats and the effect of immune suppression. The Journal of general virology 65:391-396.

58.   Bi Z, Quandt P, Komatsu T, Barna M, Reiss CS. 1995. IL-12 promotes enhanced recovery from vesicular stomatitis virus infection of the central nervous system. J Immunol 155:5684-5689.

59.   Reiss CS, Plakhov IV, Komatsu T. 1998. Viral replication in olfactory receptor neurons and entry into the olfactory bulb and brain. Ann NY Acad Sci 855:751-761.

60.   van den Pol A, Dalton K, Rose J. 2002. Relative neurotropism of a recombinant rhabdovirus expressing a green fluorescent envelope glycoprotein. J Virol 76:1309-1327.

61.   Frei K, Malipiero UV, Leist TP, Zinkernagel RM, Schwab ME, Fontana A. 1989. On the cellular source and function of interleukin-6 produced in the central nervous-system in viral diseases. European Journal of Immunology 19:689-694.

62.   Huneycutt BS, Bi Z, Aoki CJ, Reiss CS. 1993. Central neuropathogenesis of vesicular stomatitis virus infection of immunodeficient mice. J Virol 67:6698-6706.

63.   Chauhan VS, Furr SR, Sterka DG, Jr., Nelson DA, Moerdyk-Schauwecker M, Marriott I, Grdzelishvili VZ. 2010. Vesicular stomatitis virus infects resident cells of the central nervous system and induces replication-dependent inflammatory responses. Virology 400:187-196.

64.   Furr SR, Chauhan VS, Sterka D, Jr., Grdzelishvili V, Marriott I. 2008. Characterization of retinoic acid-inducible gene-I expression in primary murine glia following exposure to vesicular stomatitis virus. J Neurovirol:1-11.

65.   Furr SR, Moerdyk-Schauwecker M, Grdzelishvili VZ, Marriott I. 2010. RIG-I mediates nonsegmented negative-sense RNA virus-induced inflammatory immune responses of primary human astrocytes. Glia 58:1620-1629.

66.   Wollmann G, Rogulin V, Simon I, Rose JK, AN vdP. 2010. Some attenuated variants of vesicular stomatitis virus show enhanced oncolytic activity against human glioblastoma cells relative to normal brain cells. J Virol 84:1563-1573.

67.   Ahmed M, McKenzie MO, Puckett S, Hojnacki M, Poliquin L, Lyles DS. 2003. Ability of the matrix protein of vesicular stomatitis virus to suppress beta interferon gene expression is genetically correlated with the inhibition of host RNA and protein synthesis. J Virol 77:4646-4657.

68.   Kopecky SA, Willingham MC, Lyles DS. 2001. Matrix protein and another viral component contribute to induction of apoptosis in cells infected with vesicular stomatitis virus. J Virol 75:12169-12181.

69.   Stojdl DF, Lichty BD, tenOever BR, Paterson JM, Power AT, Knowles S, Marius R, Reynard J, Poliquin L, Atkins H, Brown EG, Durbin RK, Durbin JE, Hiscott J, JC B. 2003. VSV strains with defects in their ability to shutdown innate immunity are potent systemic anti-cancer agents. Cancer cell 4:263-275.

70.   Cary ZD, Willingham MC, Lyles DS. 2011. Oncolytic Vesicular Stomatitis Virus Induces Apoptosis in U87 Glioblastoma Cells by a Type II Death Receptor Mechanism and Induces Cell Death and Tumor Clearance In Vivo. J Virol 85:5708-5717.

71. Gaddy DF, and Lyles DS. 2005. Vesicular stomatitis viruses expressing wild-type or mutant M proteins activate apoptosis through distinct pathways. J Virol 79:4170-4179.

72. Barber GN. 2004. Vesicular stomatitis virus as an oncolytic vector. Viral Immunol 17:516-527.

73. Lichty BD, Power AT, Stojdl DF, and Bell JC. 2004. Vesicular stomatitis virus: re-inventing the bullet. Trends Mol Med 10:210-216.

74. Stojdl DF, Lichty BD, Knowles S, Marius R, Atkins H, Sonenberg N, Bell JC. 2000. Exploiting tumor-specific defects in the interferon pathway with a previously unknown oncolytic virus. Nature medicine 6:821-825.

75. Balachandran S, Barber GN. 2004. Defective translational control facilitates vesicular stomatitis virus oncolysis. Cancer cell 5:51-65.

76. Marozin S, Altomonte J, Stadler F, Thasler WE, Schmid RM, Ebert O. 2008. Inhibition of the IFN-beta response in hepatocellular carcinoma by alternative spliced isoform of IFN regulatory factor-3. Molecular therapy : the journal of the American Society of Gene Therapy 16:1789-1797.

77. Moussavi M, Fazli L, Tearle H, Guo Y, Cox M, Bell J, Ong C, Jia W, Rennie PS. 2010. Oncolysis of prostate cancers induced by vesicular stomatitis virus in PTEN knockout mice. Cancer Res 70:1367-1376.

78. Zhang KX, Matsui Y, Hadaschik BA, Lee C, Jia W, Bell JC, Fazli L, So AI, Rennie PS. 2010. Down-regulation of type I interferon receptor sensitizes bladder cancer cells to vesicular stomatitis virus-induced cell death. International journal of cancer. Journal international du cancer 127:830-838.

79. Noser JA, Mael AA, Sakuma R, Ohmine S, Marcato P, Lee PW, Ikeda Y. 2007. The RAS/Raf1/MEK/ERK signaling pathway facilitates VSV-mediated oncolysis: implication for the defective interferon response in cancer cells. Molecular therapy : the journal of the American Society of Gene Therapy 15:1531-1536.

80. Li Q, Tainsky MA. 2011. Epigenetic silencing of IRF7 and/or IRF5 in lung cancer cells leads to increased sensitivity to oncolytic viruses. PLoS One 6:e28683.

81. Oliere S, Arguello M, Mesplede T, Tumilasci V, Nakhaei P, Stojdl D, Sonenberg N, Bell J, Hiscott J. 2008. Vesicular stomatitis virus oncolysis of T lymphocytes requires cell cycle entry and translation initiation. J Virol 82:5735-5749.

82. Balachandran S, Barber GN. 2007. PKR in innate immunity, cancer, and viral oncolysis. Methods in molecular biology 383:277-301.

83. Harashima A, Guettouche T, Barber GN. 2010. Phosphorylation of the NFAR proteins by the dsRNA-dependent protein kinase PKR constitutes a novel mechanism of translational regulation and cellular defense. Genes & development 24:2640-2653.

84. Wang BX, Rahbar R, Fish EN. 2011. Interferon: current status and future prospects in cancer therapy. Journal of interferon & cytokine research : the official journal of the International Society for Interferon and Cytokine Research 31:545-552.

85. Naik S, Russell SJ. 2009. Engineering oncolytic viruses to exploit tumor specific defects in innate immune signaling pathways. Expert Opin Biol Ther 9:1163-1176.

86. Saloura V, Wang LC, Fridlender ZG, Sun J, Cheng G, Kapoor V, Sterman DH, Harty RN, Okumura A, Barber GN, Vile RG, Federspiel MJ, Russell SJ, Litzky L, Albelda SM. 2010. Evaluation of an attenuated vesicular stomatitis virus vector expressing interferon-beta for use in malignant pleural mesothelioma: heterogeneity in interferon responsiveness defines potential efficacy. Hum Gene Ther 21:51-64.

87. Linge C, Gewert D, Rossmann C, Bishop JA, Crowe JS. 1995. Interferon system defects in human malignant melanoma. Cancer Res 55:4099-4104.

88. Wong LH, Krauer KG, Hatzinisiriou I, Estcourt MJ, Hersey P, Tam ND, Edmondson S, Devenish RJ, Ralph SJ. 1997. Interferon-resistant human melanoma cells are deficient in ISGF3 components, STAT1, STAT2, and p48-ISGF3gamma. J Biol Chem 272:28779-28785.

89. Sun WH, Pabon C, Alsayed Y, Huang PP, Jandeska S, Uddin S, Platanias LC, Rosen ST. 1998. Interferon-alpha resistance in a cutaneous T-cell lymphoma cell line is associated with lack of STAT1 expression. Blood 91:570-576.

90. Matin SF, Rackley RR, Sadhukhan PC, Kim MS, Novick AC, Bandyopadhyay SK. 2001. Impaired alpha-interferon signaling in transitional cell carcinoma: lack of p48 expression in 5637 cells. Cancer Res 61:2261-2266.

91. Pfeffer LM, Wang C, Constantinescu SN, Croze E, Blatt LM, Albino AP, Nanus DM. 1996. Human renal cancers resistant to IFN's antiproliferative action exhibit sensitivity to IFN's gene-inducing and antiviral actions. J Urol 156:1867-1871.

92. Tarver T. 2012. Cancer Facts & Figures 2012. American Cancer Society (ACS). J Consum Health Internet 16:366-367.

93. Stathis A, Moore MJ. 2010. Advanced pancreatic carcinoma: current treatment and future challenges. Nature reviews. Clinical oncology 7:163-172.

94. Farrow B, Albo D, Berger DH. 2008. The role of the tumor microenvironment in the progression of pancreatic cancer. J Surg Res 149:319-328.

95. Lindsay TH, Jonas BM, Sevcik MA, Kubota K, Halvorson KG, Ghilardi JR, Kuskowski MA, Stelow EB, Mukherjee P, Gendler SJ, Wong GY, and Mantyh PW. 2005. Pancreatic cancer pain and its correlation with changes in tumor vasculature, macrophage infiltration, neuronal innervation, body weight and disease progression. Pain 119:233-246.

96. Jonckheere N, Skrypek S, Van Seuningen I. 2010. Mucins and pancreatic cancer. Cancers:1794-1812.

97. Reichert M, Rustgi AK. 2011. Pancreatic ductal cells in development, regeneration, and neoplasia. The J of Clin Investig 121:4572-4578.

98. Besmer DM, Curry JM, Roy LD, Tinder TL, Sahraei M, Schettini JL, Hwang SI, Lee YY, Gendler SJ, Mukherjee P. 2011. Pancreatic Ductal Adenocarcinoma (PDA) mice lacking Mucin 1 have a profound defect in tumor growth and metastasis. Cancer Res.

99. Horm TM, Schroeder JA. 2013. MUC1 and metastatic cancer: Expression, function and therapeutic targeting. Cell Adh Migr 7.

100. Kalra AV, Campbell RB. 2009. Mucin overexpression limits the effectiveness of 5-FU by reducing intracellular drug uptake and antineoplastic drug effects in pancreatic tumours. Eur J Cancer 45:164-173.

101. Roy LD, Sahraei M, Subramani DB, Besmer D, Nath S, Tinder TL, Bajaj E, Shanmugam K, Lee YY, Hwang SI, Gendler SJ, Mukherjee P. 2011. MUC1 enhances invasiveness of pancreatic cancer cells by inducing epithelial to mesenchymal transition. Oncogene 30:1449-1459.

102. Kalra AV, Campbell RB. 2007. Mucin impedes cytotoxic effect of 5-FU against growth of human pancreatic cancer cells: overcoming cellular barriers for therapeutic gain. Br J Cancer 97:910-918.

103. Maitra A, Hruban RH. 2008. Pancreatic cancer. Annual review of pathology 3:157-188.

104. Moerdyk-Schauwecker M, Shah NR, Murphy AM, Hastie E, Mukherjee P, Grdzelishvili VZ. 2013. Resistance of pancreatic cancer cells to oncolytic vesicular stomatitis virus: role of type I interferon signaling. Virology 436:221-234.

105. Murphy AM, Besmer DM, Moerdyk-Schauwecker M, Moestl N, Ornelles DA, Mukherjee P, Grdzelishvili VZ. 2012. Vesicular stomatitis virus as an oncolytic agent against pancreatic ductal adenocarcinoma. J Virol 86:3073-3087.

106. Habte HH, de Beer C, Lotz ZE, Tyler MG, Kahn D, Mall AS. 2008. Inhibition of human immunodeficiency virus type 1 activity by purified human breast milk mucin (MUC1) in an inhibition assay. Neonatology 93:162-170.

107. Saeland E, de Jong MA, Nabatov AA, Kalay H, Geijtenbeek TB, van Kooyk Y. 2009. MUC1 in human milk blocks transmission of human immunodeficiency virus from dendritic cells to T cells. Mol Immunol 46:2309-2316.

108. Kvistgaard AS, Pallesen LT, Arias CF, Lopez S, Petersen TE, Heegaard CW, Rasmussen JT. 2004. Inhibitory effects of human and bovine milk constituents on rotavirus infections. J Dairy Sci 87:4088-4096.

109. Walters RW, Pilewski JM, Chiorini JA, Zabner J. 2002. Secreted and transmembrane mucins inhibit gene transfer with AAV4 more efficiently than AAV5. J Biol Chem 277:23709-23713.

110. Schnell MJ, Buonocore L, Kretzschmar E, Johnson E, Rose JK. 1996. Foreign glycoproteins expressed from recombinant vesicular stomatitis viruses are incorporated efficiently into virus particles. Proc Natl Acad Sci U S A 93:11359-11365.

111. Wertz GW, Moudy R, Ball LA. 2002. Adding genes to the RNA genome of vesicular stomatitis virus: positional effects on stability of expression. J Virol 76:7642-7650.

112. Cheok CF, Verma CS, Baselga J, Lane DP. 2011. Translating p53 into the clinic. Nature reviews. Clinical oncology 8:25-37.

113. Lane DP, Cheok CF, Lain S. 2010. p53-based cancer therapy. Cold Spring Harb Perspect Biol 2:a001222.

114. Lowe J, Shatz M, Resnick MA, Mendez D. 2013. Modulation of immune responses by the tumor suppressor p53. BioDiscovery 8.

115. Heiber JF, Barber GN. 2011. Vesicular stomatitis virus expressing tumor suppressor p53 is a highly attenuated, potent oncolytic agent. J Virol 85:10440-10450.

116. Okal A, Mossalam M, Matissek KJ, Dixon AS, Moos PJ, Lim CS. 2013. A chimeric p53 evades mutant p53 transdominant inhibition in cancer cells. Molecular pharmaceutics 10:3922-3933.

117. Habte HH, Kotwal GJ, Lotz ZE, Tyler MG, Abrahams M, Rodriques J, Kahn D, Mall AS. 2007. Antiviral activity of purified human breast milk mucin. Neonatology 92:96-104.

118. Obuchi M, Fernandez M, Barber GN. 2003. Development of recombinant vesicular stomatitis viruses that exploit defects in host defense to augment specific oncolytic activity. J Virol 77:8843-8856.

119. Hastie E, Besmer DM, Shah NR, Murphy AM, Moerdyk-Schauwecker M, Molestina C, Roy LD, Curry JM, Mukherjee P, Grdzelishvili VZ. 2013. Oncolytic Vesicular Stomatitis Virus in an Immunocompetent Model of MUC1-Positive or MUC1-Null Pancreatic Ductal Adenocarcinoma. J Virol 87:10283-10294.

120. Hingorani SR, Petricoin EF, Maitra A, Rajapakse V, King C, Jacobetz MA, Ross S, Conrads TP, Veenstra TD, Hitt BA, Kawaguchi Y, Johann D, Liotta LA, Crawford HC, Putt ME, Jacks T, Wright CV, Hruban RH, Lowy AM, Tuveson DA. 2003. Preinvasive and invasive ductal pancreatic cancer and its early detection in the mouse. Cancer cell 4:437-450.

121. Morikane K, Tempero RM, Sivinski CL, Nomoto M, Van Lith ML, Muto T, Hollingsworth MA. 1999. Organ-specific pancreatic tumor growth properties and tumor immunity. Cancer Immunol, Immunother: CII 47:287-296.

122. Schroeder JA, Thompson MC, Gardner MM, Gendler SJ. 2001. Transgenic MUC1 interacts with epidermal growth factor receptor and correlates with mitogen-activated protein kinase activation in the mouse mammary gland. The J of Biol Chem 276:13057-13064.

123. Taylor-Papadimitriou J, Peterson JA, Arklie J, Burchell J, Ceriani RL, Bodmer WF. 1981. Monoclonal antibodies to epithelium-specific components of the human milk fat globule membrane: production and reaction with cells in culture. International J of Cancer 28:17-21.

124. Croce MV, Isla-Larrain M, Remes-Lenicov F, Colussi AG, Lacunza E, Kim KC, Gendler SJ, Segal-Eiras A. 2006. MUC1 cytoplasmic tail detection using CT33 polyclonal and CT2 monoclonal antibodies in breast and colorectal tissue. Histology and histopathology 21:849-855.

125. Moyer SA, Baker SC, Lessard JL. 1986. Tubulin: a factor necessary for the synthesis of both Sendai virus and vesicular stomatitis virus RNAs. Proc Natl Acad Sci USA 83:5405-5409.

126. Lawson ND, Stillman EA, Whitt MA, Rose JK. 1995. Recombinant vesicular stomatitis viruses from DNA. Proc Natl Acad Sci USA 92:4477-4481.

127. Kalvodova L SJ, Cordo S, Ejsing CS, Shevchenko A, Simons K. 2009. The lipidomes of vesicular stomatitis virus, semliki forest virus, and the host plasma membrane analyzed by quantitative shotgun mass spectrometry. J Virol 83:7996-8003.

128. Rowse GJ, Tempero RM, VanLith ML, Hollingsworth MA, Gendler SJ. 1998. Tolerance and immunity to MUC1 in a human MUC1 transgenic murine model. Cancer Res 58:315-321.

129. Tinder TL, Subramani DB, Basu GD, Bradley JM, Schettini J, Million A, Skaar T, and Mukherjee P. 2008. MUC1 enhances tumor progression and contributes toward immunosuppression in a mouse model of spontaneous pancreatic adenocarcinoma. The Journal of Immunol 181:3116-3125.

130. Spicer AP, Rowse GJ, Lidner TK, and Gendler SJ. 1995. Delayed mammary tumor progression in Muc-1 null mice. J Biol Chem 270:30093-30101.

131. Corbett TH, Roberts BJ, Leopold WR, Peckham JC, Wilkoff LJ, Griswold DP, Jr., Schabel FM, Jr. 1984. Induction and chemotherapeutic response of two transplantable ductal adenocarcinomas of the pancreas in C57BL/6 mice. Cancer Res 44:717-726.

132. Ahmed M, Marino TR, Puckett S, Kock ND, Lyles DS. 2008. Immune response in the absence of neurovirulence in mice infected with m protein mutant vesicular stomatitis virus. J Virol 82:9273-9277.

133. Johnson JE, Nasar F, Coleman JW, Price RE, Javadian A, Draper K, Lee M, Reilly PA, Clarke DK, Hendry RM, Udem SA. 2007. Neurovirulence properties of recombinant vesicular stomatitis virus vectors in non-human primates. Virology 360:36-49.

134. Dalton KP, Rose JK. 2001. Vesicular stomatitis virus glycoprotein containing the entire green fluorescent protein on its cytoplasmic domain is incorporated efficiently into virus particles. Virology 279:414-421.

135. Fernandez M, Porosnicu M, Markovic D, Barber GN. 2002. Genetically engineered vesicular stomatitis virus in gene therapy: application for treatment of malignant disease. J Virol 76:895-904.

136. Wu L, Huang TG, Meseck M, Altomonte J, Ebert O, Shinozaki K, García-Sastre A, Fallon J, Mandeli J, SL. W. 2008. rVSV(M Delta 51)-M3 is an effective and safe oncolytic virus for cancer therapy. Human Gene Therapy 19:635-647.

137. Bi Z, Barna M, Komatsu T, Reiss CS. 1995. Vesicular stomatitis virus infection of the central nervous system activates both innate and acquired immunity. J Virol 69:6466-6472.

138. Ansari D, Tingstedt B, Andersson R. 2012. Pancreatic cancer - cost for overtreatment with gemcitabine. Acta Oncol.

139. Kovarik A, Peat N, Wilson D, Gendler SJ, Taylor-Papadimitriou J. 1993. Analysis of the tissue-specific promoter of the MUC1 gene. J Biol Chem 268:9917-9926.

140. Mukherjee P, Basu GD, Tinder TL, Subramani DB, Bradley JM, Arefayene M, Skaar T, De Petris G. 2009. Progression of pancreatic adenocarcinoma is significantly impeded with a combination of vaccine and COX-2 inhibition. J Immunol 182:216-224.

141. Jonckheere N, Van Seuningen I. 2010. The membrane-bound mucins: From cell signalling to transcriptional regulation and expression in epithelial cancers. Biochimie 92:1-11.

142. Kim GE, Bae HI, Park HU, Kuan SF, Crawley SC, Ho JJ, Kim YS. 2002. Aberrant expression of MUC5AC and MUC6 gastric mucins and sialyl Tn antigen in intraepithelial neoplasms of the pancreas. Gastroenterology 123:1052-1060.

143. Muik A, Dold C, Geiß Y, Volk A, Werbizki M, Dietrich U, von Laer D. 2012. Semireplication-competent vesicular stomatitis virus as a novel platform for oncolytic virotherapy. J Mol Med (Berl).

144. Wu Y, Lun X, Zhou H, Wang L, Sun B, Bell JC, Barrett JW, McFadden G, Biegel JA, Senger DL, PA. F. 2008. Oncolytic efficacy of recombinant vesicular stomatitis virus and myxoma virus in experimental models of rhabdoid tumors. Clinical cancer research : an official journal of the American Association for Cancer Research 14:1218-1227.

145. Galivo F, Diaz RM, Wongthida P, Thompson J, Kottke T, Barber G, Melcher A, Vile R. 2010. Single-cycle viral gene expression, rather than progressive replication and oncolysis, is required for VSV therapy of B16 melanoma. Gene Ther 17:158-170.

146. Naik S, Nace R, Barber GN, Russell SJ. 2012. Potent systemic therapy of multiple myeloma utilizing oncolytic vesicular stomatitis virus coding for interferon-beta. Cancer gene therapy.

147. Chen N, Restivo A, Reiss CS. 2001. Leukotrienes play protective roles early during experimental VSV encephalitis. J Neuroimmunol 120:94-102.

148. Altomonte J, Wu L, Chen L, Meseck M, Ebert O, Garcia-Sastre A, Fallon J, Woo S. 2008. Exponential enhancement of oncolytic vesicular stomatitis virus potency by vector-mediated suppression of inflammatory responses in vivo. Molecular therapy : the journal of the American Society of Gene Therapy 16:146-153.

149. Altomonte J, Wu L, Meseck M, Chen L, Ebert O, Garcia-Sastre A, Fallon J, Mandeli J, Woo SL. 2009. Enhanced oncolytic potency of vesicular stomatitis virus through vector-mediated inhibition of NK and NKT cells. Cancer gene therapy 16:266-278.

150.   Kottke T, Diaz RM, Kaluza K, Pulido J, Galivo F, Wongthida P, Thompson J, Willmon C, Barber GN, Chester J, Selby P, Strome S, Harrington K, Melcher A, Vile RG. 2008. Use of biological therapy to enhance both virotherapy and adoptive T-cell therapy for cancer. Molecular therapy : the journal of the American Society of Gene Therapy 16:1910-1918.

151.   Qiao J, Wang H, Kottke T, Diaz RM, Willmon C, Hudacek A, Thompson J, Parato K, Bell J, Naik J, Chester J, Selby P, Harrington K, Melcher A, Vile RG. 2008. Loading of oncolytic vesicular stomatitis virus onto antigen-specific T cells enhances the efficacy of adoptive T-cell therapy of tumors. Gene Ther 15:604-616.

152.   Labib M, Zamay AS, Muharemagic D, Chechik A, Bell JC, Berezovski MV. 2012. Electrochemical sensing of aptamer-facilitated virus immunoshielding. Anal Chem 84:1677-1686.

153.   Tesfay MZ, Kirk AC, Hadac EM, Griesmann GE, Federspiel MJ, Barber GN, Henry SM, Peng KW, Russell SJ. 2013. PEGylation of vesicular stomatitis virus extends virus persistence in blood circulation of passively immunized mice. J Virol 87:3752-3759.

154.   Peng KW, Myers R, Greenslade A, Mader E, Greiner S, Federspiel MJ, Dispenzieri A, Russell SJ. 2013. Using clinically approved cyclophosphamide regimens to control the humoral immune response to oncolytic viruses. Gene Ther.

155.   Willmon C, Diaz RM, Wongthida P, Galivo F, Kottke T, Thompson J, Albelda S, Harrington K, Melcher A, Vile R. 2011. Vesicular stomatitis virus-induced immune suppressor cells generate antagonism between intratumoral oncolytic virus and cyclophosphamide. Molecular therapy : the journal of the American Society of Gene Therapy 19:140-149.

156.   Leveille S, Samuel S, Goulet ML, Hiscott J. 2011. Enhancing VSV oncolytic activity with an improved cytosine deaminase suicide gene strategy. Cancer gene therapy 18:435-443.

157.   Porosnicu M, Mian A, Barber GN. 2003. The oncolytic effect of recombinant vesicular stomatitis virus is enhanced by expression of the fusion cytosine deaminase/uracil phosphoribosyltransferase suicide gene. Cancer Res 63:8366-8376.

158.   Ebert O SK, Kournioti C, Park MS, García-Sastre A, Woo SL. 2004. Syncytia induction enhances the oncolytic potential of vesicular stomatitis virus in virotherapy for cancer. Cancer Research 64:3265-3270.

159.   Shin EJ, Chang JI, Choi B, Wanna G, Ebert O, Genden EM, Woo SL. 2007. Fusogenic vesicular stomatitis virus for the treatment of head and neck squamous carcinomas. Otolaryngol Head Neck Surg 136:811-817.

160. Chang G, Xu S, Watanabe M, Jayakar HR, Whitt MA, Gingrich JR. 2010. Enhanced oncolytic activity of vesicular stomatitis virus encoding SV5-F protein against prostate cancer. J Urol 183:1611-1618.

161. Altomonte J, Braren R, Schulz S, Marozin S, Rummeny EJ, Schmid RM, Ebert O. 2008. Synergistic antitumor effects of transarterial viroembolization for multifocal hepatocellular carcinoma in rats. Hepatology 48:1864-1873.

162. Breitbach CJ, De Silva NS, Falls TJ, Aladl U, Evgin L, Paterson J, Sun YY, Roy DG, Rintoul JL, Daneshmand M, Parato K, Stanford MM, Lichty BD, Fenster A, Kirn D, Atkins H, Bell JC. 2011. Targeting tumor vasculature with an oncolytic virus. Molecular therapy : the journal of the American Society of Gene Therapy 19:886-894.

163. Melcher A, Parato K, Rooney CM, Bell JC. 2011. Thunder and lightning: immunotherapy and oncolytic viruses collide. Molecular therapy : the journal of the American Society of Gene Therapy 19:1008-1016.

164. Boudreau JE, Bridle BW, Stephenson KB, Jenkins KM, Brunelliere J, Bramson JL, Lichty BD, Wan Y. 2009. Recombinant vesicular stomatitis virus transduction of dendritic cells enhances their ability to prime innate and adaptive antitumor immunity. Molecular therapy : the journal of the American Society of Gene Therapy 17:1465-1472.

165. Bridle BW, Hanson S, Lichty BD. 2010. Combining oncolytic virotherapy and tumour vaccination. Cytokine & growth factor reviews 21:143-148.

166. Diaz RM, Galivo F, Kottke T, Wongthida P, Qiao J, Thompson J, Valdes M, Barber G, RG. V. 2007. Oncolytic immunovirotherapy for melanoma using vesicular stomatitis virus. Cancer Res 67:2840-2848.

167. Galivo F, Diaz RM, Thanarajasingam U, Jevremovic D, Wongthida P, Thompson J, Kottke T, Barber GN, Melcher A, and Vile RG. 2010. Interference of CD40L-mediated Tumor Immunotherapy by Oncolytic VSV. Human Gene Therapy.

168. Kottke T, Galivo F, Wongthida P, Diaz RM, Thompson J, Jevremovic D, Barber GN, Hall G, Chester J, Selby P, Harrington K, Melcher A, Vile RG. 2008. Treg depletion-enhanced IL-2 treatment facilitates therapy of established tumors using systemically delivered oncolytic virus. Molecular therapy : the journal of the American Society of Gene Therapy 16:1217-1226.

169. Qiao J, Kottke T, Willmon C, Galivo F, Wongthida P, Diaz RM, Thompson J, Ryno P, Barber GN, Chester J, Selby P, Harrington K, Melcher A, Vile RG. 2008. Purging metastases in lymphoid organs using a combination of antigen-nonspecific adoptive T cell therapy, oncolytic virotherapy and immunotherapy. Nature medicine 14:37-44.

170. Willmon CL, Saloura V, Fridlender ZG, Wongthida P, Diaz RM, Thompson J, Kottke T, Federspiel M, Barber G, Albelda SM, and Vile RG. 2009. Expression of IFN-beta enhances both efficacy and safety of oncolytic vesicular stomatitis virus for therapy of mesothelioma. Cancer Research 69:7713-7720.

171. Wongthida P, Diaz RM, Galivo F, Kottke T, Thompson J, Pulido J, Pavelko K, Pease L, Melcher A, Vile R. 2010. Type III IFN interleukin-28 mediates the antitumor efficacy of oncolytic virus VSV in immune-competent mouse models of cancer. Cancer Res 70:4539-4549.

172. Kelly E, Russell SJ. 2007. History of oncolytic viruses: genesis to genetic engineering. Molecular therapy : the journal of the American Society of Gene Therapy 15:651-659.

173. Bauzon M, Hermiston T. 2014. Armed therapeutic viruses - a disruptive therapy on the horizon of cancer immunotherapy. Frontiers in immunology 5:74.

174. Russell SJ, Peng KW, Bell JC. 2012. Oncolytic virotherapy. Nature biotechnology 30:658-670.

175. Hardwick NR, Carroll M, Kaltcheva TI, Qian D, Lim D, Leong L, Chu P, Kim J, Joseph C, Fakih MG, Yen Y, Espenschied J, Ellenhorn JD, Diamond DJ, Chung V. 2014. p53MVA therapy in patients with refractory gastrointestinal malignancies elevates p53-specific CD8+ T cell responses. Clinical cancer research : an official journal of the American Association for Cancer Research.

176. Roth JA, Nguyen D, Lawrence DD, Kemp BL, Carrasco CH, Ferson DZ, Hong WK, Komaki R, Lee JJ, Nesbitt JC, Pisters KM, Putnam JB, Schea R, Shin DM, Walsh GL, Dolormente MM, Han CI, Martin FD, Yen N, Xu K, Stephens LC, McDonnell TJ, Mukhopadhyay T, Cai D. 1996. Retrovirus-mediated wild-type p53 gene transfer to tumors of patients with lung cancer. Nature medicine 2:985-991.

177. Li J, Pan J, Zhu X, Su Y, Bao L, Qiu S, Zou C, Cai Y, Wu J, Tham IW. 2013. Recombinant adenovirus-p53 (Gendicine) sensitizes a pancreatic carcinoma cell line to radiation. Chinese journal of cancer research = Chung-kuo yen cheng yen chiu 25:715-721.

178. Kusumoto M, Ogawa T, Mizumoto K, Ueno H, Niiyama H, Sato N, Nakamura M, Tanaka M. 1999. Adenovirus-mediated p53 gene transduction inhibits telomerase activity independent of its effects on cell cycle arrest and apoptosis in human pancreatic cancer cells. Clinical cancer research : an official journal of the American Association for Cancer Research 5:2140-2147.

179. Logunov DY, Ilyinskaya GV, Cherenova LV, Verhovskaya LV, Shmarov MM, Chumakov PM, Kopnin BP, Naroditsky BS. 2004. Restoration of p53 tumor-suppressor activity in human tumor cells in vitro and in their xenografts in vivo by recombinant avian adenovirus CELO-p53. Gene Ther 11:79-84.

180. Odin L, Favrot M, Poujol D, Michot JP, Moingeon P, Tartaglia J, Puisieux I. 2001. Canarypox virus expressing wild type p53 for gene therapy in murine tumors mutated in p53. Cancer gene therapy 8:87-98.

181. van Beusechem VW, van den Doel PB, Grill J, Pinedo HM, Gerritsen WR. 2002. Conditionally replicative adenovirus expressing p53 exhibits enhanced oncolytic potency. Cancer Res 62:6165-6171.

182. Heideman DA, Steenbergen RD, van der Torre J, Scheffner M, Alemany R, Gerritsen WR, Meijer CJ, Snijders PJ, van Beusechem VW. 2005. Oncolytic adenovirus expressing a p53 variant resistant to degradation by HPV E6 protein exhibits potent and selective replication in cervical cancer. Molecular therapy : the journal of the American Society of Gene Therapy 12:1083-1090.

183. Iacobuzio-Donahue CA, Herman JM. 2014. Autophagy, p53, and pancreatic cancer. The New England journal of medicine 370:1352-1353.

184. Weissmueller S, Manchado E, Saborowski M, Morris JPt, Wagenblast E, Davis CA, Moon SH, Pfister NT, Tschaharganeh DF, Kitzing T, Aust D, Markert EK, Wu J, Grimmond SM, Pilarsky C, Prives C, Biankin AV, Lowe SW. 2014. Mutant p53 drives pancreatic cancer metastasis through cell-autonomous PDGF receptor beta signaling. Cell 157:382-394.

185. Horvath MM, Wang X, Resnick MA, Bell DA. 2007. Divergent evolution of human p53 binding sites: cell cycle versus apoptosis. PLoS genetics 3:e127.

186. Shcherbo AP, Kiselev AV, Rossolovskii AP. 2007. [The need for developing a methodology of spatial rationale for a sanitary protective zone]. Gigiena i sanitariia:22-24.

187. Takaoka A, Hayakawa S, Yanai H, Stoiber D, Negishi H, Kikuchi H, Sasaki S, Imai K, Shibue T, Honda K, Taniguchi T. 2003. Integration of interferon-alpha/beta signalling to p53 responses in tumour suppression and antiviral defence. Nature 424:516-523.

188. Iwamura T, Katsuki T, K. I. 1987. Establishment and characterization of a human pancreatic cancer cell line (SUIT-2) producing carcinoembryonic antigen and carbohydrate antigen 19-9. Jpn J Cancer Res. 78:54-62.

189. Okabe T, Yamaguchi N, N. O. 1983. Establishment and characterization of a carcinoembryonic antigen (CEA)-producing cell line from a human carcinoma of the exocrine pancreas. Cancer 51:662-668.

190. Furukawa T, Duguid WP, Rosenberg L, Viallet J, Galloway DA, and Tsao MS. 1996. Long-term culture and immortalization of epithelial cells from normal adult human pancreatic ducts transfected by the E6E7 gene of human papilloma virus 16. The American journal of pathology 148:1763-1770.

191. Lee KM, Nguyen C, Ulrich AB, Pour PM, Ouellette MM. 2003. Immortalization with telomerase of the Nestin-positive cells of the human pancreas. Biochemical and biophysical research communications 301:1038-1044.

192. Shcherbo D, Merzlyak EM, Chepurnykh TV, Fradkov AF, Ermakova GV, Solovieva EA, Lukyanov KA, Bogdanova EA, Zaraisky AG, Lukyanov S, Chudakov DM. 2007. Bright far-red fluorescent protein for whole-body imaging. Nature methods 4:741-746.

193. Boyd SD, Tsai KY, Jacks T. 2000. An intact HDM2 RING-finger domain is required for nuclear exclusion of p53. Nat Cell Biol 2:563-568.

194. Kalvodova L, Sampaio JL, Cordo S, Ejsing CS, Shevchenko A, Simons K. 2009. The lipidomes of vesicular stomatitis virus, semliki forest virus, and the host plasma membrane analyzed by quantitative shotgun mass spectrometry. J Virol 83:7996-8003.

195. Bolstad BM, Irizarry RA, Astrand M, Speed TP. 2003. A comparison of normalization methods for high density oligonucleotide array data based on variance and bias. Bioinformatics 19:185-193.

196. Klimstra DS, Longnecker DS. 1994. K-ras mutations in pancreatic ductal proliferative lesions. The American journal of pathology 145:1547-1550.

197. Berrozpe G, Schaeffer J, Peinado MA, Real FX, Perucho M. 1994. Comparative analysis of mutations in the p53 and K-ras genes in pancreatic cancer. International journal of cancer. Journal international du cancer 58:185-191.

198. Deer EL, Gonzalez-Hernandez J, Coursen JD, Shea JE, Ngatia J, Scaife CL, Firpo MA, Mulvihill SJ. 2010. Phenotype and genotype of pancreatic cancer cell lines. Pancreas 39:425-435.

199. Ruggeri B, Zhang SY, Caamano J, DiRado M, Flynn SD, Klein-Szanto AJ. 1992. Human pancreatic carcinomas and cell lines reveal frequent and multiple alterations in the p53 and Rb-1 tumor-suppressor genes. Oncogene 7:1503-1511.

200. Shcherbo D, Shemiakina, II, Ryabova AV, Luker KE, Schmidt BT, Souslova EA, Gorodnicheva TV, Strukova L, Shidlovskiy KM, Britanova OV, Zaraisky AG, Lukyanov KA, Loschenov VB, Luker GD, Chudakov DM. 2010. Near-infrared fluorescent proteins. Nature methods 7:827-829.

201. Black BL, Rhodes RB, McKenzie M, Lyles DS. 1993. The role of vesicular stomatitis virus matrix protein in inhibition of host-directed gene expression is genetically separable from its function in virus assembly. J Virol 67:4814-4821.

202. Coulon P, Deutsch V, Lafay F, Martinet-Edelist C, Wyers F, Herman RC, Flamand A. 1990. Genetic evidence for multiple functions of the matrix protein of vesicular stomatitis virus. The Journal of general virology 71 (Pt 4):991-996.

203. Wollmann G, Davis JN, Bosenberg MW, van den Pol AN. 2013. Vesicular stomatitis virus variants selectively infect and kill human melanomas but not normal melanocytes. Journal of virology 87:6644-6659.

204. Ho J, Benchimol S. 2003. Transcriptional repression mediated by the p53 tumour suppressor. Cell death and differentiation 10:404-408.

205. Frank AK, Leu JI, Zhou Y, Devarajan K, Nedelko T, Klein-Szanto A, Hollstein M, Murphy ME. 2011. The codon 72 polymorphism of p53 regulates interaction with NF-{kappa}B and transactivation of genes involved in immunity and inflammation. Molecular and cellular biology 31:1201-1213.

206. Okal A, Cornillie S, Matissek SJ, Matissek KJ, Cheatham TE, 3rd, Lim CS. 2014. Re-engineered p53 chimera with enhanced homo-oligomerization that maintains tumor suppressor activity. Molecular pharmaceutics 11:2442-2452.

207. Matissek KJ, Okal A, Mossalam M, Lim CS. 2014. Delivery of a Monomeric p53 Subdomain with Mitochondrial Targeting Signals from Pro-Apoptotic Bak or Bax. Pharmaceutical research.

208. Schlehuber LD, Rose JK. 2004. Prediction and identification of a permissive epitope insertion site in the vesicular stomatitis virus glycoprotein. J Virol 78:5079-5087.

209. Dreja H, Piechaczyk M. 2006. The effects of N-terminal insertion into VSV-G of an scFv peptide. Virol J 3:69.

210. Muik A, Kneiske I, Werbizki M, Wilflingseder D, Giroglou T, Ebert O, Kraft A, Dietrich U, Zimmer G, Momma S, von Laer D. 2011. Pseudotyping vesicular stomatitis virus with lymphocytic choriomeningitis virus glycoproteins enhances infectivity for glioma cells and minimizes neurotropism. J Virol 85:5679-5684.

211. Bergman I GJ, Gao Y, Whitaker-Dowling P. 2007. Treatment of implanted mammary tumors with recombinant vesicular stomatitis virus targeted to Her2/neu. Int J Canc 121:425-430.

212. Gao Y, Whitaker-Dowling P, Watkins SC, Griffin JA, Bergman I. 2006. Rapid adaptation of a recombinant vesicular stomatitis virus to a targeted cell line. J Virol 80:8603-8612.

213. Ayala-Breton C, Barber GN, Russell SJ, Peng KW. 2012. Retargeting vesicular stomatitis virus using measles virus envelope glycoproteins. Hum Gene Ther 23:484-491.

214. Croyle MA, Callahan SM, Auricchio A, Schumer G, Linse KD, Wilson JM, Brunner LJ, Kobinger GP. 2004. PEGylation of a vesicular stomatitis virus G pseudotyped lentivirus vector prevents inactivation in serum. J Virol 78:912-921.

215. Muharemagic D, Labib M, Ghobadloo SM, Zamay AS, Bell JC, Berezovski MV. 2012. Anti-Fab aptamers for shielding virus from neutralizing antibodies. J ACS 134:17168-17177.

216. Liang M, Yan M, Lu Y, Chen IS. 2013. Retargeting VSV-G pseudotyped lentiviral vectors with enhanced stability by in situ synthesized polymer shell. Hum Gene Ther Methods.

217. Hwang BY, Schaffer DV. 2013. Engineering a serum-resistant and thermostable vesicular stomatitis virus G glycoprotein for pseudotyping retroviral and lentiviral vectors. Gene Ther.

218. Waibler Z, Detje CN, Bell JC, Kalinke U. 2007. Matrix protein mediated shutdown of host cell metabolism limits vesicular stomatitis virus-induced interferon-alpha responses to plasmacytoid dendritic cells. Immunobiology 212:887-894.

219. Wollmann G TP, van den Pol AN. 2005. Targeting human glioblastoma cells: comparison of nine viruses with oncolytic potential. J Virol 79:6005-6022.

220. Whelan SP, Ball LA, Barr JN, Wertz GT. 1995. Efficient recovery of infectious vesicular stomatitis virus entirely from cDNA clones. Proc Natl Acad Sci USA 92:8388-8392.

221. Flanagan EB, Zamparo JM, Ball LA, Rodriguez LL, Wertz GW. 2001. Rearrangement of the genes of vesicular stomatitis virus eliminates clinical disease in the natural host: new strategy for vaccine development. J Virol 75:6107-6114.

222. Novella IS, Ball LA, Wertz GW. 2004. Fitness analyses of vesicular stomatitis strains with rearranged genomes reveal replicative disadvantages. J Virol 78:9837-9841.

223. Faria PA, Chakraborty P, Levay A, Barber GN, Ezelle HJ, Enninga J, Arana C, van Deursen J, Fontoura BM. 2005. VSV disrupts the Rae1/mrnp41 mRNA nuclear export pathway. Mol Cell 17:93-102.

224. Rajani KR, Pettit Kneller EL, McKenzie MO, Horita DA, Chou JW, Lyles DS. 2012. Complexes of vesicular stomatitis virus matrix protein with host Rae1 and Nup98 involved in inhibition of host transcription. PLoS pathogens 8.

225. von Kobbe C, van Deursen JM, Rodrigues JP, Sitterlin D, Bachi A, Wu X, Wilm M, Carmo-Fonseca M, Izaurralde E. 2000. Vesicular stomatitis virus matrix protein inhibits host cell gene expression by targeting the nucleoporin Nup98. Mol.Cell 6:1243-1252.

226. Yuan H, Yoza BK, Lyles DS. 1998. Inhibition of host RNA polymerase II-dependent transcription by vesicular stomatitis virus results from inactivation of TFIID. Virology 251:383-392.

227. Kelly EJ, Nace R, Barber GN, and Russell SJ. 2010. Attenuation of vesicular stomatitis virus encephalitis through microRNA targeting. J Virol 84:1550-1562.

228. Basu M, Maitra RK, Xiang Y, Meng X, Banerjee AK, Bose S. 2006. Inhibition of vesicular stomatitis virus infection in epithelial cells by alpha interferon-induced soluble secreted proteins. The Journal of general virology 87:2653-2662.

229. Paglino JC, van den Pol AN. 2011. Vesicular stomatitis virus has extensive oncolytic activity against human sarcomas: rare resistance is overcome by blocking interferon pathways. J Virol 85:9346-9358.

230. Li Y, Fan X, He X, Sun H, Zou Z, Yuan H, Xu H, Wang C, Shi X. 2012. MicroRNA-466l inhibits antiviral innate immune response by targeting interferon-alpha. Cell Mol Immunol 9:497-502.

231. Le Boeuf F, Bell JC. 2010. United virus: the oncolytic tag-team against cancer! Cytokine Growth Factor Rev 21:205-211.

232. Egan MA, Chong SY, Rose NF, Megati S, Lopez KJ, Schadeck EB, Johnson JE, Masood A, Piacente P, Druilhet RE, Barras PW, Hasselschwert DL, Reilly P, Mishkin EM, Montefiori DC, Lewis MG, Clarke DK, Hendry RM, Marx PA, Eldridge JH, Udem SA, Israel ZR, Rose JK. 2004. Immunogenicity of attenuated vesicular stomatitis virus vectors expressing HIV type 1 Env and SIV Gag proteins: comparison of intranasal and intramuscular vaccination routes. AIDS research and human retroviruses 20:989-1004.

233. Rose NF, Marx PA, Luckay A, Nixon DF, Moretto WJ, Donahoe SM, Montefiori D, Roberts A, Buonocore L, Rose JK. 2001. An effective AIDS vaccine based on live attenuated vesicular stomatitis virus recombinants. Cell 106:539-549.

234. Jenks N, Myers R, Greiner SM, Thompson J, Mader EK, Greenslade A, Griesmann GE, Federspiel MJ, Rakela J, Borad MJ, Vile RG, Barber GN, Meier TR, Blanco MC, Carlson SK, Russell SJ, Peng KW. 2010. Safety studies on intrahepatic or intratumoral injection of oncolytic vesicular stomatitis virus expressing interferon-beta in rodents and nonhuman primates. Hum Gene Ther 21:451-462.

235. Irie T, Carnero E, Okumura A, Garcia-Sastre A, Harty RN. 2007. Modifications of the PSAP region of the matrix protein lead to attenuation of vesicular stomatitis virus in vitro and in vivo. The Journal of general virology 88:2559-2567.

236. Ozduman K, Wollmann G, Ahmadi SA, van den Pol AN. 2009. Peripheral immunization blocks lethal actions of vesicular stomatitis virus within the brain. J Virol 83:11540-11549.

237. Janelle V, Brassard F, Lapierre P, Lamarre A, Poliquin L. 2011. Mutations in the glycoprotein of vesicular stomatitis virus affect cytopathogenicity: potential for oncolytic virotherapy. J Virol 85:6513-6520.

238. Edge RE, Falls TJ, Brown CW, Lichty BD, Atkins H, Bell JC. 2008. A let-7 MicroRNA-sensitive vesicular stomatitis virus demonstrates tumor-specific replication. Molecular therapy : the journal of the American Society of Gene Therapy 16:1437-1443.

239. Alain T, Lun X, Martineau Y, Sean P, Pulendran B, Petroulakis E, Zemp FJ, Lemay CG, Roy D, Bell JC, Thomas G, Kozma SC, Forsyth PA, Costa-Mattioli M, Sonenberg N. 2010. Vesicular stomatitis virus oncolysis is potentiated by impairing mTORC1-dependent type I IFN production. Proc Natl Acad Sci U S A 107:1576-1581.

240. Nguyen TL, Abdelbary H, Arguello M, Breitbach C, Leveille S, Diallo JS, Yasmeen A, Bismar TA, Kirn D, Falls T, Snoulten VE, Vanderhyden BC, Werier J, Atkins H, Vaha-Koskela MJ, Stojdl DF, Bell JC, Hiscott J. 2008. Chemical targeting of the innate antiviral response by histone deacetylase inhibitors renders refractory cancers sensitive to viral oncolysis. Proc Natl Acad Sci U S A 105:14981-14986.

241. Le Boeuf F, Diallo JS, McCart JA, Thorne S, Falls T, Stanford M, Kanji F, Auer R, Brown CW, Lichty BD, Parato K, Atkins H, Kirn D, Bell JC. 2010. Synergistic interaction between oncolytic viruses augments tumor killing. Molecular therapy : the journal of the American Society of Gene Therapy 18:888-895.

242. Le Boeuf F, Niknejad N, Wang J, Auer R, Weberpals JI, Bell JC, Dimitroulakos J. 2012. Sensitivity of cervical carcinoma cells to vesicular stomatitis virus-induced oncolysis: Potential role of human papilloma virus infection. International journal of cancer. Journal international du cancer 131:E204-215.

243. Gaddy DF L, D.S. 2007. Oncolytic vesicular stomatitis virus induces apoptosis via signaling through PKR, Fas, and Daxx. J Virol 81:2792-2804.

244. Sharif-Askari E, Nakhaei P, Oliere S, Tumilasci V, Hernandez E, Wilkinson P, Lin R, Bell J, Hiscott J. 2007. Bax-dependent mitochondrial membrane permeabilization enhances IRF3-mediated innate immune response during VSV infection. Virology 365:20-33.

245. Hamacher R, Schmid RM, Saur D, Schneider G. 2008. Apoptotic pathways in pancreatic ductal adenocarcinoma. Mol Cancer 7:64.

246. Hanahan D, Weinberg RA. 2011. Hallmarks of cancer: the next generation. Cell 144:646-674.

247. Samuel S, Tumilasci VF, Oliere S, Nguyen TL, Shamy A, Bell J, Hiscott J. 2010. VSV oncolysis in combination with the BCL-2 inhibitor obatoclax overcomes apoptosis resistance in chronic lymphocytic leukemia. Molecular therapy : the journal of the American Society of Gene Therapy 18:2094-2103.

248. Tumilasci VF, Oliere S, Nguyen TL, Shamy A, Bell J, Hiscott J. 2008. Targeting the apoptotic pathway with BCL-2 inhibitors sensitizes primary chronic lymphocytic leukemia cells to vesicular stomatitis virus-induced oncolysis. J Virol 82:8487-8499.

249. Schache P, Gurlevik E, Struver N, Woller N, Malek N, Zender L, Manns M, Wirth T, Kuhnel F, Kubicka S. 2009. VSV virotherapy improves chemotherapy by triggering apoptosis due to proteasomal degradation of Mcl-1. Gene Ther 16:849-861.

250. Brown CW, Stephenson KB, Hanson S, Kucharczyk M, Duncan R, Bell JC, Lichty BD. 2009. The p14 FAST protein of reptilian reovirus increases vesicular stomatitis virus neuropathogenesis. J Virol 83:552-561.

251. Goel A, Carlson SK, Classic KL, Greiner S, Naik S, Power AT, Bell JC, Russell SJ. 2007. Radioiodide imaging and radiovirotherapy of multiple myeloma using VSV(Delta51)-NIS, an attenuated vesicular stomatitis virus encoding the sodium iodide symporter gene. Blood 110:2342-2350.

252. Naik S, Nace R, Federspiel MJ, Barber GN, Peng KW, Russell SJ. 2012. Curative one-shot systemic virotherapy in murine myeloma. Leukemia.

253. Altomonte J WL, Chen L, Meseck M, Ebert O, García-Sastre A, Fallon J, Woo SL. 2008. Exponential enhancement of oncolytic vesicular stomatitis virus potency by vector-mediated suppression of inflammatory responses in vivo. Molecular Therapy 16:146-153.

254. Kottke T, Hall G, Pulido J, Diaz RM, Thompson J, Chong H, Selby P, Coffey M, Pandha H, Chester J, Melcher A, Harrington K, Vile R. 2010. Antiangiogenic cancer therapy combined with oncolytic virotherapy leads to regression of established tumors in mice. J Clin Invest 120:1551-1560.

255. Nakashima H, Kaur B, Chiocca EA. 2010. Directing systemic oncolytic viral delivery to tumors via carrier cells. Cytokine Growth Factor Rev 21:119-126.

256. Power AT, Bell JC. 2008. Taming the Trojan horse: optimizing dynamic carrier cell/oncolytic virus systems for cancer biotherapy. Gene Ther 15:772-779.

257. Ikeda K, Wakimoto H, Ichikawa T, Jhung S, Hochberg FH, Louis DN, Chiocca EA. 2000. Complement depletion facilitates the infection of multiple brain

tumors by an intravascular, replication-conditional herpes simplex virus mutant. J Virol 74:4765-4775.

258. Qiao J, Wang H, Kottke T, White C, Twigger K, Diaz RM, Thompson J, Selby P, de Bono J, Melcher A, Pandha H, Coffey M, Vile R, Harrington K. 2008. Cyclophosphamide facilitates antitumor efficacy against subcutaneous tumors following intravenous delivery of reovirus. Clinical cancer research : an official journal of the American Association for Cancer Research 14:259-269.

259. Ghiringhelli F, Menard C, Puig PE, Ladoire S, Roux S, Martin F, Solary E, Le Cesne A, Zitvogel L, Chauffert B. 2007. Metronomic cyclophosphamide regimen selectively depletes CD4+CD25+ regulatory T cells and restores T and NK effector functions in end stage cancer patients. Cancer immunology, immunotherapy : CII 56:641-648.

260. Shin EJ, Wanna GB, Choi B, Aguila D 3rd, Ebert O, Genden EM, and Woo SL. 2007. Interleukin-12 expression enhances vesicular stomatitis virus oncolytic therapy in murine squamous cell carcinoma. The Laryngoscope 117:210-214.

261. Stephenson KB, Barra NG, Davies E, Ashkar AA, Lichty BD. 2012. Expressing human interleukin-15 from oncolytic vesicular stomatitis virus improves survival in a murine metastatic colon adenocarcinoma model through the enhancement of anti-tumor immunity. Cancer gene therapy 19:238-246.

262. Miller J, Bidula SM, Jensen TM, Reiss CS. 2009. Cytokine-modified VSV is attenuated for neural pathology, but is both highly immunogenic and oncolytic. Int J Infereron Cytokine Mediator Res 1:15-32.

263. Miller JM, Bidula SM, Jensen TM, Reiss CS. 2010. Vesicular stomatitis virus modified with single chain IL-23 exhibits oncolytic activity against tumor cells in vitro and in vivo. Int J Infereron Cytokine Mediator Res 2010:63-72.

264. Leveille S, Goulet ML, Lichty BD, Hiscott J. 2011. Vesicular stomatitis virus oncolytic treatment interferes with tumor-associated dendritic cell functions and abrogates tumor antigen presentation. J Virol 85:12160-12169.

265. Wongthida P, Diaz RM, Pulido C, Rommelfanger D, Galivo F, Kaluza K, Kottke T, Thompson J, Melcher A, Vile R. 2011. Activating systemic T-cell immunity against self tumor antigens to support oncolytic virotherapy with vesicular stomatitis virus. Hum Gene Ther 22:1343-1353.

266. Bridle BW, Stephenson KB, Boudreau JE, Koshy S, Kazdhan N, Pullenayegum E, Brunelliere J, Bramson JL, Lichty BD, Wan Y. 2010. Potentiating cancer immunotherapy using an oncolytic virus. Molecular therapy : the journal of the American Society of Gene Therapy 18:1430-1439.

267. Pulido J, Kottke T, Thompson J, Galivo F, Wongthida P, Diaz RM, Rommelfanger D, Ilett E, Pease L, Pandha H, Harrington K, Selby P, Melcher

A, Vile R. 2012. Using virally expressed melanoma cDNA libraries to identify tumor-associated antigens that cure melanoma. Nature biotechnology 30:337-343.

268. Wongthida P, Diaz RM, Galivo F, Kottke T, Thompson J, Melcher A, Vile R. 2011. VSV oncolytic virotherapy in the B16 model depends upon intact MyD88 signaling. Molecular therapy : the journal of the American Society of Gene Therapy 19:150-158.

269. Jensen H, Andresen L, Nielsen J, Christensen JP, Skov S. 2011. Vesicular stomatitis virus infection promotes immune evasion by preventing NKG2D-ligand surface expression. PLoS One 6:e23023.

270. Cobleigh MA, Bradfield C, Liu Y, Mehta A, Robek MD. 2012. The immune response to a vesicular stomatitis virus vaccine vector is independent of particulate antigen secretion and protein turnover rate. J Virol 86:4253-4261.

271. Nowak AK, Robinson BW, Lake RA. 2002. Gemcitabine exerts a selective effect on the humoral immune response: implications for combination chemo-immunotherapy. Cancer Res 62:2353-2358.

272. Ausubel LJ, Meseck M, Derecho I, Lopez P, Knoblauch C, McMahon R, Anderson J, Dunphy N, Quezada V, Khan R, Huang P, Dang W, Luo M, Hsu D, Woo SL, Couture L. 2011. Current good manufacturing practice production of an oncolytic recombinant vesicular stomatitis viral vector for cancer treatment. Hum Gene Ther 22:489-497.

273. Diallo JS, Vaha-Koskela M, Le Boeuf F, Bell J. 2012. Propagation, purification, and in vivo testing of oncolytic vesicular stomatitis virus strains. Methods in molecular biology 797:127-140.